The Particulate Methane Monooxygenase from *Methylococcus capsulatus* (Bath)

Balaka Piku Basu, BSc. (Hons)

A thesis submitted for the degree of

Doctor of Philosophy

Department of Biological Sciences

University of Warwick,

September 2000

PAGE NUMBERING AS ORIGINAL

For my family

Table of Contents

List of Contents

List of Figures

List of Tables

Acknowledgements

I would like to take the opportunity to thank my supervisor Professor Howard Dalton F.R.S for his patience and guidance during my studentship. I would also like to thank the members of the Biological Sciences Department with special thanks to Dr. Heather Luckarift, Sarah Dennison and Sue Slade for all their assistance.

Thanks also to my friends and collaborators, Dr. Ashraf Kitmitto (UMIST) and Dr Bettina Katterle (University of Oslo) for their guidance and support and Nice-Guy Eddie (Animal House, University of Warwick) for the pMMO antibodies.

I would also like to thank all my friends with a special mention to Erica and Cathy, for their constant support. I would like to say a heartfelt thanks to my lab mates and good friends, Anastasia Callaghan and Dr. Ekundayo Adeosun because I wouldn't have got this far without them. Finally and most importantly I would like to thank my family, particularly my parents, who have given me unconditional love and support (both financial and moral) throughout the years. I only hope this will go some way to repay my great debt to them.

Declaration

I declare that all the work reported in this thesis is the result of original research conducted by myself (under the supervision of Professor H. Dalton FRS). Additional help and information, when obtained has been referenced.

No work contained within this thesis has been previously submitted for any other degree.

BALAKA PIKU BASU

List of abbreviations

ATP	adenosine-5'-triphosphate
CHAPS	3-[(3-cholamidopropyl)dimethyl ammonio]-l-propane sulfonate
CBC	copper binding cofactor
DEAE	diethylaminoethyl
2,4-DNP	2,4-dinitrophenol
Dnase I	deoxyribonuclease I
DDTC	diethyldithiocarbamate
DTT	D,L-dithiothreitol
EDTA	ethylenediaminetetraacetic acid
EPR	electron paramagnetic resonance spectroscopy
FAD	flavin adenine dinucleotide
FDH	formaldehyde dehydrogenase
FADH	formate dehydrogenase
FPLC	fast protein liquid chromatography
GC	gas chromatography
H_4F	tetrahydrofolate
H_4F-DH	tetrahydrofolate dehydrogenase
H_4MPT	tetrahydromethanopterin
H_4MPT-DH	tetrahydromethanoperin dehydrogenase
HOQNO	2-N-heptyl-4-hydroxyquinoline-N-oxide
kDa	kilodalton
MMO	methane monooxygenase
NAD^+	nicotinamide adenine dinucleotide (oxidised form)
NADH	nicotinamide adenine dinucleotide (reduced form)
NADP	nicotinamide adenine dinucleotide phosphate (oxidised)
NADPH	nicotinamide adenine dinucleotide phosphate (reduced)
NMS	nitrate mineral salts medium
PAGE	polyacrylamide gel electrophoresis
PCR	polymerase chain reaction

PIPES	piperazine-N,N'-bis[2-ethanesulfonic acid, disodium salt]
PMS	phenyl methyl sulphate
pMMO	particulate methane monooxygenase
$pMMO^m$	membrane-bound pMMO
$pMMO^s$	pMMO solubilised using dodecyl-β-D-maltoside
$pMMO^c$	purified pMMO complex
pMMOH	pMMO hydroxylase
pMMOR	pMMO reductase
PQQ	pyrrolo-quinoline quinone
PQQH	pyrrolo-quinoline quinol
SDS	sodium dodecyl sulfate
SMMO	soluble methane monooxygenase
SPA	single particle analysis
U.V.	ultra violet

Summary

The isolation procedure for the pMMO complex has been optimised to obtain a high specific activity enzyme from *Methylococcus capsulatus* (Bath). The enzyme is comprised of the pMMO hydroxylase (pMMOH) consisting of polypeptides 47,26 and 23kDa molecular mass. In addition to this, a putative pMMO reductase (pMMOR) was also found to be necessary to maintain propylene oxidising activity. This component was found to consist of two polypeptides of approximately 63 and 8kDa. Preliminary N-terminal sequence data of the large subunit of pMMOR indicates that the sequence bears 70% similarity to the methanol dehydrogenase (MDH) from *Methylococcus capsulatus* (Bath). Therefore, we tentatively propose that the MDH can act as a reductase component to the pMMOH.

The significance of this result prompted investigations into the previous published proposals that electrons derived from the methanol oxidation reaction can be channelled back into the methane oxidation reaction by the methanol dehydrogenase, independent of NADH. Any effect of methanol to act as a reductant to pMMO in membrane preparations was lost upon isolation of the pMMO complex, indicating the necessity to maintain a fully functional methanol dehydrogenase (MDH) upon isolation. In addition to this, the *in vitro* electron donors of pMMO, NADH and duroquinol were found to act via distinct pathways of electron transfer (electron transport inhibitor studies).

Electron paramagnetic resonance (EPR) spectroscopy data provided evidence that the copper in the active site of pMMO existed as a mononuclear copper (II) centre **not** a trinuclear copper centre suggested by Chan and coworkers (Chan *et al.*, 1993; Nguyen *et al.*, 1994, 1996a, 1996b, 1998). In addition to this preliminary data also indicates the presence of an iron centre which is only EPR visible after reduction of the complex suggesting the majority of iron in the complex is EPR invisible. The exact nature of this iron centre is still unclear.

A structural study of the pMMO complex has also been undertaken using electron microscopy studies in conjunction with single particle analysis. This allowed low resolution projection maps of different views of the pMMO complex to be generated. The complex appears to exist in a polymeric state of at least a dimer, possibly a tetramer if the molecular weight analysis calculated by sedimentation equilibrium analysis is taken into account.

This study has provided some insight into basic characteristics and the structure of a duroquinol-driven pMMO complex and its interaction with other electron transfer proteins.

Scope of this thesis

Although there has been significant progress in the elucidation of the particulate methane monooxygenase (pMMO) from *Methylococcus capsulatus* (Bath) the recent reports by Zahn and DiSpirito (1996) and Nguyen et al. (1998) have given rise to some confusion in this field. Therefore, the aims of this PhD project were:

1) To develop a reproducible method for the isolation of the pMMO to obtain a high specific activity enzyme.

2) To undertake basic characterisation of the pMMO.

3) To conclusively establish the nature of the metals associated to the pMMO.

4) To investigate the structure of the membrane-bound and purified pMMO complex.

1. Introduction

1.1 Methane and the environment

Scientific interest into methane utilisation has surged in the last thirty years or so. This has been due largely to two factors.

Firstly, methane is present in ~1.8 parts per million in the atmosphere. It is twenty-six times more potent than carbon dioxide as a greenhouse gas and is a source of stratospheric water vapour, which influences ozone depletion (Lelieveld *et al.*, 1993; Shrope, 2000). Increasing concentrations of methane contribute to global warming, and therefore it follows that efforts to reduce atmospheric methane concentrations will help alleviate this effect.

Secondly, the steady decline in crude oil stocks means that the need to find a replacement energy source is imperative (Hogan *et al.,* 1991; Crutzen, 1991). Methane is currently under-utilised as an energy resource because of the difficulty in storing and transporting methane.

Both these problems could be overcome by converting methane to methanol, an easily transportable compound, without sacrificing energy content. This conversion can be carried out synthetically but it is a costly and energy-intensive process (Burch and Parkyns, 1992). The solution may lie in the exploitation of naturally occurring micro-organisms that carry out the conversion of methane to methanol. Understanding how these microbes convert methane to methanol and under what conditions this can be done efficiently may allow us to better utilise methane either by the direct exploitation of these micro-organisms or by learning lessons from the biochemical features of the enzymes that perform this reaction in order to design robust catalysts.

1.2 Methane utilising bacteria

Methylotrophs are a diverse group of micro-organisms that are "able to grow at the expense of reduced carbon compounds containing one or more carbon atoms but no carbon-carbon bonds" (Anthony, 1982). These include methane, methanol, methylated amines, formate, formamide, carbon monoxide, dimethylsulphide and trimethylsulphonium compounds. Obligate methylotrophs grow only on such compounds, whereas facultative methylotrophs are also able to grow on a variety of other organic multicarbon compounds (Zatman, 1981; Anthony, 1982; Hanson, 1992).

1.2.1 Methanotrophs

Methanotrophs are aerobic bacteria that are a subset of methylotrophs and can utilise methane as a sole carbon and energy. In 1970, Whittenbury and co-workers isolated and characterised over 100 new methane oxidising bacteria that have formed the basis of the current classification scheme. The methanotrophs were classified into five different groups based on morphology, the structure of intracytoplasmic membrane, the types of resting stages formed and physiological characteristics. The 'genera' were named *Methylomonas*, *Methylobacter*, *Methylococcus*, *Methylocystis* and *Methylosinus*. The classification was recently revised so methanotrophs were classified into three groups (Type I, e.g. *Methylomonas*, Type II, e.g. *Methylosinus* and Type X e.g. *Methylococcus*) based on the pathways used for carbon assimilation, DNA base composition and intracytoplasmic membrane structure. (Whittenbury and Dalton, 1981; Anthony, 1982; Hanson, 1992 and Hanson and Hanson, 1996)

1.3 Methane oxidation

In methanotrophs, the pathway for methane oxidation (Figure 1.1) has been largely accepted as a sequence of four successive oxidation reactions (Marison and Attwood, 1982).

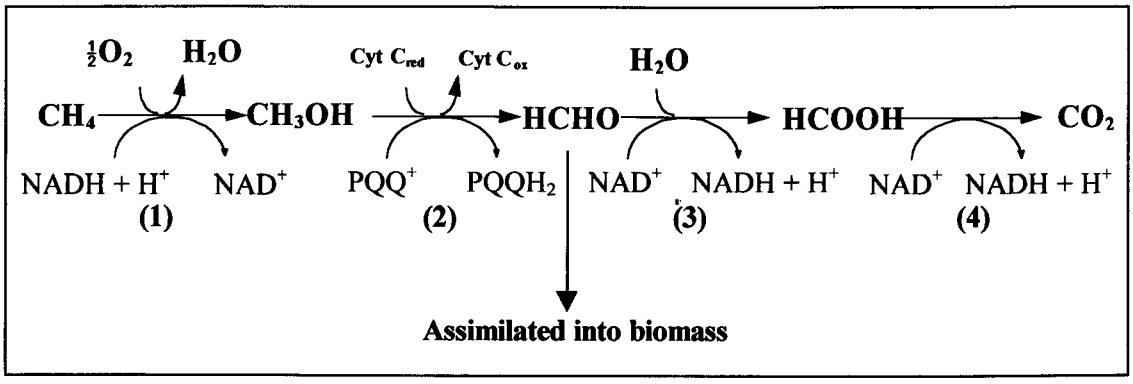

Figure 1.1 The pathway of methane oxidation in methanotrophs. The four oxidation reactions are catalysed by (1) methane monooxygenase (MMO), (2) methanol dehydrogenase (MDH), (3) formaldehyde dehydrogenase (FDH) and (4) formate dehydrogenase (FADH).

The four main enzymes involved in this pathway have been well characterised and are discussed in more detail below.

1.4 Methane Monooxygenase (MMO)

The first step in the methane oxidation pathway, the hydroxylation of methane to methanol, is catalysed by the enzyme methane monooxygenase (MMO). There are two distinct types of the MMO. These differ in cellular location and have been identified in various methanotrophs as the cytoplasmic or soluble MMO (sMMO) and the membrane-bound or particulate MMO (pMMO).

Virtually all methanotrophs possess the particulate MMO (pMMO) whereas the soluble MMO (sMMO) is restricted to a limited number of methanotroph strains e.g. *Methylosinus*, *Methylocystis*, *Methylococcus* species and some *Methylomonas* (Shigematsu *et al.*, 1999) and *Methylomicrobium* (Fuse *et al.*, 1998) species. In general, the sMMO is capable of oxidising a wide range of substrates including alicyclic and aromatic substrates. However, the particulate enzyme can only oxidise a narrow range of substrates that is restricted to alkanes and alkenes of up to five carbons in length.

1.4.1 Soluble Methane Monooxygenase (sMMO)

The soluble methane monooxygenase (sMMO) has been well characterised from M*ethylococcus capsulatus* (Bath) (Colby and Dalton, 1978; Woodland and Dalton, 1984; Green and Dalton, 1985; Liu and Lippard, 1994) and *Methylosinus trichosporium* OB3b (Fox *et al.*, 1989; Lipscomb, 1993). The sMMO has also been identified in other methanotrophs including *Methylobacterium* sp. Strain CRL-26 (Patel and Savas, 1987), *Methylosinus sporium* 5 (Pilkington and Dalton, 1991), *Methylomonas* GYJ3 (Liu et al., 1991) and *Methylocystis* sp. Strain M (Nakajima *et al.*, 1992). In general, the soluble MMO is a multi-component enzyme made up of three distinct proteins (Figure 1.2) which include an hydroxylase (protein A), a regulatory protein (protein B) and an NAD(P)H-dependent oxidoreductase (protein C).

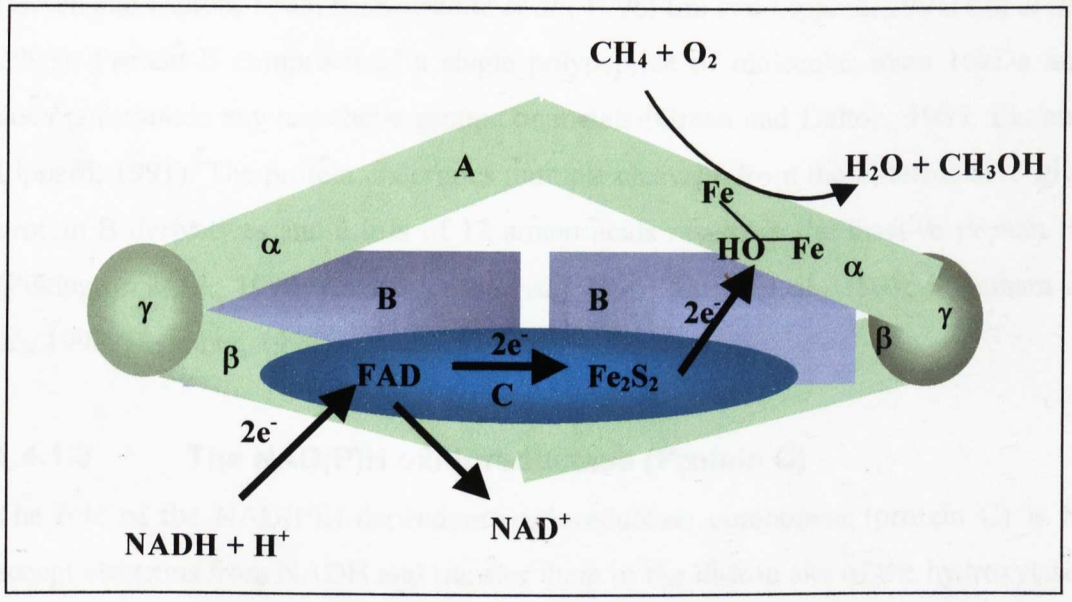

Figure 1.2 Schematic model of sMMO from *Methylococcus capsulatus* (Bath) (adapted from Rosenweig *et al.*, 1993). Protein A, Hydroxylase (green), oxidises methane at its hydroxo-bridged di-iron sites. Protein B, Regulatory (purple), converts enzyme to oxygenase in presence of substrate. Protein C, Reductase (blue), transfers reducing equivalents from NADH to protein A.

1.4.1.1 The hydroxylase component (Protein A)

The hydroxylase component (protein A) of sMMO from *Methylococcus capsulatus* (Bath) is the site of substrate oxygenation and oxygen binding (Colby and Dalton, 1978) and contains a di-iron centre coupled via a μ-oxo bridge structure (Wilkins, 1992). It exists as a dimer of molecular mass of ~250 kDa. Each monomer is comprised of the three subunits, α (60 kDa), β (45 kDa), and γ (20 kDa) in an $\alpha_2\beta_2\gamma_2$ configuration (Woodland and Dalton, 1989; Fox *et al.*, 1989; Dalton *et al.*, 1993).

1.4.1.2 The regulatory component (Protein B)

The precise role of the regulatory component (protein B) is still unclear although it is now generally accepted that it plays several roles in regulating enzymatic activity, converting sMMO from an oxidase to an oxygenase, altering the redox potential of the di-iron site and promoting electron transfer between components of the sMMO (Green and Dalton, 1985; Kazlauskaite *et al.*, 1996; Liu and Lippard, 1991; Liu *et al.*, 1995). Protein B comprises of a single polypeptide of molecular mass 16kDa and does not contain any prosthetic groups or metals (Green and Dalton, 1985; Liu and Lippard, 1991). The protein undergoes multiple cleavage from the N-terminal to give protein B derivatives and a loss of 12 amino acids results in the inactive protein B′ (Pilkington *et al.*, 1990; Kazlauskaite *et al.*, 1996; Lloyd *et al.*, 1997; Shinohara *et al.*, 1998, Bhambra, 1996).

1.4.1.3 The NAD(P)H oxidoreductase (Protein C)

The role of the NAD(P)H-dependent oxidoreductase component (protein C) is to accept electrons from NADH and transfer them to the di-iron site of the hydroxylase. Protein C is a single polypeptide of molecular mass ~39kDa, containing FAD and an Fe_2S_2 centre which are essential for MMO activity (Colby and Dalton, 1978; Colby and Dalton, 1979; Green and Dalton, 1985; Lund and Dalton, 1985; Lund *et al.*, 1985). The reductase component from *Methylococcus capsulatus* (Bath) was inhibited by copper ions (Green *et al.*, 1985) which may have important implications in the regulation of MMO activity by copper ions.

1.4.2 Particulate Methane Monooxygenase (pMMO)

The particulate methane monooxygenase (pMMO) is not as well characterised as its counterpart sMMO largely because of its lability *in vitro*. There has been recent progress in the isolation of pMMO from various methanotrophs and this is discussed in greater detail later on in this chapter (section 1.10)

1.5 Methanol dehydrogenase (MDH)

In Gram negative methylotrophs, the oxidation of methanol to formaldehyde is catalysed by the periplasmic enzyme, methanol dehydrogenase (MDH). MDH is a quinoprotein containing pyrrolo-quinoline quinone (PQQ) as its prosthetic group. The majority of methanol dehydrogenases have an approximate molecular mass of ~140kDa and exist as an $\alpha_2\beta_2$ heterotetramer (Nunn *et al.*, 1989). The α subunit has a molecular mass of ~60kDa and contains one molecule of non-covalently bound PQQ and a calcium ion, both of which are essential for enzyme activity (Anthony *et al.*, 1994). The β subunit has a molecular mass of 8.5 kDa and is generally rich in lysine residues (Patel and Felix, 1976; Anthony, 1986; Anthony *et al.*, 1994; Anthony and Ghosh, 1998).

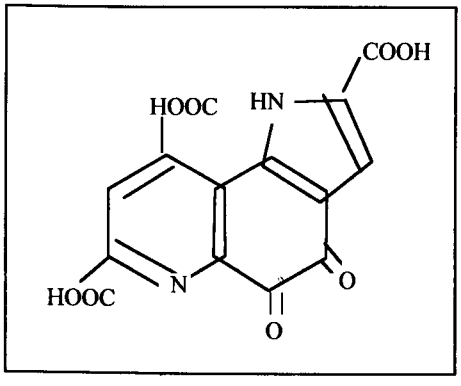

Figure 1.3 Structure of methanol dehydrogenase prosthetic group, pyrrolo-quinoline quinone (PQQ).

The physiological electron acceptor for MDH is the unique acidic cytochrome c_L, which subsequently interacts with the cytochrome aa_3 complex of the periplasmic membrane (Nunn and Anthony, 1988). Although the location of the MDH is usually associated with the periplasm, MDH activity has been observed in both the soluble

and particulate fractions of type I and type X methanotrophs (Patel and Felix, 1976; Grosse *et al.*, 1997). Anthony (1986) proposed that MDH may be at least partially bound to the membrane and could interact with electron transport chain components.

MDH can oxidise primary alcohols, short-chain aldehydes up to propionaldehyde but not secondary alcohols and has the same rate of oxidation of methanol as formaldehyde (Heptinstall and Quayle, 1970; Dunstan *et al.*, 1972; Marison and Attwood, 1982; Anthony, 1986).

1.6 Formaldehyde Dehydrogenase (FDH)

The oxidation of formaldehyde to formate is catalysed by the formaldehyde dehydrogenase (FDH) enzyme. These enzymes are divided into two groups depending on whether the electron acceptor is NAD^+ or an artificial dye e.g. 2,6-dichlorophenolindophenol.

Stirling and Dalton (1978) reported an NAD^+-dependent FDH from *Methylococcus capsulatus* (Bath) which required a protein cofactor for the oxidation of formaldehyde. Tate and Dalton (1999) suggested that the protein cofactor known as the 'modifier' was a small molecular mass protein (8kDa). In the presence of the modifier, only the oxidation of formaldehyde was observed. However, the enzyme was also able to oxidise several aldehydes and alcohols in the absence of the modifier. The FDH was shown to exist as a homotetramer of 63kDa subunits in contrast to the homodimeric structure suggested by Stirling and Dalton (1978). Preliminary N-terminal sequence information obtained for the FDH and the modifier showed no sequence similarities with other protein sequences available in the database (Tate and Dalton, 1999).

However recent studies have shown that the FDH and modifier from *Methylococcus capsulatus* (Bath) have great similarity to the large and small subunit of methanol dehydrogenases from other methylotrophs (Adeosun, 2000). This study also suggests that the source of NAD^+-linked FDH activity was due to an enzyme similar to the NADP-dependent methylene tetrahydromethanopterin dehydrogenase (H_4MPT-DH)

which has been identified and purified from *Methylobacterium extorquens* AM1 (Chistoserdova *et al.*, 1998; Vorholt *et al.*, 1998).

The NADP-dependent methylene tetrahydromethanopterin dehydrogenase (H_4MPT-DH) enzyme catalyses the dehydrogenation of methylene H_4MPT to methenyl H_4MPT. Unlike the enzyme from *Methylobacterium extorquens* AM1, the H_4MPT-DH from *Methylococcus capsulatus* (Bath) was able to catalyse the dehydrogenation of methylene H_4MPT using NAD^+ as an electron acceptor. The enzyme is important in the generation of NADH from formaldehyde oxidation.

An alternate route for formaldehyde is for it to enter into the tetrahydrofolate (H_4F) pathway. The pathway for H_4F-dependent and H_4MPT-dependent formaldehyde oxidation pathways are summarised in Figure 1.4.

1.7 Formate Dehydrogenase (FADH)

Formate dehydrogenase catalyses the oxidation of formate from various metabolic pathways. There have been two contradictory reports on the isolation of a methanotrophic FADH from *Methylosinus trichosporium* OB3b (Yoch *et al.*; Jollie and Lipscomb, 1991). The FADH was purified anaerobically by Yoch *et al.* (1990) and existed in two different forms of molecular mass 315kDa and 155kDa although both forms consisted of the same subunits α (~54kDa) and β (~102kDa). The lower molecular weight FADH existed as an $\alpha\beta$ heterodimer and the higher molecular weight FADH, as an $\alpha_2\beta_2$ tetramer. The enzyme was found to require the flavin mononucleotide FMN, for activity and contained nonhaem iron and acid-labile sulphide.

These findings were in contrast to the FADH purified by Jollie and Lipscomb (1991), which existed as 2 $\alpha\beta\gamma\delta$ protomers (α~98kDa, β~56kDa, γ~20kDa and δ~12kDa) containing iron, inorganic sulphide, molybdenum and a novel flavin cofactor.

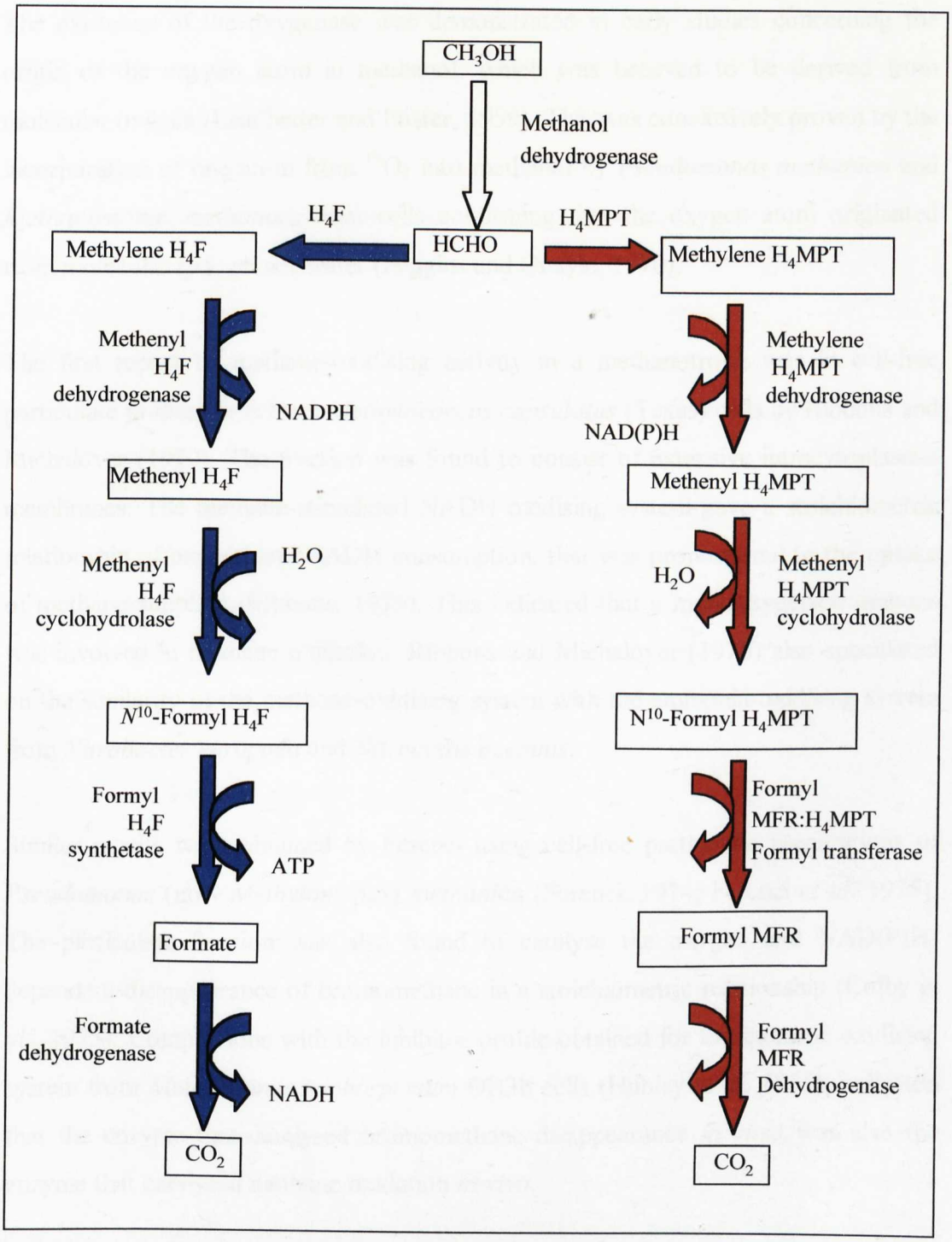

Figure 1.4 The proposed H_4F/H_4MPT pathway for formaldehyde oxidation (modified from Vorholt *et al.*, 1998). Methylene H_4F/H_4MPT, the substrate for the dehydrogenation by NADP-dependent methylene H_4F/H_4MPT dehydrogenase, is formed spontaneously from H_4F/H_4MPT and formaldehyde

1.8 Background to methane monooxygenase (MMO)

The existence of the oxygenase was demonstrated in early studies concerning the origin of the oxygen atom in methanol, which was believed to be derived from molecular oxygen (Leadbetter and Foster, 1959). This was conclusively proven by the incorporation of one atom from $^{18}O_2$ into methanol by *Pseudomonas methanica* and *Methanomonas methanooxidans* cells confirming that the oxygen atom originated from molecular oxygen not water (Higgins and Quayle, 1970).

The first report of methane-oxidising activity in a methanotroph was in cell-free particulate preparations from *Methylococcus capsulatus* (Texas) cells by Ribbons and Michalover (1970). The fraction was found to consist of extensive intracytoplasmic membranes. The methane-stimulated NADH oxidising system gave a stoichiometric relationship of oxygen and NADH consumption, that was proportional to the uptake of methane supplied (Ribbons, 1975). This indicated that a monooxygenase enzyme was involved in methane oxidation. Ribbons and Michalover (1970) also speculated on the similarity of the methane-oxidising system with the ammonia-oxidising system from *Nitrobacter europaea* and *Nitrocystis oceanus*.

Similar results were obtained by Ferenci using cell-free particulate preparations of *Pseudomonas* (now *Methylomonas*) *methanica* (Ferenci, 1974; Ferenci *et al.* 1975). The particulate fraction was also found to catalyse the oxygen and NAD(P)H-dependent disappearance of bromomethane in a stoichiometric relationship (Colby *et al.*, 1975). Comparisons with the inhibitor profile obtained for the methane oxidising system from *Methylosinus trichosporium* OB3b cells (Hubley *et al.* 1975), indicated that the enzyme that catalysed bromomethane disappearance *in vitro* was also the enzyme that catalysed methane oxidation *in vivo*.

The first report on methanol accumulation from methane was in particulate extracts from *Methylosinus trichosporium* OB3b (Tonge *et al.*, 1975). 150mM phosphate buffer was use to inhibit methanol oxidase activity which could interfere in the methanol production measurements. Values obtained for NADH and oxygen consumption were high compared to the uptake of methane utilisation and methanol

formation indicating that the stoichiometry was not consistent with a reaction catalysed by a monooxygenase. However, it was suggested that the stoichiometry would be consistent if methane caused redirection of the electron flow from oxygenation to the methane oxygenase system (Higgins *et al.*, 1976).

1.8.1 Location of the methane monooxygenase

Early reports suggested that the methane monooxygenase could exist in different intracellular locations in the cells from various methanotrophs. Stirling and Dalton (1979) obtained a soluble version of MMO from *Methylosinus trichosporium* OB3b, which was previously thought to be located in the particulate fraction, and was found to be similar to the enzyme from *Methylococcus capsulatus* (Bath). The soluble MMO from *Methylosinus trichosporium* OB3b was found to exist under defined growth conditions i.e. under methane or nitrate-limited growth conditions (Scott *et al.*, 1981a and b). During oxygen-limiting conditions the presence of intracytoplasmic membranes and the particulate form of the enzyme were observed. However, when oxygen limitation conditions were used by Stirling and Dalton (1979) only the soluble MMO was observed suggesting that regulation of the intracellular location of the MMO was due to some other factor.

Dalton *et al.* (1984) noted that soluble extracts from *Methylococcus capsulatus* (Bath) cells that had been cultured in small shake flask cultures, did not have MMO activity. However, when these cells were transferred into a 100-litre fermenter for growth, the resulting MMO activity was again detected in the soluble fraction. On further examination, it was discovered that at biomass concentrations of <0.8g/l, MMO activity was entirely located in the particulate fraction. Above this biomass concentration, MMO activity was increasingly located in the soluble fraction until at 1.6g/l, when the MMO was located entirely in the soluble fraction. This demonstrated that the intracellular switch for MMO location is related to biomass concentrations of the cell culture. In addition to this, when the copper concentrations were increased from 0.2mg/ml to 1.2mg/ml in a 15-litre batch culture MMO activity was again observed in the particulate fraction of the cell extracts at low biomass concentrations. The soluble MMO activity was not detected until the biomass concentration reached

1.4g/l dry weight. This led to the proposal that the cellular location of MMO was dependent on the concentration of copper in the growth medium. This was confirmed by the observation that in steady state cultures grown under low copper : biomass conditions, the soluble form (sMMO) was expressed and at high copper : biomass conditions, the particulate or membrane-associated form (pMMO) was expressed (Stanley *et al.*, 1983, Prior and Dalton, 1985).

1.9 Regulation of MMO gene expression

In methanotrophs which possess both pMMO and sMMO enzyme systems, e.g. *Methylococcus capsulatus* (Bath) and *Methylosinus trichosporium* OB3b, copper is believed to regulate MMO expression by a unique 'copper switch'. The exact mechanism of this switch is not known, although recent advances in the molecular biology of both methane monooxygenases have given us a clearer insight into the regulation of MMO expression by copper ions.

1.9.1 Molecular biology of soluble MMO (sMMO)

The genes encoding the soluble MMO have been cloned and sequenced from several methanotrophs including *Methylococcus capsulatus* (Bath) (Murrell, 1993 and 1994). Northern blotting and primer extension analysis using *Methylococcus capsulatus* (Bath) showed that the six open reading frames (ORFs) of the sMMO gene cluster are organised as an operon. The sMMO gene cluster (Figure 1.5) consists of the *mmo*X, *mmo*Y and *mmo*Z genes, which encode the α, β and γ subunits of the hydroxylase respectively. An open reading frame (ORF) *orf* Y, separates *mmo* Y and *mmo*Z and has no known function. The *mmo*B and *mmo*C genes encode protein B and C respectively. Transcription of the sMMO genes was only observed under low copper : biomass conditions (Neilsen *et al.*, 1996a). Primer extension analysis identified a σ^{54}-like promoter immediately upstream of the *mmo*X transcription start site in *Methylosinus trichosporium* OB3b.

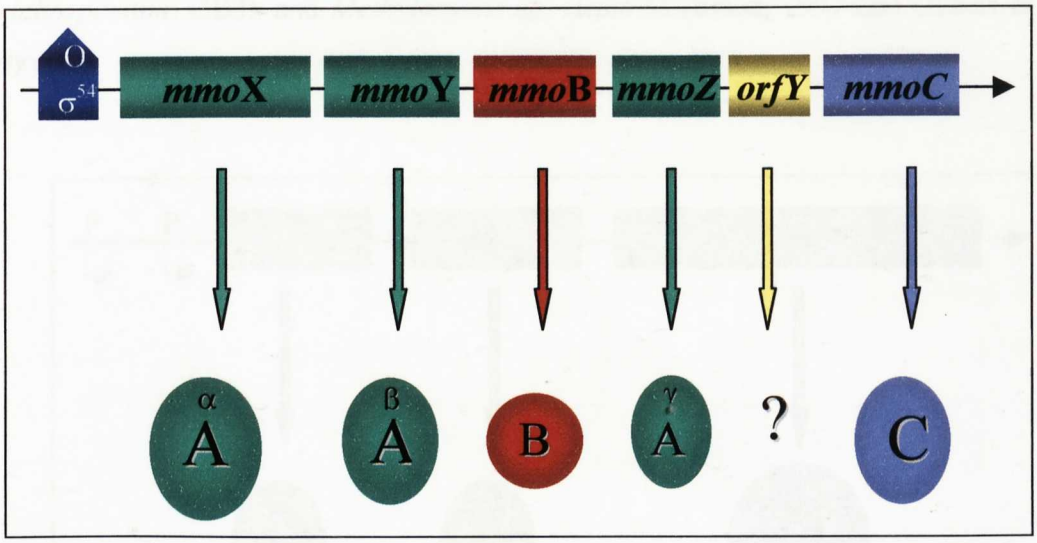

Figure 1.5 Schematic diagram depicting the soluble methane monooxygenase gene cluster and the corresponding expression of the sMMO subunits, Protein A (α,β,γ), B and C.

1.9.2 Molecular biology of pMMO

The *pmo*A and *pmo*B genes, which encode the β (27kDa) and α (46kDa) 'switchover' polypeptides of pMMO subunits respectively, were sequenced and cloned from *Methylococcus capsulatus* (Bath) (Semrau *et al.*, 1995a). An oligonucleotide probe, designed from the N-terminal sequencing of the putative 46kDa polypeptide of pMMO, was hybridised to the chromosomal DNA digest from *Methylococcus capsulatus* (Bath). A 2.1kb region of DNA was identified and was found to contain both the *pmo*A and the *pmo*B genes. A third open reading frame, designated *pmo*C which encodes the γ (25kDa) protein of pMMO was also sequenced (Costello *et. al.*, 1995; Stolyar *et al.*, 1999). There are two virtually identical copies of the genes encoding pMMO (*pmo*CAB) in the chromosome of *Methylosinus capsulatus* (Bath) and a third, separate copy of *pmo*C has also been identified (Semrau *et al.*, 1995a; Costello *et. al.*, 1995; Stolyar *et al.*, 1999).

The open reading frames for the *pmo*CAB genes are contiguous on the chromosome of *Methylococcus capsulatus* (Bath) (Figure 1.6) and are transcribed into the same mRNA. Smaller transcripts of individual genes have also been detected and gene specific probing indicated the presence of a transcript encoding *pmo*CA (Nielsen *et al.*, 1996b). The *pmo* genes have also been cloned and sequenced from *Methylosinus*

trichosporium, OB3b and *Methylocystis sp.* strain M (Finch, 1997 and Gilbert *et al.*, 2000).

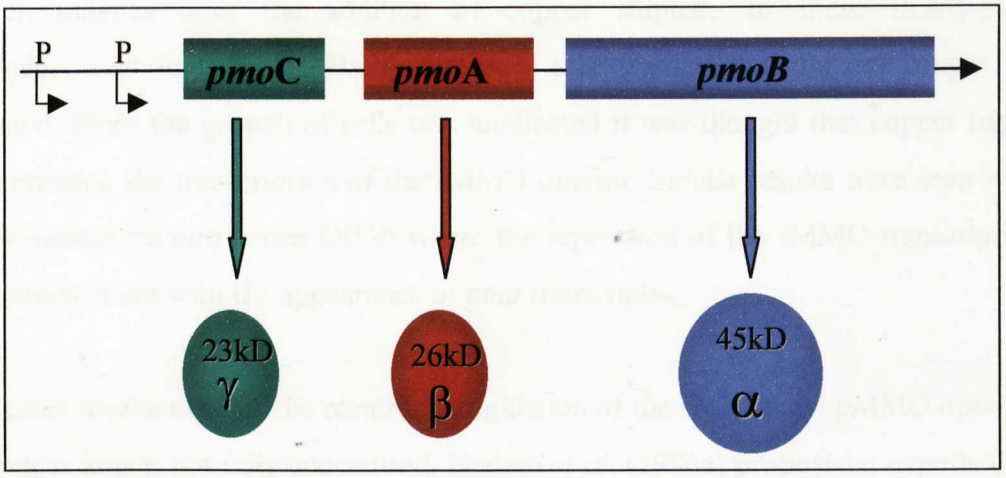

Figure 1.6 Schematic diagram of the *pmo* gene cluster from *Methylococcus capsulatus* (Bath) and the corresponding pMMO hydroxylase subunits (α, β and γ) expressed. P = Putative promoters.

The presence of multiple gene copies has also been observed encoding the analogous enzyme, ammonia monooxygenase (AMO) (Sayavedra-Soto *et al.*, 1996). A comparative study was carried out on *pmo* and *amo* genes from various methanotrophs and nitrifiers from α,β,γ subdivisions of Proteobacteria. Degenerate oligonucleotide primers, designed from homologous regions of *pmoA* and *amoA* sequences were used to amplify *pmo* and *amo* gene sequences. Analysis revealed strong conservation between the sequences. The *amoA* from *Nitrosococcus oceanus* showed higher identity to *pmo*A sequences from other γ-Proteobacteria than sequences of *amo*A. This provided evidence that pMMO and AMO are evolutionarily related despite their different roles in methanotrophs and ammonia-oxidising bacteria (Holmes *et al.*, 1995; Murrell and Holmes, 1996).

1.9.3 Models of the 'copper switch' mechanism

Neilsen *et al.* (1996) identified a 5.5kb transcript in copper-depleted *Methylococcus capsulatus* (Bath) cultures, which was thought to encode the entire sMMO operon. Fifteen minutes after the addition of copper sulphate to these steady-state *Methylococcus capsulatus* (Bath) cultures, this transcript could no longer be detected. Since the growth of cells was unaffected it was thought that copper might be repressing the transcription of the sMMO operon. Similar results were seen with *Methylosinus trichosporium* OB3b where the repression of the sMMO transcription was concomitant with the appearance of *pmo* transcripts.

The exact mechanism for the reciprocal regulation of the sMMO and pMMO operons by copper ions is not fully understood. Neilsen *et al.* (1996a) proposed a hypothetical classic repressor model for the possible role of copper in the transcriptional regulation of the *smmo* gene cluster (Figure 1.7). At high copper growth conditions, the transcriptional regulator protein binds Cu^{2+} ions causing a conformational change and allowing it to bind to the operator regions on the promoter, which in turn blocks the transcription of the *smmo* genes.

Murrell *et al.* (2000) proposed a number of models for reciprocal regulation of the *pmo* and *smmo* operons. One probable model involves the positive control of sMMO gene regulation, where Cu^{2+} binds and inactivates an 'activator protein'. This model is preferred as there is evidence to suggest that all known σ^{54} promoters rely on activator proteins for transcription (Wösten, 1998).

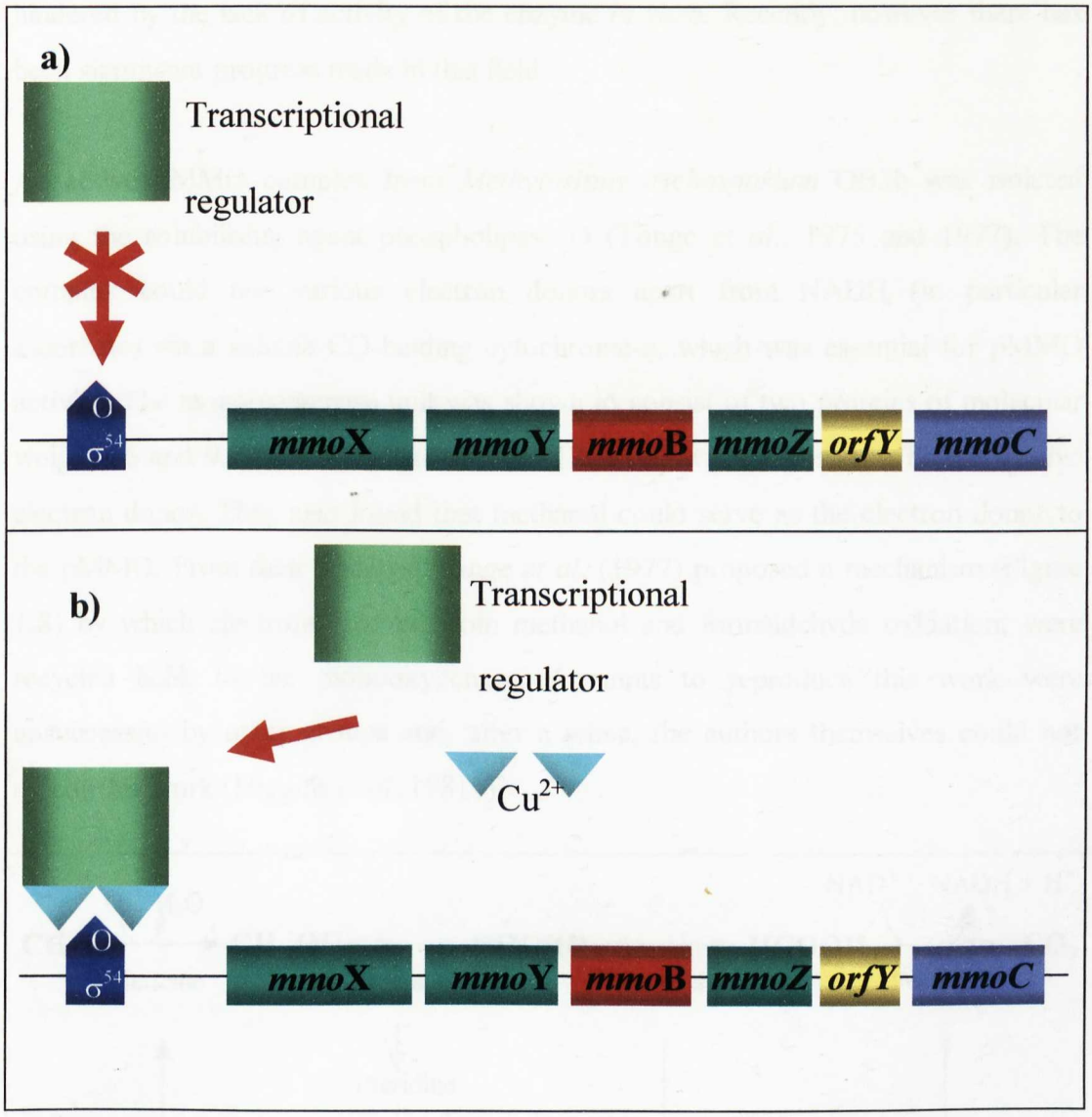

Figure 1.7 Model proposed for reciprocal transcription of the *smmo* operon. (Adapted from Charlton, 1997). In the absence of copper the transcriptional regulator is not able to bind to the operator sequence (O) of the σ^{54} promoter and the RNA polymerase transcribes the *smmo* operon. In the presence of copper, the transcriptional regulator binds to the operator sequence of the promoter and the transcription of *smmo* genes is repressed.

1.10 Isolation of the particulate methane monooxygenase

The purification of the particulate methane monooxygenase (pMMO) has been hindered by the lack of activity of the enzyme *in vitro*. Recently, however there has been significant progress made in this field.

An active pMMO complex from *Methylosinus trichosporium* OB3b was isolated using the solubilising agent phospholipase D (Tonge *et al.*, 1975 and 1977). The complex could use various electron donors apart from NADH (in particular ascorbate) via a soluble CO-binding cytochrome-*c*, which was essential for pMMO activity. The monooxygenase unit was shown to consist of two proteins of molecular weight 46 and 9.4kDa. The cytochrome (12.5kDa) was proposed to be the *in vivo* electron donor. They also found that methanol could serve as the electron donor to the pMMO. From their findings, Tonge *et al.* (1977) proposed a mechanism (Figure 1.8) by which electrons derived from methanol and formaldehyde oxidation, were recycled back to the monooxygenase. Attempts to reproduce this work were unsuccessful by other groups and, after a while, the authors themselves could not repeat this work (Higgins *et al*, 1981b).

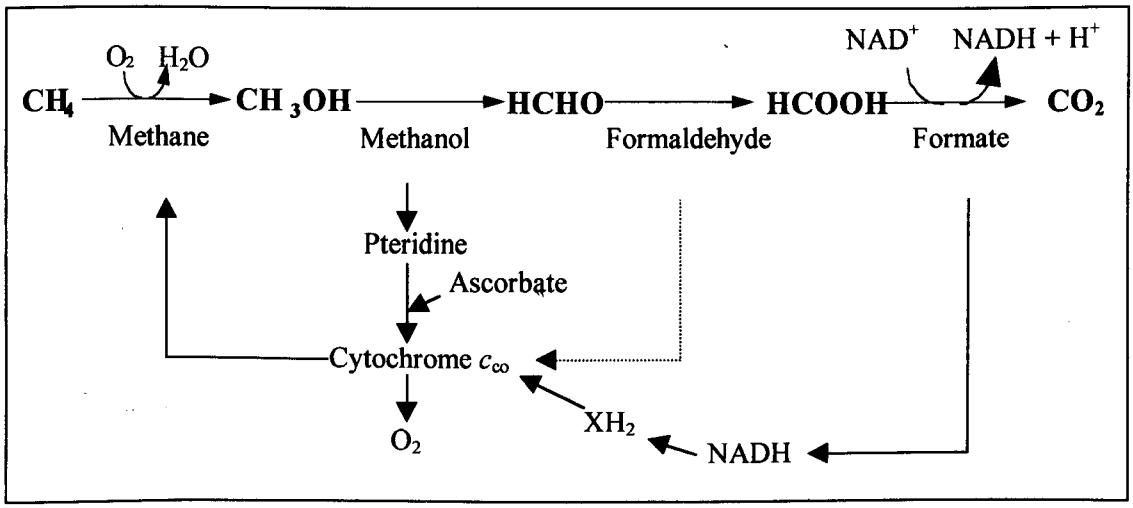

Figure 1.8 Tentative mechanism for methane oxidation adapted from Tonge *et al.* (1975). Electrons derived from methanol and formaldehyde oxidation are recycled in to the methane oxygenation reaction via the immediate physiological electron donor, the CO-binding cytochrome-*c*, which is reduced in turn by methanol dehydrogenase.

Gvozdev and coworkers (1984) solubilised a pMMO complex from *Methylococcus capsulatus* (Strain M) using the detergent sodium deoxycholate. They proposed that upon solubilisation an inhibitor was released, which could inactivate the enzyme. This could be overcome if the solubilisation was carried out in the presence of hydroxyapatite since the inhibitor preferentially reacted with the adsorbent. They then went on to purify a complex by ion exchange chromatography (Akent'eva and Gvozdev, 1988). The complex was found to be composed of a monooxygenase component and an NADH oxidoreductase and had a specific activity of 3600nmoles/min/mg based on the disappearance of methane.

Smith and Dalton (1989) were the first to attempt a detailed purification of the pMMO from *Methylococcus capsulatus* (Bath). In their studies they used the non-ionic detergent dodecyl-β-D-maltoside to solubilise the enzyme system at a detergent: protein ratio of 0.5. No activity was detectable in the directly solubilised fraction using a variety of electron donors including NADH and ascorbate. However, removal of the detergent using Bio-Beads SM2 and addition of the egg or soya bean lecithin restored enzyme activity. Attempts to further purify the solubilised MMO were unsuccessful and resulted in inactivation of the enzyme. The enzyme was found to consist of the polypeptides 49, 23 and 22kDa. The loss of enzyme activity on solubilisation was proposed to be due to the detergent-induced disruption of the electron transport chain from NADH to the pMMO.

Shiemke *et al.* (1995) published details of a reproducible method for the solubilisation of pMMO from *Methylococcus capsulatus* (Bath) based on the earlier work of Smith and Dalton (1989). In this study, a variety of reductants were tested for their ability to donate electrons to solubilised pMMO. Various quinols, in particular the plastoquinol analogues, duroquinol and decyl-plastoquinol (Figure 1.9) were found to be most effective, whereas ubiquinone analogues were ineffective as electron donors to pMMO. They found that a detergent : protein ratio of 1.7 was optimal for solubilisation of an active pMMO.

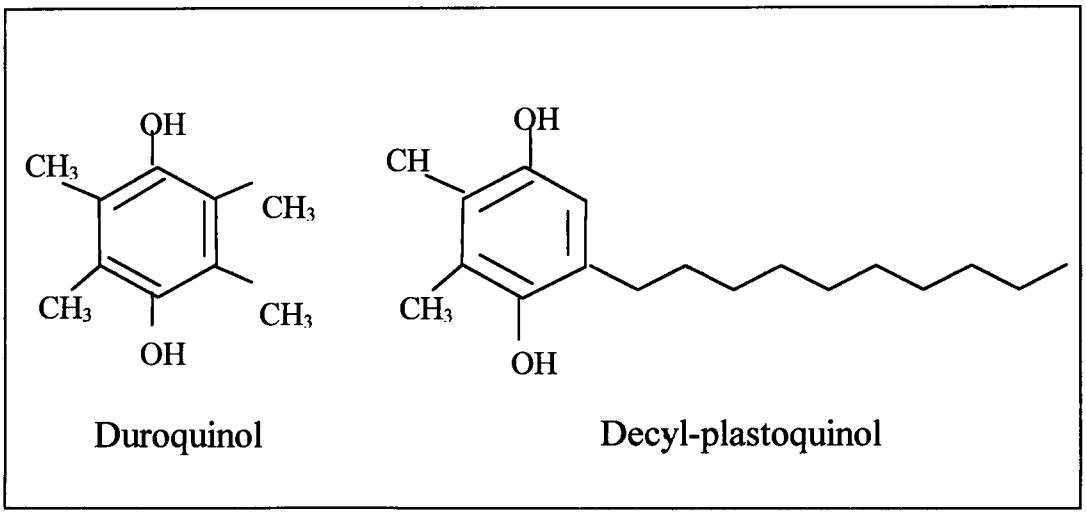

Figure 1.9 Structures of the plastoquinol analogues duroquinol and decyl-plastoquinol

The ability of plastoquinol analogues to serve as reductants for pMMO electrons was proposed to be due to their similarity in structure and redox potential to the *in vivo* electron donor, which was not identified in their study. In whole cells of *Nitrosomonas europaea* (Shears and Wood, 1986) quinols could act as reductants to the analogous enzyme, ammonia monooxygenase. The rate of reduction of the endogenous quinone pool was inversely proportional to the redox potential of the exogenous quinol. No such correlation was observed with pMMO indicating that it was unlikely that the quinols were interacting with pMMO via an endogenous quinone pool, which would have been depleted in solubilised extracts anyway. Shiemke and coworkers (1995) proposed that the quinol was interacting directly with the pMMO or a pMMO reductase closely associated with pMMO.

Shiemke and co-workers (Cook and Shiemke, 1997) also observed that the addition of catalytic amounts of exogenous quinones in solubilised extracts could restore the role of NADH as a reductant to pMMO. This indicated that an NADH:quinone oxidoreductase might be involved in the reduction of pMMO by NADH *in vivo*. They also claimed to have purified small amounts of a NADH:quinone oxidoreductase (36kDa) which was thought to mediate this reaction, although there have been no subsequent reports on the isolation of this enzyme.

The pMMO from *Methylococcus capsulatus* (Bath) was purified using anion exchange and hydrophobic interaction chromatography columns under anaerobic conditions (Zahn and DiSpirito, 1996). The anaerobic conditions were necessary to maintain enzyme activity. *Methylococcus capsulatus* (Bath) were grown with high copper and high iron concentrations in the growth medium to achieve optimal cell-free pMMO activity. The pMMO was solubilised using dodecyl-β-D-maltoside and duroquinol was used as the reductant in propylene oxidising activity assays.

The enzyme consisted of three polypeptides of molecular masses 46, 27 and 25kDa and contained 14.5 copper and 2.5 iron atoms per 99kDa of enzyme. The enzyme had a specific activity of approximately 11 nmoles/min/mg. The 47 and 27kDa switchover polypeptides were isolated after Triton X-100 or CHAPS solubilisation, using a sucrose gradient and were found to contain one nonhaem atom, one copper atom and one acid-labile sulphur. Two contaminating polypeptides (37 and 20kDa) that co-purified with the pMMO were identified as cytochrome *b*-559/569. Efforts to remove these polypeptides resulted in a total loss of activity. They also observed copper binding cofactors (CBCs) of molecular mass 618Da, associated with the pMMO, which were believed to have a role in sequestering copper. A model was proposed based on these findings (Figure 1.10).

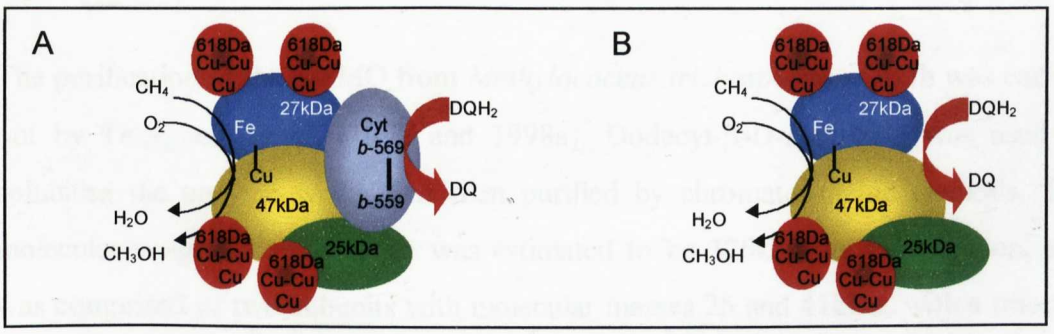

Figure 1.10 Proposed mechanism of methane oxidation by pMMO. Using duroquinol as a reductant with (A) cytochrome *b*-559/569 as the initial electron donor and with (B) duroquinol oxidised directly by the pMMO. (adapted from Zahn and DiSpirito, 1996)

Recently, Nguyen *et al.* (1998) published protocols to purify the pMMO hydroxylase from *Methylococcus capsulatus* (Bath) using either ion exchange or affinity chromatography under anaerobic and partially anaerobic conditions. Cultivation of *Methylococcus capsulatus* (Bath) cells was optimised to obtain maximal pMMO activities. The enzyme was solubilised using dodecyl-β-D-maltoside and NADH was used as the reductant in activity assays. The purified enzyme had specific activities of 2-5 nmoles propylene oxide produced/min/mg. The hydroxylase was composed of subunits of molecular mass 46, 26 and 23kDa, designated α, β and γ respectively. In addition to this they also found a proteolytically-cleaved version of the enzyme α', with a molecular mass of 35kDa. Metal analysis of the pMMO showed it had approximately 12-15 copper ions per 94kDa monomeric unit but no iron was detected in these preparations.

Nguyen *et al.* (1998) proposed that a pMMO reductase must exist since NADH is a two electron donor and each copper is a one electron acceptor. Therefore a mediator would be required to pass electrons one at a time to the recipient pMMO. They also claim to have purified an NADH-oxidoreductase, which can be added back to the purified pMMO to enhance NADH-linked activity (Nguyen *et al.*, 1998). As yet, details for the purification of the NADH-oxidoreductase have not been published.

The purification of the pMMO from *Methylococcus trichosporium* OB3b was carried out by Takeguchi *et al.* (1997 and 1998a). Dodecyl-β-D-maltoside was used to solubilise the enzyme which was then purified by chromatographic methods. The molecular weight of the enzyme was estimated to be 326kDa by gel filtration, and was comprised of two subunits with molecular masses 25 and 41kDa, with a trace of a contaminating polypeptide (26kDa). The enzyme was found to contain 0.9 iron atoms and 12.8 copper atoms per molecule.

1.11 Properties of the pMMO

1.11.1 Substrate analysis of the pMMO

Smith and Dalton (1989) performed substrate analysis studies on pMMO-containing membranes and solubilised pMMO from *Methylococcus capsulatus* (Bath). They found that *n*-alkanes up to and including butane were oxidised efficiently with a preference for hydroxylation at the C-2 position.

The epoxidation of substrates, such as propylene and butene, was also observed. Epoxidation of propylene gave only propylene oxide as a product and this reaction is currently used as a standard activity assay for MMO. The epoxidation and oxidation of 1-butene was observed, resulting in the formation of 3-buten-2-ol. Both but-2-ene isomers were oxidised by the pMMO. The *cis*-but-2-ene underwent an epoxidation reaction whereas the *trans*-but-2-ene underwent an epoxidation reaction as well as terminal oxidation yielding a crotyl alcohol. This is in contrast to the findings of Nguyen *et al.* (1996a) where only the epoxidation reaction was observed for both the but-2-ene isomers in pMMO-containing membranes from *Methylococcus capsulatus* (Bath). Nguyen *et al.*, (1996a) also found that propane was only oxidised to propan-2-ol, which is in contrast to the findings of Smith and Dalton (1989) where both the propan-1-ol and propan-2-ol were produced.

Using stereochemical analysis, Nguyen *et al.*, (1996a) found that substrates of three carbons or higher were generally oxidised to (R)-2-alcohols with virtually no detectable primary alcohol product. This chiral distribution of products demonstrated that the pMMO exhibited regioselectivity.

1.11.2 Metal components associated with of pMMO

Electron paramagnetic resonance (EPR) investigations have been carried out on particulate MMO from various methanotrophs and are discussed here briefly and in more detail in Chapter 5 of this thesis. EPR spectroscopy is a useful technique for investigating the ligand environment of metals in a metalloprotein.

The most controversial EPR studies on pMMO were carried out by Chan and co-workers on pMMO-containing membranes and the purified enzyme (Chan *et al.*,

1993; Nguyen *et al.*, 1994, 1996a, 1996b, 1998). Although they observed a type-2 copper EPR signal in their pMMO samples, when pMMO was oxidised with ferricyanide, this signal gave rise to a broad isotropic signal which was proposed to be due to a trinuclear copper cluster. Subsequent analysis of the enzyme showed that the pMMO contained 15-21 copper ions arranged in 5-7 mixed-valence trinuclear copper clusters. They postulated that these trinuclear copper clusters could be classified into groups according to their role in catalysis (C-clusters) and electron transfer (E-clusters). The 2-3 C-clusters were proposed to function as the catalytic core of the enzyme and the 3-4 E-clusters were presumed to be the source of endogenous reducing equivalents (Nguyen *et al.*, 1996b).

Zahn and DiSpirito (1996) presented an alternative model in which the enzyme involves both iron and copper. Their EPR spectra were consistent for a type 2 copper centre but also gave a weak high spin iron signal (g=6.0) and a broad low field signal at g=12.5. The low-field signal is typical for a protein containing a diferric cluster e.g. soluble methane monooxygenase although DiSpirito and coworkers dispute this. Zahn and DiSpirito (1996) also suggest that the loosely bound copper ions associated with copper binding cofactors (CBCs) may be responsible for the broad isotropic signal observed by Chan and coworkers.

Similar findings of a trinuclear copper cluster model for pMMO has only been reported for the enzyme from *Methylosinus trichosporium* OB3b (Takeguchi *et al.*, 1997 and 1999). Takeguchi and coworkers (1997, 1998 and 1999) also suggested the existence of two classes of trinuclear copper clusters with similar roles as previously proposed by Chan and coworkers. However, a high spin iron signal was also observed, which was proposed to originate from the active site of pMMO, since when duroquinol or acetylene were added to the pMMO sample, the high spin iron signal decreased.

Antholine and coworkers (Yuan *et al.*, 1997, 1998a and b, 1999; Lemos *et al.*, 2000) carried out X-band and S-band EPR studies on whole cells and membranes from *Methylococcus capsulatus* (Bath) and *Methylomicrobium albus* BG8, which were grown in media enriched with ^{63}Cu and ^{15}N. They concluded that their S-band EPR

spectra unambiguously established that there was one cupric ion co-ordinated to four nitrogen donor atoms i.e. a type 2 copper.

1.11.3 Active site of pMMO

The 47kDa and 27kDa polypeptides are believed to be the polypeptides expressed when the cells switch from soluble MMO expression to particulate MMO and are known as the 'switchover polypeptides'. Studies have been carried out on the pMMO from *Methylococcus capsulatus* (Bath) using radio-labelled acetylene, which is a suicide substrate of pMMO as it binds irreversibly to the active site of pMMO thus inactivating it (Prior and Dalton, 1985b). The resultant banding patterns were analysed by SDS-PAGE and fluorography and showed that the ^{14}C-acetylene bound irreversibly to the 26kDa polypeptide of pMMO, which was therefore proposed to contain the active site. This phenomenon has been observed in both soluble and particulate MMO from other methanotrophs (DiSpirito *et al.*, 1992) and ammonia monooxygenase (AMO) from nitrifiers e.g. *Nitrosomonas europaea* (Hynes and Knowles, 1982). However, recent studies by Zahn and DiSpirito (1996) demonstrated that the 47kDa subunit of pMMO from *Methylococcus capsulatus* (Bath) was also labelled by ^{14}C-acetylene and was thought to be due to the increased sensitivity of the phosphorescence image technique over fluorograms. Similar findings were also observed in ammonia monooxygenase of the *Nitrosomonas europaea* (Hyman and Arp, 1992)

The 47kDa α subunit and 27kDa β subunit contain six and five histidine residues respectively in their protein sequences (Semrau *et al.*, 1995). Seven of these histidines are conserved when compared to the protein sequence of ammonia monooxygenase from *Nitrosomonas europaea* (Bergmann and Hooper, 1994; McTavish *et al.*, 1993). This indicates that they may have an important role i.e. in copper ligation. This is in agreement with the findings of Elliot *et al.* (1998), who performed pulsed EPR studies on pMMO membrane samples from *Methylococcus capsulatus* (Bath). Their data supported histidine ligation to EPR-detectable copper and the copper sites were proposed to be in the 27kDa β subunit involving the His38, His40 and/or His168 at the membrane-periplasmic interface.

However, Yuan *et al.* (1999) proposed that the α subunit of pMMO contained a potential type 2 site for Cu^{2+} as it had a conserved histidine (His33) as the amino-terminal residue after the putative leader sequence. Therefore, they used a synthetic amino acid fragment designed from the first twenty amino acids of the amino terminal of the α subunit of pMMO from *Methylococcus capsulatus* (Bath). When copper ions were added to the synthetic peptide, EPR signals similar to those usually associated with the pMMO were observed. They suggested that the amino-terminal end in the α subunit would be a good bidentate chelator, as depicted in Figure 1.11, and if the 47kDa subunit existed as a dimer, the cupric ion could stabilise the dimer by coordination with four approximately equivalent nitrogen donor atoms.

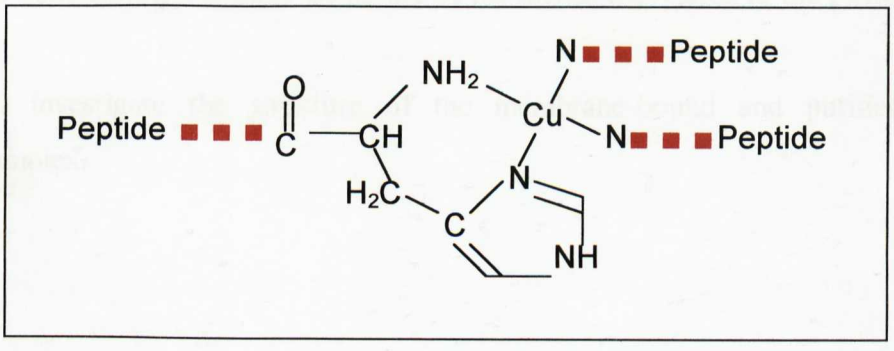

Figure 1.11 Schematic diagram for the binding of cupric ion to the amino-terminal sequence for which histidine is the first amino acid (adapted from Yuan *et al.*, 1999). Nitrogen donor atoms from the imidazole of histidines provide the third and fourth nitrogen donor atoms. Alternatively, another bidentate amino-terminal histidine of another α subunit could complete the square planar configuration resulting in the formation of *cis* and *trans* dimers.

1.12 Scope of this thesis

Although there has been significant progress in the elucidation of the particulate methane monooxygenase (pMMO) from *Methylococcus capsulatus* (Bath) the recent reports by Zahn and DiSpirito (1996) and Nguyen et al. (1998) have given rise to some confusion in this field. Therefore, the aims of this PhD project were:

1) To develop a reproducible method for the isolation of the pMMO to obtain a high specific activity enzyme.

2) To undertake basic characterisation of the pMMO.

3) To conclusively establish the nature of the metals associated to the pMMO.

4) To investigate the structure of the membrane-bound and purified pMMO complex.

2. Materials and Methods

2.1 Chemicals and Biochemicals

All chemicals were of analytical grade and obtained from BDH Chemicals Ltd., Dorset, UK; Boehringer Mannheim UK (Diagnostics and Biochemicals) Ltd., East Sussex, UK; Sigma-Aldrich Chemical Company Ltd., Dorset, UK. Dodecyl-β-D-maltoside was of Ultrol grade and was purchased from Calbiochem (California, USA). Argon, hydrogen, methane/carbon dioxide and nitrogen were of technical grade and obtained from Linde Gas Ltd., Stoke on Trent, UK.

2.2 Methanotroph

Methanotroph strains	**Class**
Methylomicrobium album BG8	Type I
Methylosinus trichosporium OB3b	Type II
Methylococcus capsulatus (Bath)	Type X

All methanotrophs were obtained from the University of Warwick culture collection.

2.3 Growth and maintenance of micro-organisms

All media were made using distilled water and autoclaved for 20 minutes at 121°C and 15 lb/in^2. Volumes greater than 5 litres were sterilised by autoclaving for 60 minutes at 121°C and 15lb/in^{2}and were allowed to cool overnight. Heat labile solutions were sterilised using 0.2μm pore-size disposable sterile filter units (Millipore, Watford, UK).

2.3.1 Culturing Methanotrophs

Methanotrophs were grown in Nitrate Minimal Salts (NMS) medium (Whittenbury *et al.*, 1970). The constituents of the stock solutions are given in Table 2.1

NMS	$MgSO_4$	1 g l^{-1}
	KNO_3	1 g l^{-1}
	$CaCl.2H_2O$	0.2 g l^{-1}
	*Trace element solution	1 ml l^{-1}
	$NaMoO_4.2H_2O$	0.5 mg l^{-1}
	FeEDTA	3.8 mg l^{-1}
	CuEDTA can also been used to replace FeEDTA	
***Trace element**		
	$FeSO_4.5H_2O$	0.5 g l^{-1}
	$ZnSO_4.7H_2O$	0.4 g l^{-1}
	H_3BO_3	0.015 g l^{-1}
	$CoCl_3.6H_2O$	0.05 g l^{-1}
	Na_2EDTA	0.25 g l^{-1}
	$MnCl_2.4H_2O$	0.02 g l^{-1}
	$NiCl_2.6H_2O$	0.01 g l^{-1}
	$CuSO_4.5H_2O$	0.5/1.5 g l^{-1}
Phosphate buffer	KH_2PO_4	26 g $litre^{-1}$
	$NaHPO_4.12H_2O$	71.6 g $litre^{-1}$

Table 2.1 Constituents of the stock solutions of NMS media.

The higher concentration of copper sulphate (1.5gl^{-1}) was used in the trace elements solution when particulate methane monooxygenase expressing cells were grown. This was added to the media after autoclaving. For preparation of sterile solid NMS, 2 % (w/v) Bacto-agar (Difco) was added to the basic NMS medium prior to sterilisation. With both types of media, phosphate was autoclaved separately to avoid precipitation and added to the NMS media after cooling.

2.3.2 Maintenance of Methanotrophs

Cultures of methanotrophs were maintained on NMS agar plates as described by Whittenbury and Dalton (1981). Culture plates were placed in plastic Tupperware™ boxes, gassed with methane/carbon dioxide mixture, sealed and incubated at 30°C for *Methylosinus trichosporium,* OB3b or 45°C for e.g. *Methylococcus capsulatus* (Bath) for 3-5 days.

Small-scale growth of methanotrophs was carried out in 250ml 'Quickfit flasks' (Fisher Scientific UK Ltd) containing 50ml of NMS medium. Flasks were inoculated with a single colony of the methanotroph of choice and aseptically sealed with rubber suber-seals (W.H. Freeman, Barnsley, UK). 60ml of air was removed from the flask and 60ml of methane/CO_2 mixture (95% and 5%, v/v, respectively) was injected. Cultures were incubated for 3-5 days, shaking at 200rpm, at 30°C or 45°C.

2.3.2.1 Continuous fermentation of methanotrophs

500ml of a starting culture was used to inoculate the fermenter (LH 2000 or LH 210 series fermenter, L.H. Engineering). When the culture had reached an OD_{550} of 6, a steady state was maintained by automatic addition of media and simultaneous overflow of cultures into a 20 litre vessel. Working volumes of between 2-4 litres of media with a dilution rate of 0.05 hr^{-1} were used. Methane (20 %, v/v, in air) was supplied as the sole carbon source. The culture was grown at the appropriate temperature and maintained at a neutral pH.

Cells were harvested from the 20 litre overflow vessel by centrifugation at 3000 x g in a Westfalia continuous centrifuge (Westfalia Separator Ltd, Milton Keynes, UK). Harvested cells were resuspended in the appropriate buffer.

2.3.2.2 Batch growth of *Methylococcus capsulatus* (Bath)

Large-scale batch growth of *Methylococcus capsulatus* (Bath) was performed in a 100 litres fermenter (LH Engineering Ltd, UK). NMS medium was supplemented with an additional 1.0 g $litre^{-1}$ KNO_3 to prevent cells from becoming nitrate limited during the later stages of growth (Charlton, 1997). The fermenter was inoculated with 10 litres of a continuous culture overflow. Methane was provided as a

methane/air mixture (20%, v/v, in air). Cells were harvested after an OD_{550} of 7 was obtained (for pMMO expressing cells) by centrifugation at 3000 x g in a Westfalia continuous centrifuge (Westfalia Separator Ltd, Milton Keynes, UK). Harvested cells were resuspended in the appropriate buffer.

2.3.2.3 Analysis of culture purity

Cultures of methanotrophs were routinely checked for purity by streaking on to nutrient agar (NA) plates (Sambrook *et al.*, 1989). Plates were incubated aerobically at 30°C for a couple of days. Growth of colonies on NA plates indicated contamination. Contamination was verified by phase contrast microscopy.

2.4. Preparation of cell free extracts

Particulate extracts were initially prepared as described by Charlton (1997). Modified procedures used in this study are described below and in Chapter 3.

2.4.1 Preparation of sMMO extracts

sMMO whole cells were harvested at 10,000 x g for 15min at 4°C. The cells were re-suspended in of 25 mM 3-[N-morpholino]propanesulfonic acid, sodium salt (MOPS) buffer pH7 containing 1mM benzamidine, 5mM D, L-dithiothreitol (DTT) and 5mM sodium thioglycollate. A few crystals of Deoxyribonuclease I (DNAse I) were added to the cells before passing them two times through a pre-cooled cell disrupter (Constant Systems Ltd., UK) at a pressure of 172 MPa. The resulting cell suspension was centrifuged at 38,000 x g for 45 minutes at 4°C. The supernatant was drop frozen and could then be stored at –80°C until further use.

2.4.2 pMMO extracts

Cells expressing pMMO were harvested by centrifugation at 10,000 x g for 15 minutes at 4°C and resuspended in 25mM Piperazine-N, N'-bis[2-ethanesulfonic acid, disodium salt] PIPES buffer, pH7.25. A few crystals of DNAse I and 1mM benzamidine were added to the cell suspension and the cells were then broken by two to three passes through a Constant cell disrupter at 172 MPa until a smooth paste was obtained. Unbroken cells and cell debris were removed by centrifugation at 10,000g for 30 minutes.

2.5 Isolation of intracytoplasmic membrane (ICMs)

Intracytoplasmic membranes (ICMs) were collected by centrifugation at 150,000 x g for 60-90 minutes (depending on volume) at 4°C and the pellet containing the ICMs was resuspended in 25mM Pipes, pH7.25, 0.5M NaCl and 1mM benzamidine. This process was repeated at least twice to remove soluble proteins until the supernatant was clear, before finally resuspending the pellet in 25mM Pipes pH7.25, 0.5M NaCl and 1mM benzamidine. The membrane-bound pMMO extract ($pMMO^m$) was assayed for activity (Section 2.9.2) could then be drop frozen in liquid nitrogen and stored at -80°C until further use.

2.5.1 Sucrose gradient sedimentation

A 20-60% sucrose step gradient was prepared by making up the appropriate % solutions of sucrose in 10mM Pipes, pH7.25 (using a refractometer for accuracy). The solutions were then slowly layered into Beckman SW41Ti centrifuge tubes starting with a 60% sucrose cushion. 1ml of membrane sample (50mg/ml) was applied to the top of the gradient. The tubes were centrifuged for 14 hours at 38,000rpm at 4°C in a Beckman ultracentrifuge. Membrane fractions (gelatinous masses) were decanted slowly and assayed separately for enzyme activity using gas phase activity assays.

2.5.2 Triton separation of ICMs

For preferential solubilisation of inner membranes triton X-100 and X-114 (Sigma) were used (Fjellbirkeland *et al.*, 1997). This was carried out by resuspending the particulate extract (Section 2.4.2) in a working buffer containing 2% (v/v) Triton. The resulting suspension was stirred at room temperature for 1 hour, centrifuged at 100,000 x g for 1 hour and the soluble fraction containing ICMs was collected, assayed for activity and analysed by SDS-PAGE.

2.6 Solubilisation of ICMs

The particulate extract was thawed and assayed for activity. Extracts with high specific activities (>75nmoles of propylene oxide produced/min/mg of protein) and consisting of at least 60% of the polypeptides associated with pMMO (as analysed by SDS-PAGE) were used for the solubilisation stage. The extract was centrifuged at 150,000 x g for 30 minutes at 4°C. The pellet was resuspended in a freshly made

buffer of 25mM Pipes pH7.25, 0.5M NaCl and 1mM benzamidine. Copper sulphate was added to give a final concentration of 40μM.

Solubilisation was performed by adding the dissolved anionic detergent dodecyl-β-D-maltoside to give a detergent:protein ratio of 1.5, to the particulate extract. The detergent was added drop-wise, whilst stirring constantly on ice. The particulate extract was then left for 1hour on ice with continuous but gentle stirring. After this time the extract was then centrifuged at 150,000 x g for 90 minutes. The solubilised extract was assayed for propylene oxidising activity using duroquinol as the reductant and analysed by SDS-PAGE. Solubilised pMMO ($pMMO^{s}$) extracts were drop-frozen in liquid nitrogen and stored at -80°C until further use.

2.7 Purification methods

Fast Protein Liquid Chromatography (FPLC) equipment, columns and accessories used in this study were obtained from Amersham Pharmacia Biotech (St Albans, UK). Chromatographic procedures for protein purification were performed on a Pharmacia 'FPLC Basic' system, complete with two P-500 pumps, an LCC 500 programmable pump controller, a monitor UV-M detector system, and a FRAC-100 fraction collector. The media were packed into the Pharmacia XK columns. All FPLC columns were washed with two column volumes of degassed distilled water before equilibrating with the appropriate buffer before each purification run. Purification procedures were carried out as described by Zahn and DiSpirito (1996), Charlton, (1997) and Nguyen *et al.*, (1998) under anaerobic and aerobic conditions. When isolation was performed under anaerobic conditions the working buffers were firstly degassed, either 5mM dithionite or ascorbate was added and then the buffer was kept deoxygenated by constantly bubbling argon through the buffer. The buffers were tested for 'anaerobicity' using a solution of the indicator methyl viologen (Sigma).

The anion exchange chromatography media used was DEAE-Cellulose, DE52 and DEAE-Sepharose, CL-6B (Whatman). The hydrophobic interaction chromatography (HIC) media used in this study was Phenyl Sepharose High Performance or Phenyl Sepharose CL-4B (Amersham Pharmacia Biotech). Procedures were carried out as described by Zahn and DiSpirito (1996), Charlton (1997) and Nguyen *et al.* (1998). A

working buffer of 10mM Pipes, pH 7.25 was used with an increasing salt or detergent gradient to elute bound proteins from the column.

Lysine-Agarose (Sigma) affinity columns were used in this study in a procedure similar to that described by Nguyen *et al.* (1998). A salt gradient was used to elute bound proteins from the column.

Superdex 200 preparative grade (Amersham Pharmacia Biotech), either XK 26/600 (2.6 x 68cm) and XK 16/200 (1.5 x 68cm), depending on the concentration of protein was used during purification. Calibration of the Superdex 200 for molecular weight estimation was carried out by equilibrating the column with 10mM Pipes, pH7.25 containing 0.01% dodecyl-β-D-maltoside. The molecular weight determination of pMMO was made by comparing the ratio of V_e/V_0 of pMMO with the ratio of V_e/V_0 of five proteins of known molecular mass (BIORAD calibration kit), where V_e is the elution volume and V_0 is the void volume of the column. The void volume was taken as the elution volume required for the elution of Blue Dextran (M_r 2000kDa) from the column. A calibration curve was prepared by plotting the logarithms of the known molecular weights of the protein standards against their V_e/V_0 values. The corresponding molecular mass could then deduced from the calibration curve by using the experimental V_e/V_0 of pMMO.

Protein samples were desalted using disposable PD10 or G25 columns desalting media (Amersham Pharmacia Biotech) under gravity feed. Elution volumes shown in typical FPLC traces are measured after the void volume of the column.

2.8 Isolation of the pMMO complex

Solubilised pMMO was concentrated using an Amicon stirred cell with XM50 filter (Amicon Corporation, Danvas, M.A.) to 20mg/ml (further concentration at this stage can lead to precipitation). The concentrated extract was then filtered through a 0.2μM Whatman syringe filter and applied to a pre-cooled (4°C) Superdex 200 column (1.5 x 68 cm) which was equilibrated in 25mM Pipes buffer, pH7.25 supplemented with 0.03% dodecyl-β-d-maltoside and 1mM benzamidine. The column was run at a flow rate of 1.5ml/min.

Fractions containing pMMOH were pooled from numerous S200 runs and finally concentrated using an Amicon stirred cell concentrator with an XM50 filter membrane to give >50mg/ml of protein. The protein was then re-applied to the S200 column. Fractions containing the pMMO were collected and concentrated using an Amicon stirred cell with a XM50 ultrafiltration. The sample could then be drop frozen in liquid nitrogen and stored at -80°C until further use. The sample could then be analysed by electron microscopy to ensure complex homogeneity.

2.8.1 Separation of components of the pMMO complex

A DEAE-cellulose, DE52 (Whatman) ion exchange column (1.5 x 15cm) was used to separate the components of the pMMO complex. Concentrated pMMO complex obtained from the S200 column (>15mg/ml) was then filtered through a 0.2 μM syringe filter and applied to a cooled (4°C) DE52 column which was equilibrated in 10mM Pipes buffer, pH7.25 supplemented with 0.01% dodecyl- β-D-maltoside and 1mM benzamidine. The flow rate of the column was 2ml/min. An increasing salt gradient was applied to elute bound proteins. Fractions corresponding to the hydroxylase and the reductase were collected and concentrated using an Amicon stirred cell with a PM10 ultrafiltration membrane

2.9 Enzyme activity assays

Methane monooxygenase (MMO) activity was assayed by following the oxidation of propylene to propylene oxide. The data in this study are the mean and standard error (as calculated using the package Microcal Origin, version 4.10) from at least two assays unless otherwise stated. Propylene oxide was measured using a Pye Unicam Series 104 gas chromatograph (Pye Unicam, Cambridge, UK) fitted with a Porapak Q column (4mm x 1m, Waters Associates, Milford. Massachusetts, USA). Nitrogen was the carrier gas with a flow rate ~ 30ml/min and oven temperatures of 150-200°C. This system was linked to a Hewlett-Packard 3390A integrator (Hewlett-Packard, Avondale, Pennsylvania, USA).

A 2mM standard of the appropriate product was used to calibrate the column. Either a 5μl liquid or 0.5ml of gas sample was injected into the gas chromatograph depending on which phase was being used in the experiment.

2.9.1 Whole cell MMO activity

Assays for whole cell activity were performed in 5ml flasks containing 1ml of an OD_{550} 20 cell suspension. The flask was sealed, 3ml of air was extracted and replaced with 4ml of propylene. The flask was then incubated in a 45°C water bath for 1 minute before 100mM sodium formate was added. The sample was injected onto the column at 3 minute intervals.

2.9.2 Cell-free extract MMO assays

MMO activity in cell-free extracts was determined using NADH (or occasionally duroquinol for particulate extracts) as the electron donor. Samples (10mg/ml) were placed in a 2ml vial containing the appropriate buffer (25mM MOPS buffer, pH7 for sMMO extracts and 10mM PIPES buffer, pH7.25 for the pMMO) in a final volume of 100ml. The flask was sealed and 0.5ml of air was replaced with 0.6ml of propylene. The flask was then incubated in a 45°C water bath for 1 minute before NADH was added to give a final concentration of 5mM. The 0.5ml of gas phase sample was injected onto the column.

2.9.3 Activity assays for $pMMO^s$ and $pMMO^c$ assays

The electron donor used in these assays was 5-25mM duroquinol. Duroquinol was dried onto the base of a 2ml vial. The protein sample and 10mM PIPES buffer, pH 7.25 was added to give a final volume in the vial was 100µl. 0.6ml of air was extracted from the vial and 1ml of propylene was injected into the vial. The reactions were supplemented with 50µM copper sulphate to give optimal activity. During kinetic analysis of pMMO appropriate volumes of methane were injected into the sample vial to obtain the desired final concentration of methane in the assay. A 0.5µl liquid phase sample was then injected onto the column and methanol production was measured. 0.5µl of a 2mM methanol standard was used for calibration.

2.9.4 Test for sMMO activity in whole cells

Whole cell activity of sMMO for batch and continuous fermentation cultures was assessed by following the oxidation of naphthalene. This assay was used routinely to determine whether *Methylococcus capsulatus* (Bath) cells were expressing sMMO or pMMO. 1ml of culture was incubated in 1.5ml Eppendorf tubes in the presence of a

small naphthalene crystal and agitated for 30 minutes at 30°C. 100 µl of a fresh 0.2 % (w/v) solution of tetrazotised-σ-dianisidine (TOD) was added to the sample. Formation of a purple diazo dye indicated the presence of naphthols, which indicated the presence of sMMO activity, since pMMO is unable to oxidise naphthalene.

2.9.5 Assay for methanol dehydrogenase

Methanol dehydrogenase (MDH) activity was measured spectrophotometrically at 45°C with phenazine ethosulphate (PES) and 2,6-dichlorophenolindophenol (DCPIP) as electron acceptors. The reaction mixture (total volume 500µl) contained 50 mM Tris-HCl buffer (pH 9.0), 0.1mM DCPIP, 15mM NH_4Cl, 10mM methanol, 5mM KCN and 500µg MDH. The reaction was started by the addition of 1.0 mM PES, and the decrease in absorbance of DCPIP at 600nm (ε = 1.91 M^{-1} cm^{-1}) was measured. One unit of MDH activity was defined as 1µmol DCPIP reduced per min per mg protein.

2.10 Analytical determinations

2.10.1 Estimation of protein concentration

Protein concentrations were estimated using a modified dye-binding method of Bradford (1976) using bovine serum albumin (BSA) as a standard. An alternative assay modified from that described by Lowry, 1977 was used which was more suitable for detergent containing samples. Both procedures were carried out using the BioRad Reagent and the Detergent compatible (Dc) Reagent (BioRad Ltd, Watford, Hertfordshire, and UK).

2.10.2 Estimation of metal content

Copper and iron metal content of samples were estimated using Inductively Coupled Plasma Emission Spectroscopy by Dr. Karen Sanders at the Warwick analytical centre, University of Warwick. Samples were prepared by acid washing in Nitric acid (Primar grade) as described by the Warwick analytical centre guidelines. A control sample of buffer alone was also prepared in the same way and values obtained for this control were subtracted for the experimental protein sample values.

2.10.3 Sedimentation equilibrium experiments

Sedimentation equilibrium experiments were carried out in collaboration with Dr. K. Jumel at NCMH, University of Nottingham. The pMMO complex and pMMO hydroxylase were analysed at a concentration of 5mg/ml in 20mM Pipes buffer, pH 7.2. Measurements were made using a Beckman Optima XL-A analytical ultra-centrifuge (Beckman Instruments Inc., Palo Alto, CA, USA) at a temperature of 4°C. Protein was prepared as described in Section 2.6.

Buffers containing D_2O/H_2O ratios between 0 and 50% were prepared, the protein was added to the appropriate buffer and samples were concentrated to give a final volume of 200µl. Buffer and detergent densities were measured at 4°C using a Precision Density Meter (Model 02C, Anton Paar, Graz, Austria).

Samples and their appropriate buffers were loaded into their respective channels in 12mm multichannel cells. Equilibrium runs were carried out on a Beckman XL-A analytical ultracentrifuge (Beckman, Palo Alto, CA) at a temperature of 4°C and speeds of 3,000, 6,000, and 9,000rpm for the pMMO complex and 10,000, 12,000 and 15,000rpm for the hydroxylase sample until equilibrium was achieved at each speed. Samples were prespeeded at 45,000rpm to obtain the baseline absorbance for each sample. Molecular weights for the proteins at each D_2O/H_2O ratio were obtained using the manufacturers software package (Beckman Instruments, Inc. Fullerton, CA 1993).

2.10.4 Electron microscopy

Electron microscopy studies were carried out in collaboration with Dr. A. Kitmitto and Dr. R. Ford at the University of Manchester, Institute of Science and Technology (UMIST). The $pMMO^m$ samples were pelleted and resuspended in 25mM Pipes buffer, pH 7.25 containing 100mM NaCl and 10mM EDTA. Membranes were diluted to protein concentrations of 100-150µg/ml. Samples were mounted onto colloidion-carbon coated 3000 mesh/inch copper grids and negatively stained using 4% uranyl acetate as described before and examined in a Phillips 400 transmission electron microscope operated at an accelerating voltage of 100keV. Micrographs were recorded at a calibrated magnification x 43,600 on Kodak electron microscope film

(ESTAR thick base 4489*). Electron micrographs were digitised (Zeiss SCAI scanner) resulting in a pixel size of 6.4Å at the specimen level.

SPIDER and WEB image processing packages were employed on an indigo-silicon graphics workstation. The image was first band pass-filtered. Particles were selected interactively using the program WEB, using reference–free alignment algorithm the particles were rotationally and translationally aligned. An average image was calculated from a sum of the aligned particles.. Correspondence analysis and hierarchical ascendant classification using complete linkage as a merging criterion was performed to separate out and average particles within in each group. The threshold level was determined by visual inspection of particles randomly selected from each group to check for agreement of particle orientation shape and size.

2.10.5 Electron Paramagnetic Resonance Spectroscopy

Electron paramagnetic resonance (EPR) spectroscopy studies were carried out in collaboration with Dr. B. Katterle and Professor K.Andersson at the University of Oslo, Norway. EPR spectra were recorded on a Bruker ESP300 instrument equipped with an helitram liquid helium set-up. Samples were prepared at the University of Warwick as described in Section 2.6. Samples were measured at approximately 10K for copper signal analysis and 4K for iron signal analysis. Protein concentration of extracts used in EPR experiments varied. Final sample volumes of 200µl were used and were frozen slowly in EPR tubes at -80°C.

The appropriate chemical solution e.g. ammonia, potassium cyanide etc., was added to protein samples to give a final concentration of 500µM, unless stated otherwise. Excess chemicals were removed by applying treated protein samples to G25-packed disposable columns and centrifuging them for 3 minutes at 3,000rpm. Ascorbate and dithionite reduction experiments were performed in an anaerobic chamber while flushing with argon/nitrogen. 1mM of the reductants were added to the sample while using phenyl methyl sulphate (PMS) as the mediator of the reaction.

During the copper titration experiment, samples were washed twice with 10mM Pipes, pH 7.25, 0.03% dodecyl-β-D-maltoside, 10mM EDTA before washing with

10mM Pipes, pH 7.25, 0.03% dodecyl-β-D-maltoside alone. Sample washing took place using a PM10 centricon (Amicon Corporation, Danvas, M.A.) which were centrifuged at 3000rpm, 4°C. Increasing concentrations of copper were added.

2.10.6 Spectrophotomeric procedure

Routine UV/vis spectrophotometry were carried out on a UV/vis HP8452A Diode Array Spectrophotometer.

2.11 Other procedures

2.11.1 Polyacrylamide gel electrophoresis (PAGE)

Sodium dodecyl sulphate (SDS) PAGE was performed (adapted from Laemmli, 1970) using a Mini PROTEAN II system (BIO-RAD, Hemel Hempstead, UK) or a Hoefer SE 600 series standard dual cooled units using a BIO-RAD PowerPac 300 and a BIO-RAD PowerPac 1000 power supply.

The gel were prepared using a discontinuous buffer system containing 0.375M Tris-HCl (pH 8.8) in the upper (resolving) gel, and 0.125 M Tris-HCl (pH 6.8) in the lower (stacking) gel. Samples were diluted with an equal volume of SDS sample buffer (100mM Tris-HCl , pH 6.8; 200mM DTT; 4 % ,w/v, SDS; 0.2 %, w/v, Bromophenol Blue; and 20 %, v/v, glycerol) and boiled (100°C) for 1 minute. The samples were then loaded onto 12 % (wt/vol) homogenous acrylamide gels with a 4 % stacking gel. The reservoir buffer was a 25mM Tris-glycine (pH 8.3) reservoir buffer; all buffers used in SDS-PAGE were supplemented with 0.1% SDS. The proteins were visualised on the gel by a >30 minute incubation with Coomassie Brilliant Blue stain (0.1 % Coomassie Blue R-250 in a solution of methanol: glacial acetic acid: water, 3:1:6 by volume). The gel was then de-stained by a >30 minute incubation in a solution of methanol: glacial acetic acid: water (4:1:5 by volume). SDS-PAGE gels were calibrated using Dalton Mark VII-L markers (Sigma Chemical Company Ltd) bovine albumin, 66 kDa; egg albumin, 45 kDa; glyceraldehyde-3-P-dehydrogenase, 36 kDa; bovine carbonic anhydrase, 29 kDa; bovine pancreas trypsinogen, 24 kDa, soybean trypsin inhibitor, 20 kDa; and bovine milk α-lactalbumin, 14.2 kDa.

2.11.2 Production of anti-sera to the pMMO

A band containing the 47 kDa polypeptide of pMMO was cut out from a 12% SDS PAGE gel and electro-eluted for 4 hours. Anti-sera were raised in Dwarf-lop rabbits by the subcutaneous injection of 0.5-1.0mg aliquots of purified protein homogenised with Moris's modification of Freund's adjuvant (V. Cooper, University of Warwick, UK). Bleeds were taken at 1month intervals and stored at 4°C for 16 hours. The coagulated blood proteins were discarded carefully and the clear supernatant was removed carefully and stored on ice. An optimal volume of 50µl antiserum was found to give an effective reaction to the 47 kDa polypeptide of pMMO as visualised by Western blot analysis (Section 2.9.4). The antiserum was stored in 50µl aliquots at -20°C until further use.

2.11.3 Protein electro-elution

Protein samples were excised from SDS-PAGE gels and electro-eluted under conditions as described in the instructions for the BIO-RAD Model 422 Electro-eluter.

2.11.4 Western blots analysis

Protein samples (1-5µg) were run on SDS-PAGE gel and the marker lane cut off and stained with Coomassie Brilliant Blue. The remaining part of the gel was soaked in transfer buffer (20 mM Tris-HCl, pH 8.0, 150 mM glycine, 20 % (v/v) methanol) for 30 minutes at room temperature. Proteins from the gel were electroblotted onto hybond-C nitrocellulose membrane (Amersham life sciences Limited, Buckinghamshire, UK) in an X-Cell blot module (Novex) at 25V constant potential difference for 2 hours.

Non-specific protein-binding sites on the membrane were blocked by soaking in 2% (wt/vol) skimmed milk powder in 20ml TBST (50mM Tris-HCl, pH 8.0; 150mM NaCl; 0.1 % (v/v) Tween 20) for 1 hour at room temperature or overnight at 4°C. The membrane was then soaked in 20ml TBST containing 2 % (wt/vol) skimmed milk powder and 50µl of primary antiserum with gentle shaking for 90 minutes. The blot was washed in three rinses with TBST (10 minutes per wash). The membrane was then soaked in TBST containing 2% Marvel skimmed milk powder and secondary

antibody (50µl anti-rabbit, anti-goat IgG-peroxidase conjugate, Sigma) for 90 minutes. Unbound secondary antibody was removed by three washes in TBST and two washes in TBS (TBST without Tween 20) for 10 minutes each. The bound antibody-peroxidase conjugate was visualised staining the membrane for peroxidase with stain solution for 5-10 minutes at room temperature.

The stain solution was freshly prepared as follows:
Solution A: 1.5g NaCl and 1ml of 1M Tris-HCl, pH 7.5 were dissolved in 50ml distilled water.
Solution B: 30mg chloronaphthol dissolved in 10ml methanol and diluted to 50ml with distilled water.
50µl of 8M hydrogen peroxide was added to solution B, which was then combined with solution A immediately before use.
The blot was rinsed in water and dried on tissue paper after it had been developed to the desired extent.

2.11.5 Western blotting for N-terminal sequencing

Protein samples were run on SDS-PAGE gel alongside Dalton Mark VII-L markers (Sigma) leaving an empty lane between the markers and samples. The stacking gel and unused lanes were cut off and the remainder of the gel soaked in transfer buffer (250ml solution containing 10mM 3-[cyclohexamino]-1-propanesulphonic acid (CAPS) buffer and 25ml methanol) for 5 minutes at room temperature. A piece of polyvinylidine difluoride (PVDF) membrane (Amersham Pharmacia Biotech, UK), cut to size 1mm larger than the gel in both directions, was soaked briefly in methanol before transferring to transfer buffer for a few minutes. Protein from the gel was electroblotted onto the PVDF membrane in an X-Cell blot module (Novex) at 25V constant potential difference for 2 hours.

The PVDF membrane was prepared for staining by rinsing with water followed by methanol before staining with Coomassie Brilliant Blue solution (0.1% Coomassie Brilliant Blue R-250, water:methanol:acetic acid (5:4:1) for 1 minute. The membrane was subsequently de-stained in three changes of 50% methanol for 1-2 minutes each by which time the protein bands were visible on the blot. The blot was dried overnight

at room temperature on a sheet of blotting paper before sending it to Dr. Arthur Moir, Department of Biological Sciences, University of Sheffield, for sequencing.

2.11.6 Quinol Preparation

Quinones e.g. duroquinone (tetramethyl-p-benzoquinone) were obtained from Sigma and were reduced to the corresponding quinol using sodium borohydride (Shiemke *et al.*, 1995). Acidified ethanol solution (3mM HCl) of the quinone was made anaerobic by adding excess sodium dithionite (20mg/ml) and gassing the solution with argon. The quinone was reduced by the addition of a 1.5 fold molar excess of solid sodium borohydride. The yellow solution was gassed with argon until it became colourless. Approximately 200ml of 3mM HCl solution was added to precipitate the dissolved quinol. The precipitate was collected by filtration and washed three to five times with 3mM HCl. The dried precipitate was dissolved in acidified ethanol and stored in crimp capped 2ml vials under an atmosphere of argon at –20°C until required. The concentration of the duroquinol was calculated from the absorbance of the solution based on its extinction coefficient of $2140 M^{-1} cm^{-1}$ at 283nm.

3. Purification of the pMMO complex

3.1 Introduction

There have been published protocols for the isolation of pMMO from various methanotrophs. Early reports by Tonge *et al.* (1975 and 1977) describe the purification of a pMMO complex from *Methylosinus trichosporium* OB3b using phospholipase D as the solubilising agent with ascorbate as well as NADH as electron donors. The methane-oxidising complex consisted of three components, two proteins consisting of molecular weight 46kDa and 9.4kDa and a CO-binding cytochrome-*c*. The complex was purified by using ultrafiltration techniques and ion-exchange (DEAE-cellulose), gel filtration (Sephadex G150 and G50) and an hydroxyapatite chromatography.

Akent'eva and Gvozdev (1988) published details of the purification of an NADH-utilising pMMO from *Methylococcus capsulatus* (Strain M). The purification involved salt-washing and fractionation of the membrane using 0-20% sodium sulphate. The enzyme was solubilised using 1% sodium deoxycholate followed by 5% sodium deoxycholate. An ion exchange chromatography column (DEAE-cellulose DE32) was then used to purify the pMMO to homogeneity. The enzyme was found to consist of two subunits, a monooxygenase component and an NADH reductase. The purified enzyme had a specific activity of 3600nmoles/min/mg based on the disappearance of methane. This organism is unavailable to other labs so this work has not been reproduced elsewhere.

A reproducible procedure for the solubilisation of the pMMO from *Methylococcus capsulatus* (Bath) was published by Smith and Dalton (1989) using the non-ionic detergent dodecyl-β-D-maltoside. All NADH-dependent activity was lost upon solubilisation although activity could be restored if the solubilised pMMO was reconstituted with egg or soya bean lecithins. Further purification of the pMMO resulted in total loss of activity. The major polypeptides thought to be associated with the pMMO were of molecular weights 49, 23 and 22kDa.

Zahn and DiSpirito (1996) published details on the purification of the pMMO from *Methylococcus capsulatus* (Bath). Here, the non-ionic detergent dodecyl-β-D-maltoside was again used to solubilise the pMMO. The enzyme was then isolated using ion-exchange (DEAE-cellulose) and hydrophobic interaction chromatography (Phenyl Sepharose) while maintaining anaerobic conditions. The pMMO did not bind to the ion exchange column but was present in the flow through fractions. These were combined and loaded onto the hydrophobic interaction column from which the pMMO-containing fractions were eluted with an increasing detergent concentration gradient (0.01-0.9%). Contaminating polypeptides were also observed (37kDa and 20kDa) and were identified as the cytochrome *b*-559/569. Removal of these polypeptides resulted in enzyme inactivation.

In order to purify pMMO from *Methylococcus capsulatus* (Bath), Charlton (1997) investigated various purification techniques including sucrose gradient sedimentation, immobilised metal ion affinity chromatography (IMAC), gel filtration and ion exchange chromatography among others. These protocols were performed under aerobic conditions but were not successful in producing purified pMMO with good activity and the specific activities of partially purified extracts decreased during the purification process.

Nguyen *et al.* (1998) used methane-limiting conditions during the growth of *Methylococcus capsulatus* (Bath) cells to obtain membranes highly enriched in pMMO. Purified active pMMO was obtained by solubilisation with dodecyl-β-D-maltoside and subsequent isolation with affinity (Lysine Agarose) or ion exchange (DEAE sepharose Fast Flow) chromatography. An excess of reductants (dithionite or ascorbate) was used to maintain anaerobic conditions and enzyme activity during solubilisation and purification. NADH was used as the reductant with the purified pMMO. A proteolytically processed version of the enzyme was found with a modified α subunit of 35kDa (α' subunit). The normal sized α subunit had a molecular weight of approximately 47kDa. Minor protein and haem contaminants were also observed.

3.2 Investigating published protocols

Historically, pMMO has proved notoriously difficult to purify in a reproducible manner, which has hindered any subsequent characterisation of the enzyme. The aims in this part of the study were concerned with finding a reproducible procedure to isolate the pMMO so a detailed characterisation of the pMMO enzyme could be undertaken.

The published methods of both Zahn and DiSpirito (1996) and Nguyen *et al.* (1998) were individually repeated under both anaerobic and aerobic conditions. Following Zahn's procedure, the dodecyl-β-D-maltoside solubilised pMMO extract (60mg) was applied to a pre-cooled (4°C) DEAE-cellulose column (4.5 x 10cm) equilibrated with 25mM Pipes, pH 7 and 0.01% dodecyl-β-D-maltoside. The pMMO did not bind to the column and was eluted in the flow-through fraction. This fraction was applied to a pre-cooled (4°C) Phenyl Sepharose HP column (4.5 x 10cm) equilibrated with 25mM Pipes, pH 7 and 0.01% dodecyl-β-D-maltoside with or without excess reductants depending on whether anaerobic or aerobic conditions were being used. The pMMO bound to the column and was eluted using an increasing dodecyl-β-D-maltoside concentration (0.01%-0.9%). This fraction was concentrated using a PM30 cut-off membrane Amicon concentrator and applied to a SDS-PAGE gel to assess purity (Figure 3.1) and measured for activity using the standard propylene to propylene oxide detection assay with 25mM duroquinol as the reductant (Table 3.1).

Following Nguyen's protocol, the solubilised pMMO extract (60mg) was either applied to a Lysine Agarose or a DEAE Sepharose column which was cooled to 4°C and equilibrated with 50mM Pipes, pH 7.25 containing 0.05% dodecyl-β-D-maltoside, 200mM copper sulphate and 5mM ascorbate. Excess reductants were omitted when protocols were performed under aerobic conditions. Three fractions were eluted from the Lysine Agarose column, the pMMO was eluted in the second slow-moving fraction. When using DEAE Sepharose, the pMMO fraction was eluted from the column using ~100mM NaCl. Fractions containing pMMO were concentrated using a PM30 cut-off membrane Amicon concentrator and applied to an SDS-PAGE gel to assess purity (Figure 3.1).

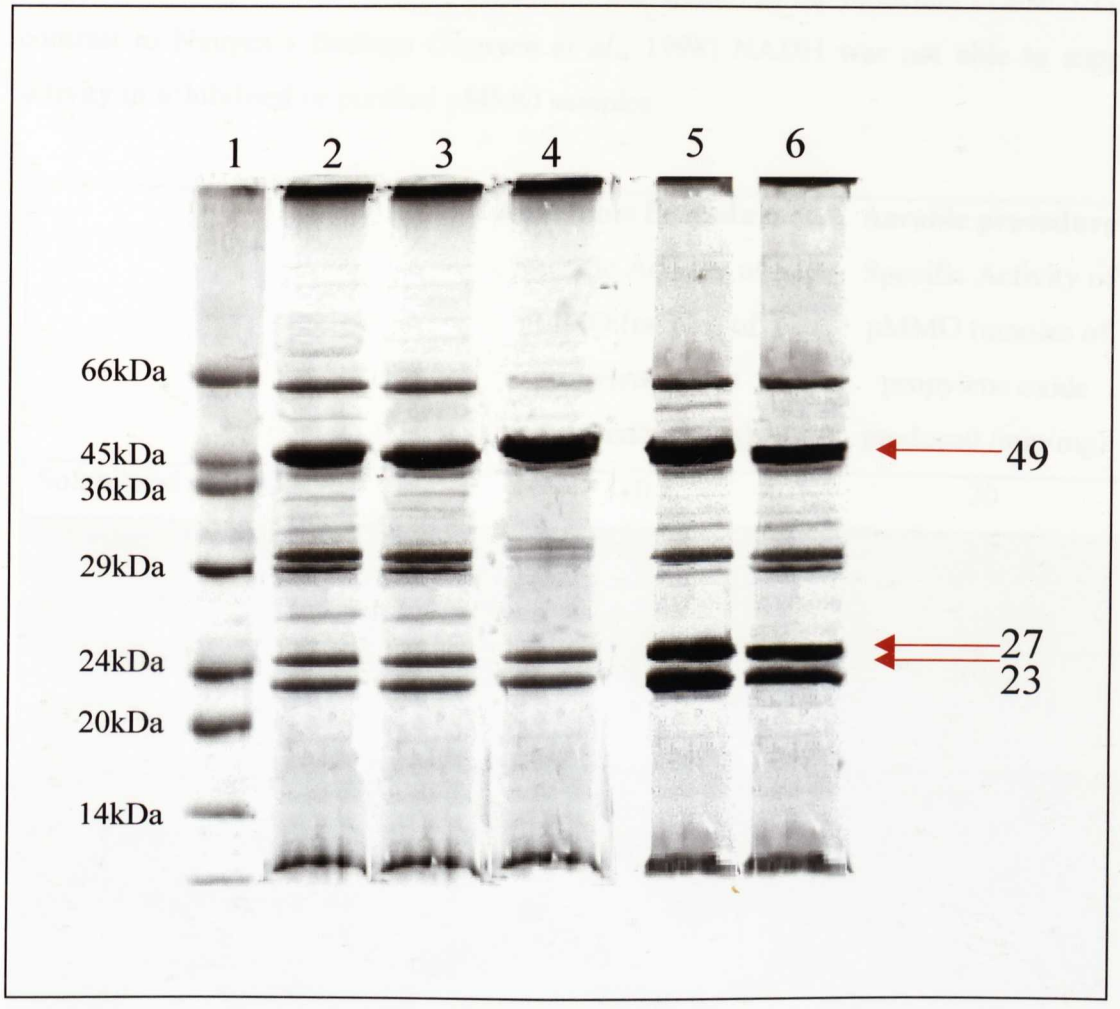

Figure 3.1 12% SDS-PAGE gel of proteins eluted during different stages of the purification protocols

Lane 1 Sigma Dalton-VII molecular weights

Lane 2 Starting preparation of solubilised pMMO^{s} extract

Lane 3 Flow through fraction containing pMMO, from DEAE cellulose column for application to Phenyl Sepharose HP column using (Zahn's protocol)

Lane 4 Fraction eluted from Phenyl Sepharose HP column using an increasing dodecyl-β-D-maltoside concentration (0.01-0.9%) (Zahn's protocol)

Lane 5 Slow moving fraction containing pMMO from Lysine-Agarose affinity (Nguyen's protocol)

Lane 6 Bound fraction of pMMO eluted from DEAE Sepharose column at 100mM NaCl (Nguyen's protocol)

Proteins were visualised by staining with Coomassie brilliant blue R-250.

The pMMO samples were measured for activity using the standard propylene to propylene oxide detection assay with 25mM duroquinol as the reductant (Table 3.1). In contrast to Nguyen's findings (Nguyen *et al.*, 1998) NADH was not able to support activity in solubilised or purified pMMO samples.

	Anaerobic Procedure Specific Activity of pMMO (nmoles of propylene oxide produced/min/mg)	**Aerobic procedure** Specific Activity of pMMO (nmoles of propylene oxide produced /min/mg)
Solubilised pMMO	10	20
Flowthrough fraction from DEAE cellulose*	3	12
pMMO fraction from Phenyl Sepharose*	0	0
Slow moving pMMO fraction from Lysine Agarose+	8	15
pMMO fraction eluted from DEAE sepharose with 100mM NaCl+	3	10

Table 3.1 Purification of pMMO using either anaerobic or aerobic conditions. Each fraction was concentrated and assessed for pMMO activity using the standard propylene to propylene oxide production assay with 25mM duroquinol as the reductant described in (Chapter 2, Section 2.9.3)

*-Protocol carried out as described in Zahn and DiSpirito (1996)

+-Protocols carried out as described in Nguyen *et al.* (1998)

Although, all activity was lost at the Phenyl Sepharose step in Zahn and DiSpirito's protocol (Table 3.1) the polypeptides of the pMMO hydroxylase (pMMOH) were present (Lane 4 of Figure 3.1). These results are in contrast to those seen by Zahn and DiSpirito (1996) where a specific activity of 11.08 nmoles of propylene oxide produced/min/mg was obtained at this stage. This protocol was believed to be unsuitable as the pMMO was inactive and the high concentration of expensive detergent required was not cost-effective. It is not clear how Zahn and DiSpirito (1996) obtained active pMMO using this protocol but they did observe major contaminating polypeptides (identified as the cytochrome-*b* 556/569) which were not detected in this study.

Using the protocol of Nguyen *et al.* (1998), under either anaerobic or aerobic conditions, resulted in active pMMO preparations (Table 3.1). These activities of 3-15 nmoles propylene oxide produced/min/mg were generally higher than those activities obtained by Nguyen and co-workers (1998). However, the degree of purification in this study is lower, as analysed by SDS-PAGE (Figure 3.1).

In general, the purification procedures carried out under aerobic methods gave more than 50% higher activities than those carried out under anaerobic procedures (Table 3.1). The polypeptide profiles were identical whether aerobic or anaerobic protocols were used.

3.2.1 Anaerobic versus aerobic methods

In this study and that of Charlton (1997), aerobic conditions were found to be sufficient to maintain activity of solubilised pMMO. This is in direct contrast to the findings of Zahn and DiSpirito (1996) and Nguyen *et al.* (1998), where anaerobic conditions were necessary to maintain the activity of the pMMO. In this part of the study, the solubilised extracts were initially from the same batch of cells, maintained under either anaerobic or aerobic conditions, and had the same starting specific activity. It was found that the use of ascorbate in the protocols as described by Nguyen et al. (1998) masked protein absorption at A_{280nm} and was therefore routinely omitted during the aerobic procedure so that protein elution could be monitored by A_{280nm}. It is unclear how Nguyen and co-

workers monitored protein elution in the presence of ascorbate. Since starting and resultant enzyme activities during the anaerobic procedure were so much lower than using aerobic conditions, the anaerobic conditions were abandoned during subsequent procedures.

3.2.2 Summary

In this study, the procedure using Lysine Agarose as described by Nguyen *et al.* (1998) yielded higher specific activities when compared to those obtained by the method of Zahn and DiSpirito (1996) where no activity was seen in the final preparation. However, the extent of purification, as analysed by SDS-PAGE, was limited as protein contaminants were observed (Figure 3.1).

Attempts to purify an active pMMO using gel filtration, metal chelating and chromatographic methods described by Charlton (1997) were unsuccessful. Electron microscopy analysis indicated that particulate extracts prepared by protocols described by Zahn and DiSpirito (1996) and Charlton (1997) were heavily contaminated with soluble proteins namely high molecular weight and sMMO polypeptides (confirmed using antibodies raised to the hydroxylase of sMMO, data not included). The consequences of this contamination could result in misleading information being obtained i.e. specific activity and metal analysis, when using these published protocols. This observation was also made by Nguyen *et al.* (1998).

In light of the failure to obtain active purified pMMO using protocols previously described and working from possibly contaminated sources, it was decided that the knowledge gained from previous literature could be used as a foundation in order to develop a more successful approach.

3.3 Optimisation of intracytoplasmic membrane (ICM) isolation

The growth of intracytoplasmic membranes (ICMs) has been correlated with the presence of pMMO in *Methylococcus capsulatus* (Bath), (Prior and Dalton, 1985). Investigations were carried out in order to optimise the isolation of the ICMs, thereby reducing contamination of possible soluble or outer membrane proteins and increasing the abundance of pMMO in the starting preparations.

ICMs were subjected to a discontinuous sucrose (60-20%) gradient, (Chapter 2, section 2.5.1) in an attempt to separate inner and outer membranes, therefore reducing contamination sources. Good separation was achieved and the small amounts of ICM with pMMO activity were isolated as shown in Figure 3.2 and Table 3.2. However, attempts to then solubilise an active pMMO were unsuccessful. The sucrose in the sample was thought to be affecting solubilisation as there was a low yield of solubilised proteins and no activity in the supernatant. Attempts at dialysing out the sucrose before solubilisation resulted in a decrease in activity and subsequent solubilisation of these dialysed membranes resulted in no enzyme activity as shown in Table 3.2.

Triton X-100 and Triton X-114 were used as detergents in an attempt to solubilise the cytoplasmic membranes in preference to outer membranes as previously carried out by Fjellbirkeland *et al.* (1997). This was performed by resuspending the particulate extract (Chapter 2, section 2.5.2) in a working buffer containing 2% (v/v) Triton. The resulting suspension was stirred at room temperature for 1 hour, centrifuged at 100,000xg for 1 hour and the soluble fraction containing ICMs was collected, assayed for activity and analysed by SDS-PAGE. The polypeptides thought to correspond to the pMMO hydroxylase were observed (Figure 3.2) however, no propylene oxidising activity was detected in the fraction possibly because of inactivation of the enzyme by the detergent.

Both methods were unsuccessful in isolating high activity, membrane bound pMMO ($pMMO^m$). However, a successful method was developed which combined extra ultracentrifugation steps and ionic washes to remove outer membranes and soluble or periplasmic proteins. This washing technique is described in more detail in Chapter 2, section 2.5. Briefly, cells were broken, whole cells debris was removed by centrifugation and the supernatant was centrifuged at 150,000 x g for 90 minutes. The resulting pellet was then resuspended in excess working buffer and centrifuged at 150,000 x g for 60 minutes at least twice until the supernatant became clear. The pellet was finally resuspended in minimal working buffer. Membrane samples ($pMMO^m$) were tested for activity (Table 3.2) by measuring the epoxidation of propylene with NADH as the reductant, as described in Chapter 2, section 2.9.2. The $pMMO^m$ sample was estimated to contain ~60% of the polypeptides associated with pMMO. The stringent washing protocol removed high molecular weight and soluble proteins as observed by electron microscopy (Chapter 6, Figure 6.6).

Method of ICM isolation	Specific Activity (nmoles of propylene oxide produced /min/mg)
Sucrose gradient	52
Sucrose gradient and dialysis	16
Sucrose gradient and dodecyl-β-D-maltoside solubilisation	0
ICM preferential solubilisation by Triton	0
Stringent washing technique	75

Table 3.2 Specific activities of intracytoplasmic membranes after specified isolation procedure. Activities of isolated ICMs (10mg/ml) were measured using the detection of propylene oxide produced from propylene with NADH as a reductant as described in Chapter 2, section 2.9.2.

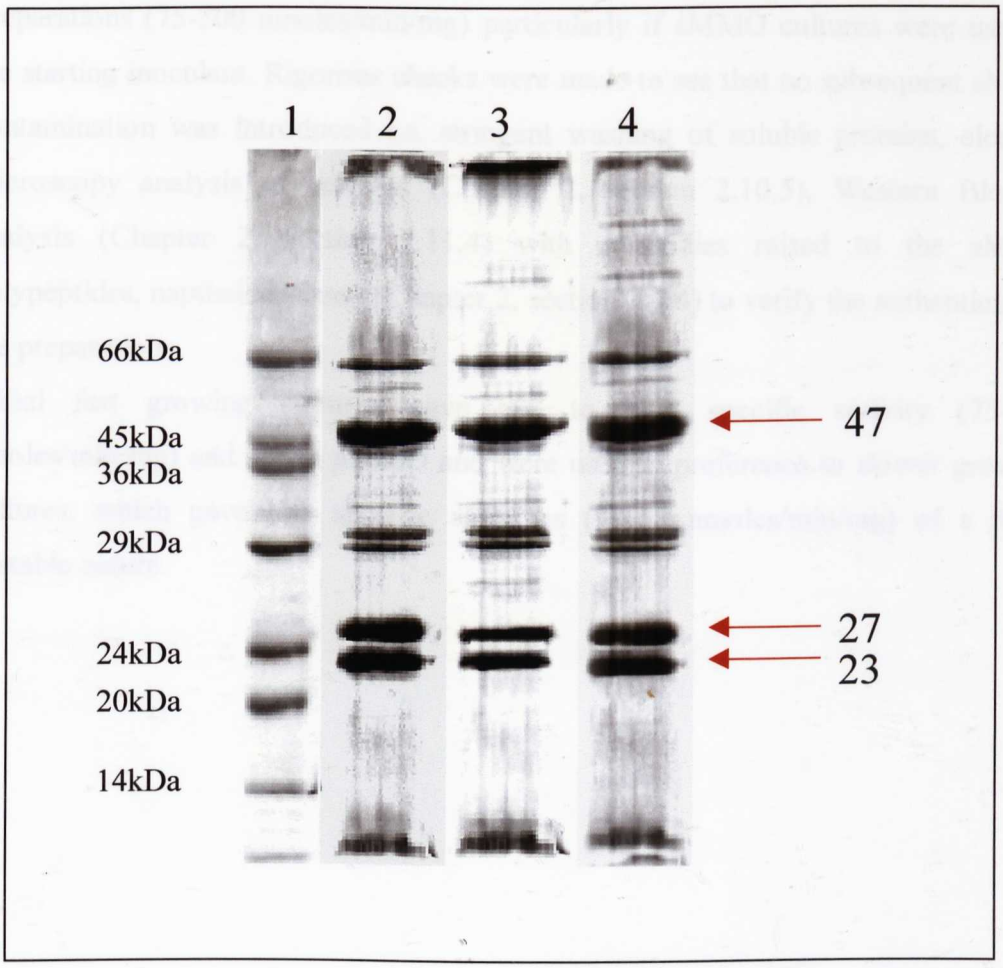

Figure 3.2 12% SDS PAGE gel of intracytoplasmic membranes isolated by different procedures.

Lane 1 Dalton VII molecular weight markers
Lane 2 ICMs isolated using Triton X-100 preferential solubilisation
Lane 3 ICMs isolated using a discontinuous sucrose gradient (60-20%)
Lane 4 ICMs isolated using the stringent washing technique. The membrane pellet was resuspended in excess working buffer and washed at least twice by centrifugation at 150,000g for 60minutes.
Proteins were visualised by staining with Coomassie brilliant blue R-250.

3.3.1 Useful observations

Several observations were made during the course of this study that may be useful as a guide for obtaining high activity membrane preparations.

1) Batch cultures (100L) appeared to produce high specific activity pMMO preparations (75-200 nmoles/min/mg) particularly if sMMO cultures were used as the starting inoculant. Rigorous checks were made to see that no subsequent sMMO contamination was introduced i.e. stringent washing of soluble proteins, electron microscopy analysis of cultures (Chapter 2, section 2.10.5), Western Blotting analysis (Chapter 2, section 2.11.4) with antibodies raised to the sMMO polypeptides, napthalene assay (Chapter 2, section 2.9.4) to verify the authenticity of the preparations.
2) Initial fast growing cultures gave rise to high specific activity (75-200 nmoles/min/mg) and stable pMMO and were used in preference to slower growing cultures, which gave low specific activities (30-50 nmoles/min/mg) of a more unstable nature.

3.4 Solubilisation of the pMMO complex

An intrinsic difficulty in the purification of membrane protein complexes is their tendency to dissociate in detergent solutions. Previous studies with various detergents (Smith and Dalton, 1989; Charlton, 1997) concluded that dodecyl-β-D-maltoside is the only detergent to yield an active pMMO enzyme. This is because non-ionic detergents such as decyl and dodecyl maltosides are generally milder than other detergents, therefore preserving intact complexes. Dodecyl-β-D-maltoside was the choice of detergent in this study. An active pMMO was solubilised using a 1.5mg dodecyl-β-D-maltoside /mg protein and 40μM copper sulphate in a manner similar to that described by Charlton (1997) (Chapter 2, section 2.6). However, this detergent to protein ratio was only effective when the membrane pellet was repeatedly resuspended in buffer containing 0.5M NaCl prior to solubilisation. This yielded enzyme activities in the range of 15-30 nmoles of propylene oxide produced /min/mg protein (Table 3.3).

Concentration of NaCl in resuspension buffer (M)	Specific activity of pMMO after solubilisation (nmoles of propylene oxide/min/mg)	
	No copper sulphate added	40μM of copper sulphate added
0	0	0
0.5	0	30
1.0	0	19

Table 3.3 Effect of NaCl concentration in resuspension buffer on resultant activities of pMMO during solubilisation with dodecyl-β-D-maltoside. Prior to solubilisation with dodecyl-β-D-maltoside, the membrane pellet was resuspended in minimal volumes of Pipes, pH7 buffer containing either 0.5 or 1.0M NaCl, with or without the addition of 40μM copper sulphate. Solubilised samples were assayed by measuring the production of propylene oxide from propylene using 25mM duroquinol as described in Chapter 2, Section 2.9.3.

It is not known why the addition of salt in the resuspension buffer allows the solubilisation of an active enzyme. However, salt can stabilise interactions within protein complexes and it is possible that this then allows an intact and therefore active protein complex to be solubilised.

The effectiveness of solubilisation was hard to decipher since membrane-associated protein preparations are often difficult to visualise on gels as membrane-bound proteins can be retarded in the gel because of the associated lipids, leading to smearing. In addition to this, complete solubilisation of the membrane preparation in sample buffer is often hard to do and therefore, the visual representation is often not an accurate depiction of the total membrane protein population in the preparation. However, the solubilised extracts were estimated to contain ~75% of the polypeptides associated with the pMMOH as analysed by SDS-PAGE (Figure 3.3). Other bands in the solubilised extract could not be identified but were proposed to be involved in membrane electron transport e.g. cytochromes etc.

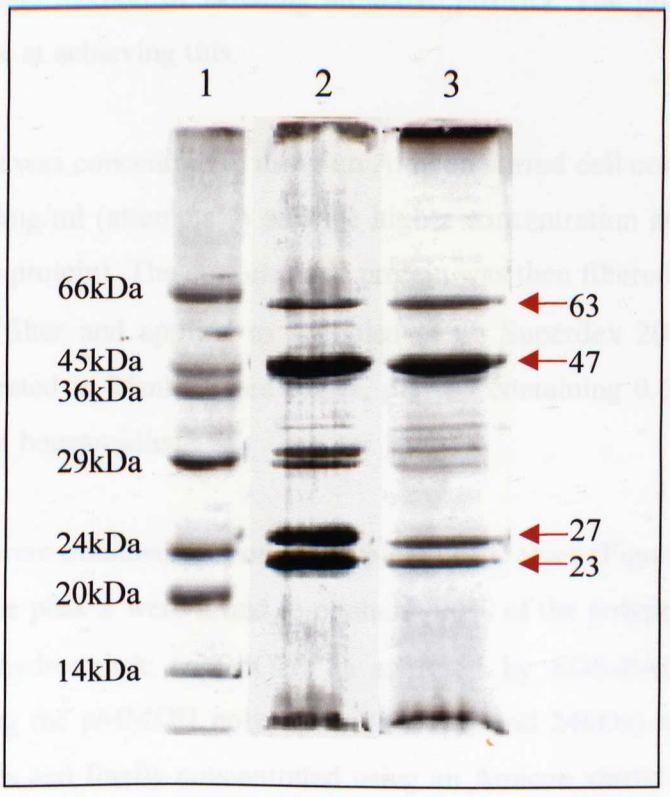

Figure 3.3 12% SDS PAGE gel of dodecyl-□-D-maltoside solubilised ICM from Methylococcus capsulatus (Bath).
Lane 1 Sigma Dalton-VII molecular weight markers
Lane 2 Intracytoplasmic membrane from *Methylococcus capsulatus* (Bath) prior to solubilisation. (5μg applied to gel)
Lane 3 Dodecyl-β-D-maltoside solubilised pMMO extract (5μg applied to gel)
Proteins were visualised by staining with Coomassie brilliant blue R-250.

3.6 Purification of the pMMO complex

Having obtained active solubilised pMMO ($pMMO^s$) extract it was then necessary to devise a reproducible method of isolating an active pMMO. The procedure described below was effective at achieving this.

Solubilised pMMO was concentrated, using an Amicon stirred cell concentrator with an XM50 filter, to 20mg/ml (attempts to achieve higher concentration at this stage led to precipitation of the protein). The concentrated protein was then filtered through a 0.2μm Whatman syringe filter and applied to a cooled (4°C) Superdex 200 (S200) column which was equilibrated in 25mM Pipes buffer, pH7.25 containing 0.03% dodecyl-β-d-maltoside and 1mM benzamidine.

Three main peaks were obtained as seen in a typical FPLC trace (Figure 3.4a). Fractions corresponding to the peak 2 were found to contain ~90% of the polypeptides associated with the pMMO hydroxylase (pMMOH) as analysed by SDS-PAGE (Figure 3.5). Fractions containing the pMMOH polypeptides (47, 27 and 24kDa) were pooled from numerous S200 runs and finally concentrated using an Amicon stirred cell concentrator with an XM50 filter to give >50mg/ml of protein. The protein was then re-applied to the S200 column as previously described. Only one main peak (2), which contained pMMOH, was obtained (Figure 3.4b). These fractions (peak 2) were collected, concentrated and drop frozen in liquid nitrogen and stored at -80°C until further use.

a)

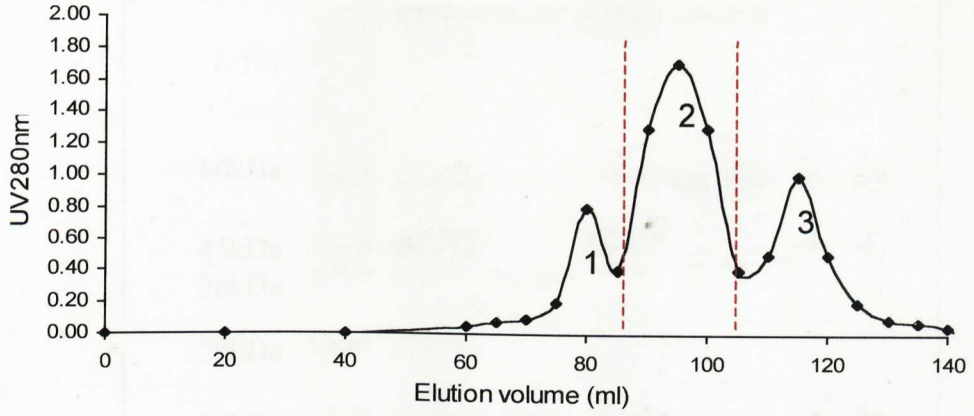

Figure 3.4 A typical FPLC trace showing the elution of proteins of *Methylococcus capsulatus* (Bath) from a) first and b) second Sephadex 200 column. 20-50mg pMMO^{s} was loaded onto a pre-cooled S200 column. The column was run at a flow rate of 1.5ml/min with an elution buffer of 25mM Pipes buffer, pH7.25 containing 0.03% dodecyl-β-D-maltoside and 1mM benzamidine. Eluted fractions corresponding to protein peaks were collected and concentrated. Peak 2 corresponds to the pMMO complex (pMMO^{c}).

b)

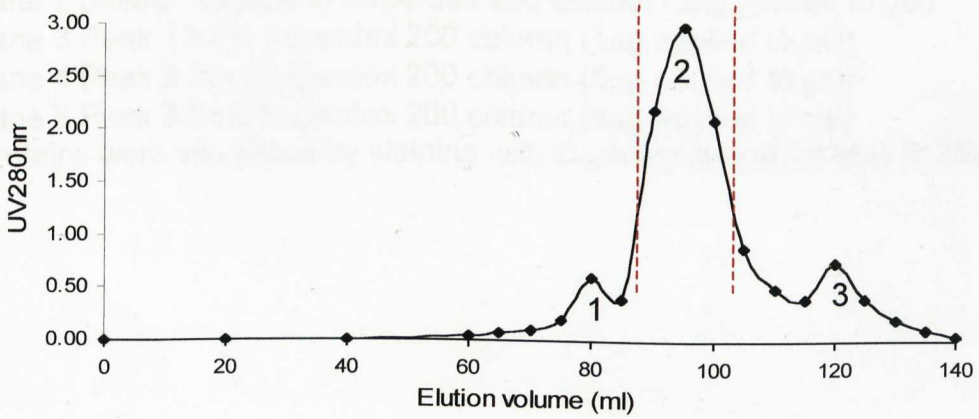

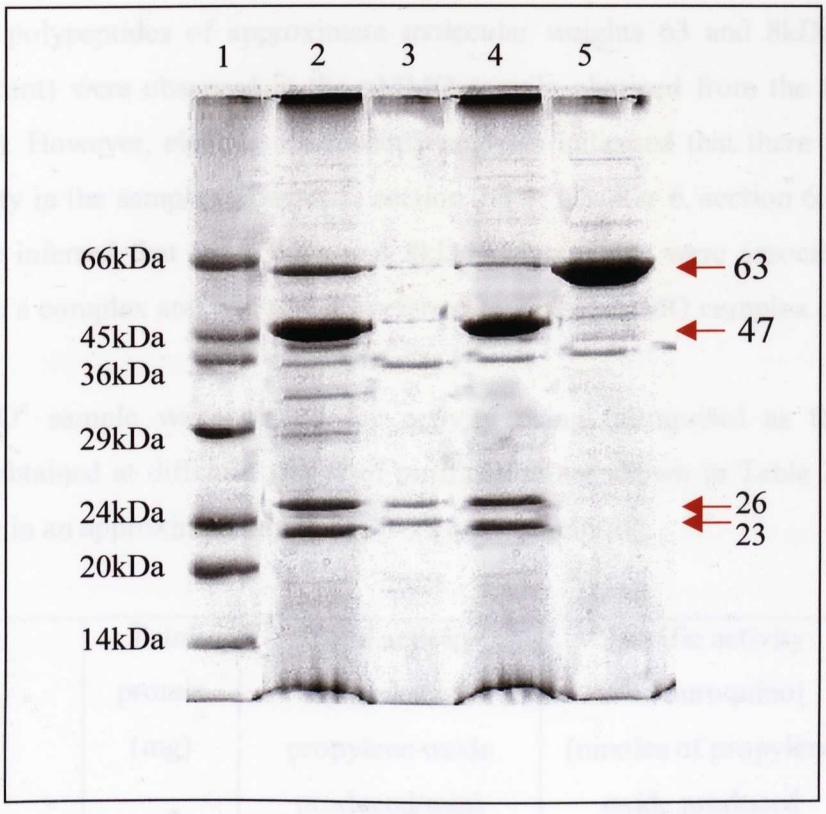

Figure 3.5 12% SDS-PAGE gel depicting the polypeptide profiles of the peaks collected from the size-exclusion Superdex 200 column.
Lane 1 Sigma Dalton-VII molecular weight markers
Lane 2 pMMO^{s} applied to Superdex 200 column (5μg applied to gel)
Lane 3 Peak 1 from Superdex 200 column (1μg applied to gel)
Lane 4 Peak 2 from Superdex 200 column (5μg applied to gel)
Lane 5 Peak 3 from Superdex 200 column (5μg applied to gel)
Proteins were visualised by staining with Coomassie brilliant blue R-250.

Additional polypeptides of approximate molecular weights 63 and 8kDa (often runs with dye-front) were observed in the pMMO sample obtained from the S200 column (figure 3.5). However, electron microscopy analysis indicated that there was complex homogeneity in the sample (Chapter 2, section 2.8.4; Chapter 6, section 6.6). From this it could be inferred that the 63kDa and 8kDa polypeptides were associated with the pMMOH in a complex and will now be referred to as the pMMO complex or $pMMO^c$.

The $pMMO^c$ sample was assayed for activity using duroquinol as the reductant. Activities obtained at different stages of purification are shown in Table 3.4 and were found to be in an approximate range of 30-75 nmoles/min/mg.

Protein Sample	Total protein (mg)	Total activity (nmoles of propylene oxide produced/min)	Specific activity with duroquinol (nmoles of propylene oxide produced /min/mg)	Yield (%)
$pMMO^m$	300	5700	19	100
$pMMO^s$	150	4550	30	79
$pMMO^c$	70	3150	53	55

Table 3.4 Purification of the pMMO complex from *Methylococcus capsulatus* (Bath). Activity measurements were made using the standard propylene to propylene oxide detection assay as described in Section 2.9.3. The activity measurement of $pMMO^c$ was assayed using the optimised conditions stated in Chapter 4, Section 4.2.

The degree of purification was high and specific activities increased by ~3-fold during the purification process suggesting that a duroquinol-driven pMMO complex was being purified. This was the first time a complex containing the pMMOH and the 63 and 8 kDa polypeptides had been observed. Therefore, it was necessary to assess whether the 63 and 8 kDa polypeptides had any role in pMMO activity or were adventitiously bound to the pMMOH.

3.7 Separation of the components of the pMMO^c

Although, the complex is known to comprise of a hydroxylase component, other component(s) in pMMO^c have not been identified. In order to verify the importance of the 63 and 8kDa polypeptides in the 'pMMO complex' it was necessary to firstly isolate the individual components separately.

This was achieved by using an anion exchange column (DEAE-cellulose, DE52). The concentrated pMMO^c sample obtained off the S200 column (>15mg/ml) was filtered through a 0.2μm syringe filter and applied to a cooled DEAE cellulose column which was equilibrated in 10mM Pipes buffer, pH7.25, 0.01% dodecyl-β-D-maltoside, 1mM benzamidine. Three peaks were obtained as seen in the typical FPLC trace (Figure 3.6). Two peaks were obtained in the void volume. Fractions corresponding to the different peaks were collected, concentrated using a PM10 cut off membrane in an Amicon concentrator.

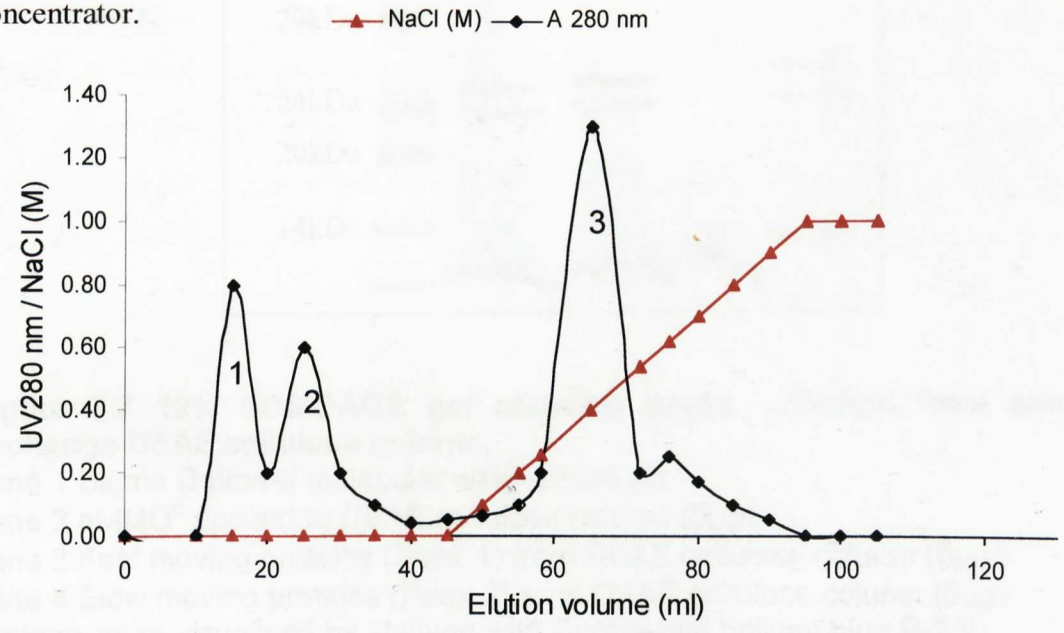

Figure 3.6 A typical FPLC trace showing the elution of proteins of *Methylococcus capsulatus* (Bath) anion exchange DEAE cellulose column. The column was equilibrated with 25mM Pipes buffer, pH7.25 containing 0.03% dodecyl-β-D-maltoside and 1mM benzamidine. The column was run at a flow rate of 2ml/min. Peak 3 was eluted with an increasing NaCl gradient.

The first peak (Figure 3.6) was found to contain polypeptides (63kDa and 8kDa) as analysed by SDS-PAGE (Figure 3.7). Their co-purification indicates that they may exist together as a component of unknown function. Fractions corresponding to the second peak contained only the polypeptides associated with the pMMOH. A final peak was eluted at 0.3M NaCl using an increasing salt gradient and contained the undissociated pMMO complex.

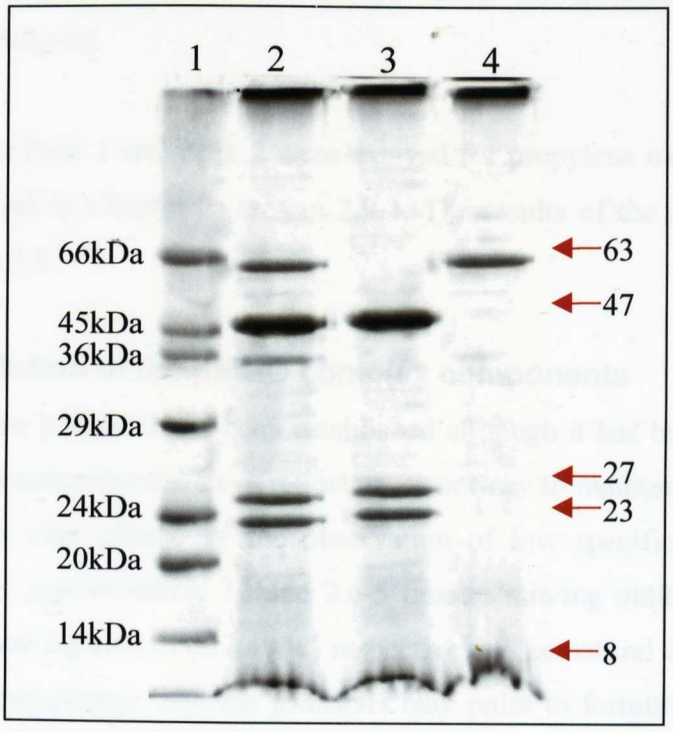

Figure 3.7 12% SDS-PAGE gel showing peaks collected from anion-exchange DEAE cellulose column.
Lane 1 Sigma Dalton-II molecular weight markers
Lane 2 pMMO^{c} applied to DEAE cellulose column (5μg)
Lane 3 Fast moving proteins (Peak 1) from DEAE cellulose column (5μg)
Lane 4 Slow moving proteins (Peak 2) from DEAE cellulose column (5μg)
Proteins were visualised by staining with Coomassie brilliant blue R-250.

The results presented in Figure 3.6 and 3.7 indicate that the $pMMO^c$ can be dissociated into its two components under gentle conditions (during the washing step). This may suggest that after isolation, the complex constituents are naturally dissociating and associating at a low rate, as the majority of protein still exists in the complex form. Concentrations of pure components obtained using DEAE-cellulose FPLC were typically low at <5mg/ml.

The fractions from Peak 1 and Peak 2 were assayed for propylene oxidising activity as previously described in Chapter 2, section 2.9.3. The results of the activity assays are detailed in section 3.8.

3.8 Reconstitution of the pMMO complex components

The existence of the pMMOH has been established although it has been suggested that there may be extra component(s) i.e. a reductase, necessary to maintain pMMO activity. This suggestion is also upheld by the observation of low specific activities of the purified pMMO of approximately 10 and 2.6-5 nmoles/min/mg obtained by Zahn and DiSpirito (1996) and Nguyen *et al.* (1998) respectively. The natural dissociation of the 63kDa and 8kDa component with the pMMOH may point to fortuitous binding of the proteins however, this could only be determined by assessing if the unknown component had any role in supporting pMMO activity. The 63 and 8kDa component has been designated as the putative reductase (pMMOR) for the purposes of this study.

	Total protein (mg)	Mean activity (nmoles of propylene oxide produced/min)	Specific Activity (nmoles of propylene oxide produced/min/mg)	% Activity
$pMMO^c$	0.5	13.75 ± 0.25	27.5	100
$pMMO^c$ + pMMOH	0.6	17.15 ± 0.45	28.6	105
$pMMO^c$ + pMMOR	0.6	16 ± 5	26.6	100
pMMOH + pMMOR	0.5	1.3 ± 0.6	2.6	9.5
$pMMO^c$ + pMMOH + pMMOR	0.7	19 ±3	27.1	95
pMMOH	0.5	0	0	0
pMMOR	0.5	0	0	0

Table 3.5 Specific activities of reconstituted proteins. MMO assays were carried out using the detection of propylene oxide production using 10mM Pipes, pH7.25, 25mM duroquinol and 0.05mM copper sulphate as described in detail in chapter 2, section 2.9.3 Results are an average of at least two experiments

The results presented in Table 3.5 indicate that when isolated components (pMMOH and pMMOR) are added back to the purified pMMO complex the activity is increased but the specific activity (28 nmoles of propylene oxide produced/min/mg) remains approximately the same. Neither the hydroxylase nor the reductase can support activity alone suggesting both are necessary for propylene oxidising activity. The reconstitution procedure (hydroxylase and the reductase in the absence of complex) was not effective, yielding only 10% of the activity of the as-isolated pMMO complex. This could be due to a missing component necessary for activity e.g. haem, or the loss of major structural integrity of the complex.

These findings indicate that the 63kDa and 8kDa (pMMOR) component is a vital constituent of the pMMO complex.

3.9 Discussion

In the preliminary study, the lysine agarose protocol described by Nguyen *et al.* (1998) yielded higher specific activities (~8-15 nmoles/min/mg) than that of Zahn and DiSpirito (1996) where no activity was seen in the final preparation. However, major contaminating polypeptides of unknown function, were observed in the samples prepared by the one-step protocols of Nguyen *et al.* (1998), as analysed by SDS PAGE (Figure 3.1). The observations presented in this study appear to be in contrast to the results presented in the original publications where Zahn and DiSpirito (1996) obtained impure preparations of high activity (11.08 nmoles/min/mg) and Nguyen *et al.* (1998) obtained purer preparations of low activity (2.6-5.1 nmoles/min/mg).

These differences may be explained by the fact that the starting preparations used in the unmodified protocol were purer than those used by Zahn and DiSpirito (1996) but were not as pure as those used by Nguyen *et al.* (1998). Only minor haem and protein contaminants were present in the purified pMMO samples of Nguyen *et al.* (1998). Professor S.I. Chan, (pers. com.) suggests that further purification of the pMMO hydroxylase (pMMOH) should be avoided as it results in the inactivation of the enzyme.

The success of the purification protocol hinges on the fact that initial membrane preparations are enriched with pMMO i.e. ~60% of the total proteins were identified as the polypeptides associated with the pMMO hydroxylase (pMMOH). Solubilisation of the membranes with dodecyl-β-D-maltoside. further serves to act as a purification procedure resulting in ~75% of the total proteins being identified as the polypeptides associated with the (pMMOH)

The essential difference in the pMMO preparations obtained in this study and those obtained by other groups is the presence of the putative reductase (pMMOR). The findings have shown that pMMOR can naturally dissociate from the pMMOH but that it is also essential for maintaining an efficient and functional duroquinol-driven pMMO complex. The protocols developed in this study may serve to stabilise the interactions between the pMMOR and the pMMOH, perhaps because of the addition of salt to

resuspension buffer. The preparations in this study were highly stable, with respect to activity after prolonged storage, and have the highest recorded activities in this field to date (Table 3.6).

The isolation of a pMMO reductase is not unprecedented as it has been suggested that high pMMO activities can be obtained when a purified NADH reductase is added back to the activity assay (Nguyen *et al.*, 1998; Chan, S.I. {pers. com.}). As yet there has been no published procedure to confirm the existence and subsequent isolation of an NADH reductase, so this could not be followed up.

The findings in this study are in contrast to previous studies carried out by Charlton, (1997), Zahn and DiSpirito (1996) and Nguyen *et. al.* (1998)

Summary of major findings

1) Charlton (1997) found that a breakage buffer CHAPS was essential for maintenance of activity in particulate extracts. This result is in contrast with the findings from this study and other published protocols. (Smith and Dalton, 1986; Prior and Dalton, 1985; Zahn and DiSpirito, 1996 and Nguyen *et al.*, 1998.)

2) Soluble proteins are expected to be a major source of contamination in preparations described by Zahn and DiSpirito (1996) and Charlton (1997) since some appear to associate quite strongly with the membrane. These can be removed while still maintaining high levels of pMMO activity (~75nmoles of propylene oxide produced/min/mg) using the stringent washing protocol that has been described in this study. This step is essential prior to solubilisation since failure to remove contamination can lead to misleading results particularly where the polypeptides of the soluble methane monooxygenase (sMMO) are present, as they may give a positive result in the MMO assay if propylene is used as the substrate.

3) In contrast to the observations of Zahn and DiSpirito (1996) and Nguyen *et. al.* (1998), anaerobic conditions were not found to be necessary during solubilisation and purification of the pMMO in this study. Indeed, such conditions were found to be detrimental to enzyme activity (Table 3.1). This is consistent with previous studies carried out in our laboratory group where aerobic conditions were also used during

solubilisation and purification of the enzyme (Prior and Dalton, 1985; Smith and Dalton, 1986 and Charlton, 1997).

Following these general principles, pMMO extracts were produced which had varying but high specific activities (50-200 nmoles/mg/min) and were stable in storage at –80°C for 1year. The activities of pMMO obtained in different studies are summarised in Table 3.6. The specific activities observed in this study were similar to those activities observed in previous studies in our laboratory (Smith and Dalton 1986, and Prior and Dalton, 1985) and are generally higher than those obtained by any other group.

Reference	pMMO sample	pMMO specific activity (nmoles/min/mg protein)	
		NADH as Reductant	Duroquinol as reductant
This study	$pMMO^m$	50-200	19
	Purified pMMO	-	50-75
Nguyen et al (1998)	$pMMO^m$	9.66-12.5	-
	Purified pMMO	2.6-5.1	-
Charlton (1997)	$pMMO^m$	60-90	-
	$pMMO^s$	-	30
Zahn and DiSpirito (1996)	$pMMO^m$	-	10.4
	Purified pMMO	-	11.08
Cook and Shiemke (1996)	$pMMO^s$	-	8.0
Shiemke et al. (1995)	$pMMO^s$	-	6.2
Semrau et al. (1995b)	$pMMO^m$	23.0	-
Chan et al. (1993)	$pMMO^m$	20-30	
Smith and Dalton (1989)	$pMMO^m$	172.0	-
Prior and Dalton (1985)	$pMMO^m$	114	

Table 3.6 - A comparison of activity of pMMO preparations in *Methylococcus capsulatus* (Bath) by different research groups.

The results indicate that both the pMMOH and the putative duroquinol-dependent pMMO reductase (pMMOR) are necessary for maintaining pMMO activity and are referred to as the pMMO complex or $pMMO^c$ for the remainder of this study. A series of experiments were undertaken to characterise the $pMMO^c$ and its components.

4 Characterisation of the pMMO complex

4.1 Introduction

The three polypeptides (47, 27 and 23kDa) of pMMO hydroxylase (pMMOH) have been purified to homogeneity from *Methylococcus capsulatus* (Bath) (Zahn and DiSpirito, 1996; Nguyen *et al.*, 1998). However, subsequent characterisation of the purified pMMO at a chemical and physical level has been slow in coming, largely due to the decrease in specific activity on solubilisation and isolation of the pMMOH. This indicates either the presence of an inhibitory substance in the preparation, denaturation of proteins or the loss of a component vital for methane monooxygenase activity. The results presented in the Chapter 3 suggested that the latter suggestion is true.

The aims of this part of the study were to undertake characterisation of the pMMO using the high specific activity pMMO complex purified as described in the previous chapter.

4.2 Optimisation of the pMMO assay

Before characterisation of the purified pMMO complex could be undertaken, it was necessary to ensure that the maximum activity of the enzyme was obtained. The following experiment was carried out to optimise the concentrations of duroquinol and copper ions used in the activity assay.

4.2.1 Optimisation of duroquinol concentration

The optimal concentration of duroquinol to attain maximal activity of pMMO samples was determined by using 40μM of $CuSO_4$ in the reaction mixture. Increasing concentrations of duroquinol (prepared as described in Chapter 2, section 2.11.6) were used for the propylene oxidising activity assay (Chapter 2, section 2.9.3). The $pMMO^s$ and $pMMO^c$ samples were prepared as previously described in Chapter 3, section 3.6.

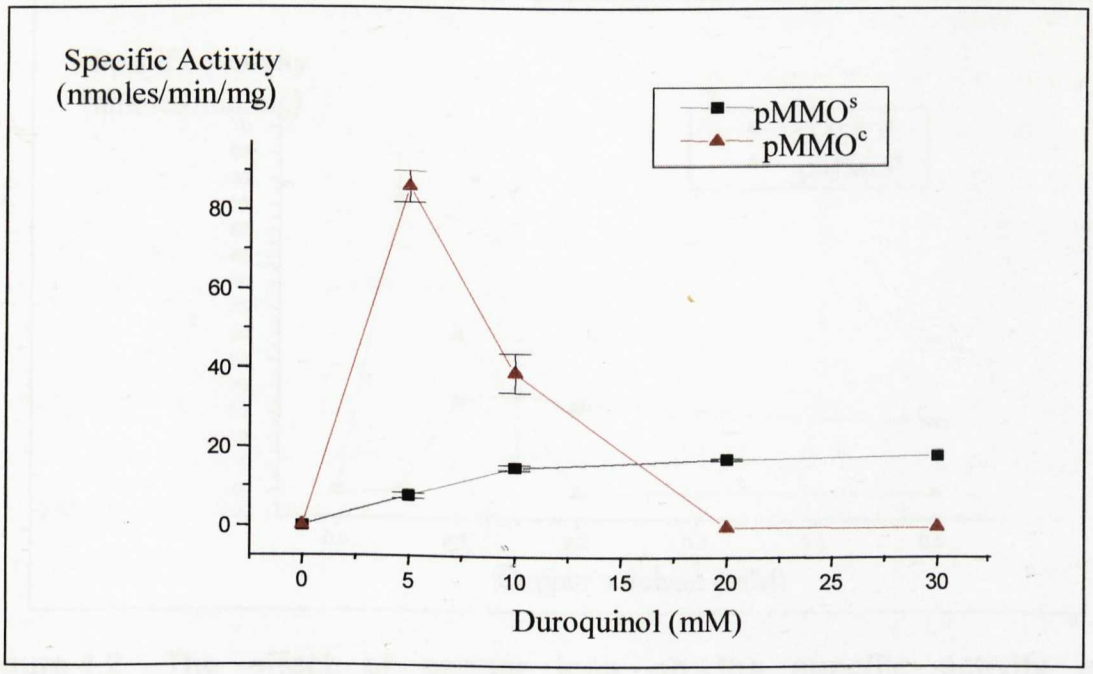

Figure 4.1 The effect of duroquinol concentration on the specific activity of solubilised pMMO extract ($pMMO^s$) and purified pMMO complex ($pMMO^c$). Results were an average of at least two assays. Assays were supplemented with 40μM copper sulphate and carried out as described in Chapter 2, section 2.7. The $pMMO^s$ and $pMMO^c$ samples were prepared as described in Chapter 3, section 3.6 and were used at a final concentration of 1mg/ml in the assay.

The results from Figure 4.1 indicate that a duroquinol concentration of 5mM gave maximal $pMMO^c$ activity of ≈83nmoles/min/mg, which is in contrast to $pMMO^s$ which required an optimal concentration of 20mM duroquinol (≈17nmoles/min/mg). Having ascertained the optimal concentration of duroquinol for $pMMO^c$ activity, the following experiment was carried out to determine the optimal concentration of copper sulphate needed for activity of pMMO.

4.2.2. Optimisation of copper sulphate concentration

The optimal concentrations of copper sulphate for obtaining maximal activities of $pMMO^s$ and $pMMO^c$ samples were determined by using concentrations of 20mM and 5mM of duroquinol respectively. Increasing concentrations of copper sulphate were added in a manner similar to that described previously in section 4.2.1.

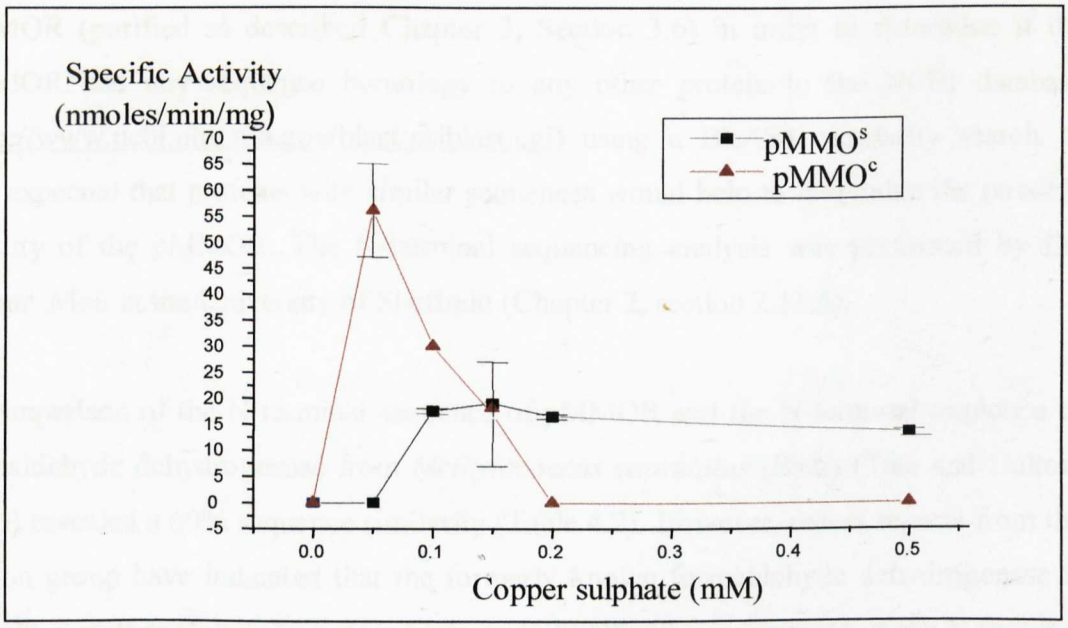

Figure 4.2 The effect of copper ions on the specific activity of solubilised pMMO extract ($pMMO^s$) and purified pMMO complex ($pMMO^c$) using 20mM and 5mM duroquinol respectively. Results were an average of at least two assays. The $pMMO^s$ and $pMMO^c$ samples were prepared as described in Chapter 3, section 3.6 and were used at a final concentration of 1mg/ml in the assay.

Maximal enzyme activity was obtained at a copper sulphate concentration of 0.05mM for the pMMO complex (≈56nmoles/min/mg), in contrast to 0.15mM for solubilised pMMO, which gave ≈19nmoles/min/mg. The higher concentration of copper needed by $pMMO^s$ may be due to the association of copper by other proteins in the impure sample. Higher concentrations of both duroquinol and copper ions were found to inhibit $pMMO^c$ activity. This may be because the excess co-substrates are binding to their binding sites causing saturation of these sites and preventing enzyme turnover. 5mM duroquinol and 0.05mM copper sulphate were used in all subsequent assays to give maximal $pMMO^c$ activity.

4.3 N-terminal sequencing of the putative reductase

N-terminal sequence analysis was carried out on the putative pMMO reductase, pMMOR (purified as described Chapter 3, Section 3.6) in order to determine if the pMMOR had any sequence homology to any other protein in the NCBI database (http://www.ncbi.nlm.nih.gov/blast/psiblast.cgi) using a BLAST similarity search. It was expected that proteins with similar sequences would help to determine the possible identity of the pMMOR. The N-terminal sequencing analysis was performed by Dr. Arthur Moir at the University of Sheffield (Chapter 2, section 2.11.5).

A comparison of the N-terminal sequence of pMMOR and the N-terminal sequence of formaldehyde dehydrogenase from *Methylococcus capsulatus* (Bath) (Tate and Dalton, 1996) revealed a 60% sequence similarity (Table 4.2). However, recent reports from the Dalton group have indicated that the formerly known formaldehyde dehydrogenase is actually a methanol dehydrogenase (Adeosun, 2000) and a comparison of the N-terminal sequence of pMMOR and the N-terminal sequence of the methanol dehydrogenase revealed a 70% sequence similarity.

A higher percentage sequence similarity (~95%) of the N-terminal sequences would be required to conclusively confirm the identity of the pMMOR as the methanol dehydrogenase from *Methylococcus capsulatus* (Bath). However, these findings in conjunction with the uncanny similarity between the estimated sizes of the subunits of

the pMMOR (~63kDa and 8kDa) and the methanol dehydrogenase (~63.615 and 8.211kDa, Adeosun, 2000) led us to conclude that the putative reductase (pMMOR) of the pMMO complex is also a methanol dehydrogenase from *Methylococcus capsulatus* (Bath).

1) *Putative reductase (pMMOR)* (This study)	NGELDRNSKG
2) *Formaldehyde dehydrogenase* (Tate and Dalton, 1996)	NSELDRLXKF
3) *Methanol dehydrogenase* (Adeosun, 2000)	NSELDRLSKD

Table 4.1 A comparison of N-terminal sequence of putative reductase from the pMMO complex with the N-terminal sequences of formaldehyde and methanol dehydrogenase *from Methylococcus capsulatus* (Bath). Differences in sequence 1) and 3) are designated in red. Differences in sequence 1) and 2) are designated in blue.

Since, the pMMOR is an essential component of the pMMO complex as determined by activity assays in Chapter 3, section 3.8, it can be inferred that the methanol dehydrogenase interacts with the pMMO hydroxylase to form an efficiently functioning pMMO complex *in vitro*. The significance of this phenomenon compels us to reinvestigate proposals by Tonge and coworkers (1975 and 1977) that the *in vivo* electron transfer to the pMMO might occur via a mechanism in which methanol dehydrogenase (MDH) recycles electrons generated from methanol oxidation back to the pMMO.

4.4 Electron donor specificity of the pMMO complex

4.4.1 *In vivo* electron donors for pMMO

Although NADH can support crude extracts of pMMO activity *in vitro*, it has been postulated that *in vivo* electron transfer might occur via a mechanism in which methanol dehydrogenase (MDH) recycles electrons generated from methanol oxidation back to the pMMO without the involvement of NADH (Tonge *et. al.*, 1977). Although, it has not been possible for other groups to reproduce their work, there have been subsequent reports that support this theory. Methanol, ethanol and higher primary alcohols, which are incapable of directly reducing NAD(P), could act as electron donors in pMMO-expressing *Methylococcus capsulatus* (Bath) cell suspensions although the ability was lost in sMMO-expressing cells (Leak and Dalton, 1983; Stanley *et al.*, 1983). Ethanol was also shown to act as an *in vivo* electron donor for pMMO in *Methylomonas methanica* (Ferenci *et al.*, 1975; Leak and Dalton, 1983). Since these reports indicate that methanol can provide electrons for methane oxidation in pMMO-expressing cells and as primary alcohols are oxidised by methanol dehydrogenase in methanotrophs, it can be inferred from this that electrons derived from methanol oxidation can be recycled into the methane oxidation reaction by methanol dehydrogenase, as previously proposed by Tonge *et al.* (1977).

To determine the validity of this proposal, various reductants were used to test their ability to donate electrons to the membrane associated and purified pMMO. Samples of $pMMO^m$ and $pMMO^c$ were prepared as described in Chapter 3 and used at final concentrations of 5mg/ml and 1mg/ml respectively in the reaction mixture. Activity assays were performed as outlined in Chapter 2, section 2.9.2 and 2.9.3, with the addition of 50μM $CuSO_4$ and the various electron donors. Reaction mixtures were incubated for 1 minute before initiation of the reaction by the addition of propylene. This method was used in preference to the initiating the reaction with the addition of reductants, for comparative assays, since plastoquinols are dried to the bottom of the assay vial and therefore present at the start of the reaction. Control experiments were carried out in the absence of reductant.

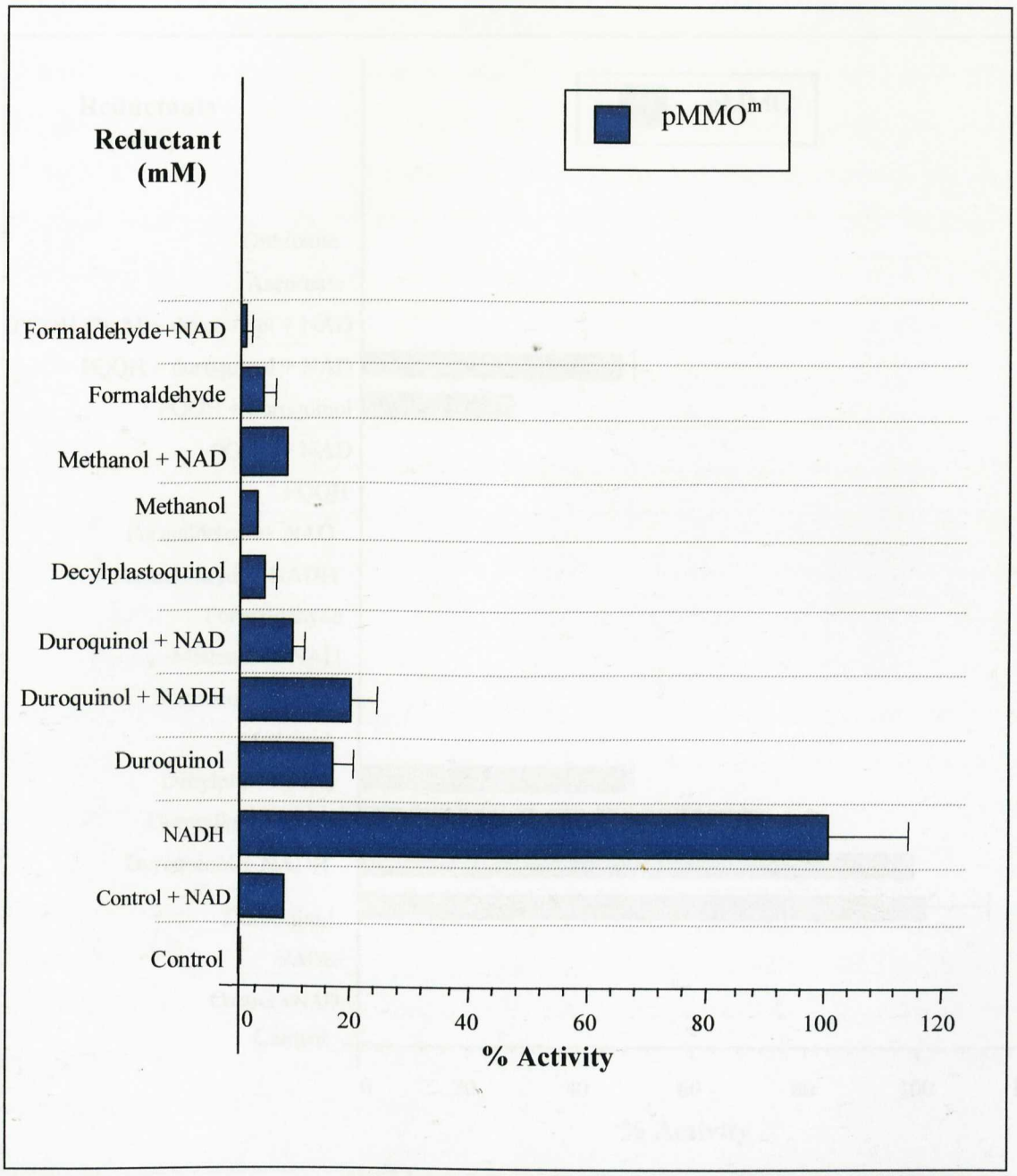

Figure 4.3 Relative propylene oxidising activities of pMMO^m with different reductants. The final concentration of the particulate extract in the assay was 5mg/ml. Final concentrations of reductants in the reaction mixture were 5mM for NAD, NADH, methanol and formaldehyde and 1mM for duroquinol, decyl-plastoquinol unless otherwise stated. NAD was added at a final concentration of 5mM. Average NADH-linked activity was 30 nmoles of propylene oxide produced/min/mg and was taken as 100% activity.

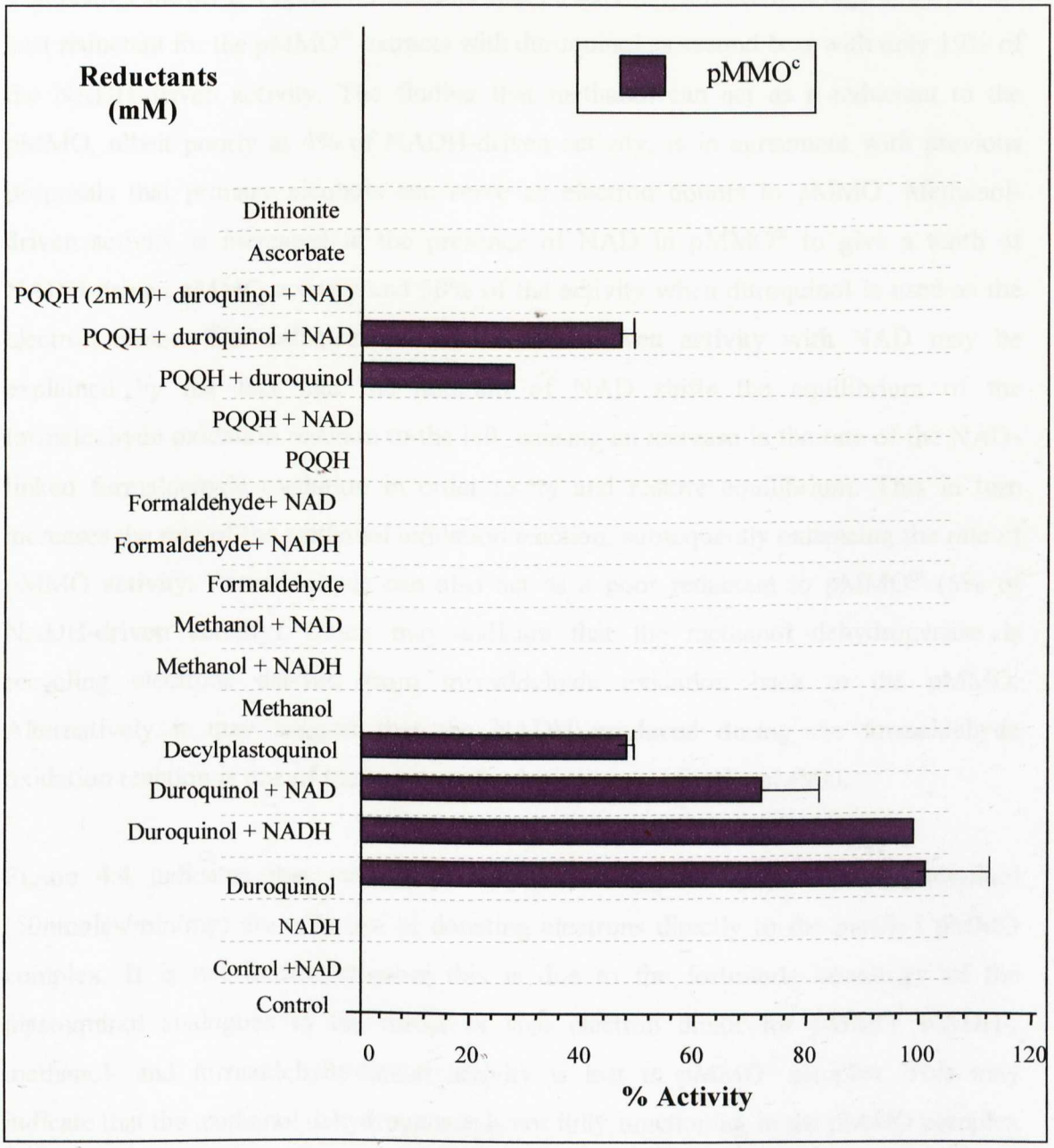

Figure 4.4 Relative propylene oxidising activities of the pMMO complex with different reductants. The pMMO complex (1mg/ml.) was purified as described in Chapter 3, section 3.6. Final concentrations of reductants in the assay were 5mM for NADH, methanol and formaldehyde and 1mM for duroquinol, plastoquinol and PQQ (pyrroloquinoline quinone) unless otherwise stated. NAD was added at a final concentration of 5mM. Average duroquinol-linked activity was 50 nmoles of propylene oxide produced /min/mg and was taken as 100% activity.

The results shown in Figure 4.3 indicate that NADH (30 nmoles/min/mg) is by far the best reductant for the $pMMO^m$ extracts with duroquinol as second best with only 19% of the NADH-driven activity. The finding that methanol can act as a reductant to the pMMO, albeit poorly at 4% of NADH-driven activity, is in agreement with previous proposals that primary alcohols can serve as electron donors to pMMO. Methanol-driven activity is increased in the presence of NAD in $pMMO^m$ to give a tenth of NADH-driven pMMO activity and 50% of the activity when duroquinol is used as the electron donor. The enhancement of methanol-driven activity with NAD may be explained by the fact that the addition of NAD shifts the equilibrium of the formaldehyde oxidation reaction to the left, causing an increase in the rate of the NAD-linked formaldehyde oxidation in order to try and restore equilibrium. This in turn increases the rate of the methanol oxidation reaction, subsequently enhancing the rate of pMMO activity. Formaldehyde can also act as a poor reductant to $pMMO^m$ (5% of NADH-driven activity) which may indicate that the methanol dehydrogenase is recycling electrons derived from formaldehyde oxidation back to the pMMO. Alternatively it may suggest that the NADH produced during the formaldehyde oxidation reaction is one of the sources of reducing power for the pMMO.

Figure 4.4 indicates that various plastoquinol analogues, in particular duroquinol (50nmoles/min/mg) are effective at donating electrons directly to the purified pMMO complex. It is not known whether this is due to the fortuitous homology of the plastoquinol analogues to the direct *in vivo* electron donor for pMMO. NADH-, methanol- and formaldehyde-linked activity is lost in $pMMO^c$ samples. This may indicate that the methanol dehydrogenase is not fully functioning in the pMMO complex or an unknown electron transport component necessary for coupling reducing equivalents from MDH or NADH to the pMMO has been removed during purification.

The methanol dehydrogenase co-factor, pyrroloquinoline quinonone, PQQ (in the reduced form, PQQH) does not act as a reductant to $pMMO^c$ and may reflect the need to obtain a fully functional PQQH. Addition of PQQH (1mM) actually inhibits duroquinol-driven activity of $pMMO^c$ although NAD appears to slightly lessen the effect of

inhibition. A higher concentration of PQQH (2mM) causes total inhibition of activity. This indicates that there may be competition for binding to a quinone-binding site in the complex.

In contrast to the findings of Tonge *et al.* (1975) and Nguyen *et al.* (1998), both ascorbate and dithionite were unable to donate electrons to pMMO but this result is perhaps unsurprising as they have previously been shown to inhibit pMMO activity in this study (Chapter 3, Table 3.1).

4.4.2 *In vitro* Electron Donors for pMMO

The results of the previous section indicate that NADH is a highly efficient electron donor to the pMMO when it is present in the membrane but once pMMO is purified, NADH ceases to act as a reductant. However, plastoquinol analogues, in particular decylplastoquinol and duroquinol were shown to be capable of providing reducing power to the $pMMO^c$ which is in agreement with the findings of Shiemke *et al.*, 1995. The findings indicate that NADH may not be the *direct* electron donor to pMMO *in vivo* but is probably the ultimate source of reducing power via an electron transport chain.

Preliminary electron transport inhibitor studies were performed using the particulate system from *Methylosinus trichosporium* OB3b by Tonge and coworkers (1975). Amytal was found to inhibit the transport of electrons to pMMO from NADH but not from ascorbate, indicating that NADH is not the direct *in vitro* electron donor of pMMO. Prior and Dalton (1985) proposed that the inhibition of NADH-driven pMMO activity in intracytoplasmic membranes from *Methylococcus capsulatus* (Bath) by potassium cyanide and sodium azide was due to the fact that NADH was not the direct electron donor to pMMO *in vitro*. This proposal was upheld by the findings of Charlton (1997) on the effect of electron transport inhibitors on $pMMO^m$ and $pMMO^s$ samples from *Methylococcus capsulatus* (Bath) using the electron inhibitors antimycin A, oligomycin, rotenone, 2,4-DNP and HOQNO. The different electron transport inhibitor profiles obtained for NADH- and duroquinol-driven pMMO activity indicated that these reductants transfer electrons to the pMMO via two different systems.

The rationale behind the following series of experiments was to ascertain whether specific electron transport proteins play a role in NADH- or duroquinol-driven pMMO activity in the membranes or the purified complex from *Methylococcus capsulatus* (Bath).

Electron transport inhibitors (detailed in Table 4.2) were made up in 10mM Pipes, pH7.25 by ultrasonic dispersion in a manner similar to that described by Colby and Dalton (1976) at final concentrations stated in this study. The $pMMO^m$ and $pMMO^c$ samples were prepared as described in Chapter 3 and were used at final concentrations of 10mg/ml and 1mg/ml respectively, in the reaction. pMMO samples were preincubated for 1 minute with the inhibitor prior to the addition of propylene to start the reaction. MMO activity was determined by measuring the epoxidation of propylene by gas chromatography. Control reactions were carried out with the absence of the electron transport inhibitor for each series of experiment.

Inhibitors	Mode of action
Antimycin A	Inhibits electron flow between flavoproteins and cytochrome *b*. Inhibits electron flow between *b* and c_1.
Oligomycin	Prevents the final ATP formation.
Rotenone	Inhibits the transfer of electrons from NADH to flavoproteins.
2,4-DNP	An uncoupling agent that allows electron flow but not phosphorylation.
HOQNO	Inhibits electron transport between cytochromes *b* and *c* or flavoprotein and cytochrome *b*.
KCN	Inhibition of terminal oxidase- may act to bind to the terminal oxidase, where it reacts with the ferric form of haem a_3 to block the electron flow in cytochrome oxidase.

Table 4.2 The electron transport inhibitors used in this study and their modes of inhibition. Abbreviations are: 2,4-DNP=2,4 dinitrophenol, HOQNO=2-*N*-heptyl-4-hydroxyquinoline-*N*-oxide, KCN=Potassium cyanide.

Figure 4.5 indicates that HOQNO (10^{-3}M) causes inhibition, giving 40% of pMMO activity in the membrane-associated system when NADH was used as a reductant. This is in contrast to the results observed by Charlton (1997) who observed total inhibition of NADH-driven pMMO^{m} activity at this concentration of HOQNO. Although, total inhibition could be obtained at higher concentrations of HOQNO (>10^{-2}M). The discrepancy was thought to be due to the limited solubility of the HOQNO. This result, in conjunction with the observation that rotenone (a flavoprotein inhibitor) only causes 5% inhibition of NADH-driven pMMO^{m} indicates that *b*- and *c*- type cytochromes are involved. HOQNO had no effect in the duroquinol-driven systems (Figure 4.6 and 4.7) at any concentration indicating that cytochromes *b* and *c* do not play a role in electron transfer between duroquinol and pMMO. Cyanide (10^{-3}M) inhibited NADH–driven pMMO^{m} activity giving 80% of the original activity, total inhibition of pMMO activity was achieved at higher concentrations of cyanide (10^{-2}M). This suggests that NADH is not the direct *in vitro* electron donor to pMMO^{m} and could indicate the possible involvement of a KCN-sensitive protein possibly a cytochrome, in the transfer of electrons to the pMMO. The other electron transport inhibitors did not affect NADH-linked pMMO activity in membranes indicating that there was unlikely to be any other electron transport protein involved in the transfer of electrons from NADH to pMMO.

An interesting result shown in Figure 4.6, is that the duroquinol-driven pMMO^{m} activity was inhibited by 2,4 dinitrophenol (2,4-DNP, 10^{-2}M), which gave 70% of pMMO^{m} activity in the presence of duroquinol. It is possible that the 2,4-DNP may be inhibiting a pump necessary for maintaining a proton motive force (*pmf*) or for transporting the reductant to a binding site, across the membrane since the pMMO complex is restricted in one main orientation in the membrane. This may then explain the lesser effect of 2,4-DNP in the purified pMMO as either the *pmf* would be dissipated or the reductant binding site may be more accessible. Duroquinol-driven pMMO^{m} activity is also inhibited by cyanide (10^{-3}M), which gave 57% of original pMMO activity (total inhibition at 10^{-2}M cyanide) indicating the presence of a cyanide sensitive protein in the transfer of electrons from duroquinol to pMMO. The rest of the electron inhibitors have

much less of an effect in the duroquinol-driven pMMO^{m} indicating that there are no other electron proteins involved in electron transfer from duroquinol to pMMO.

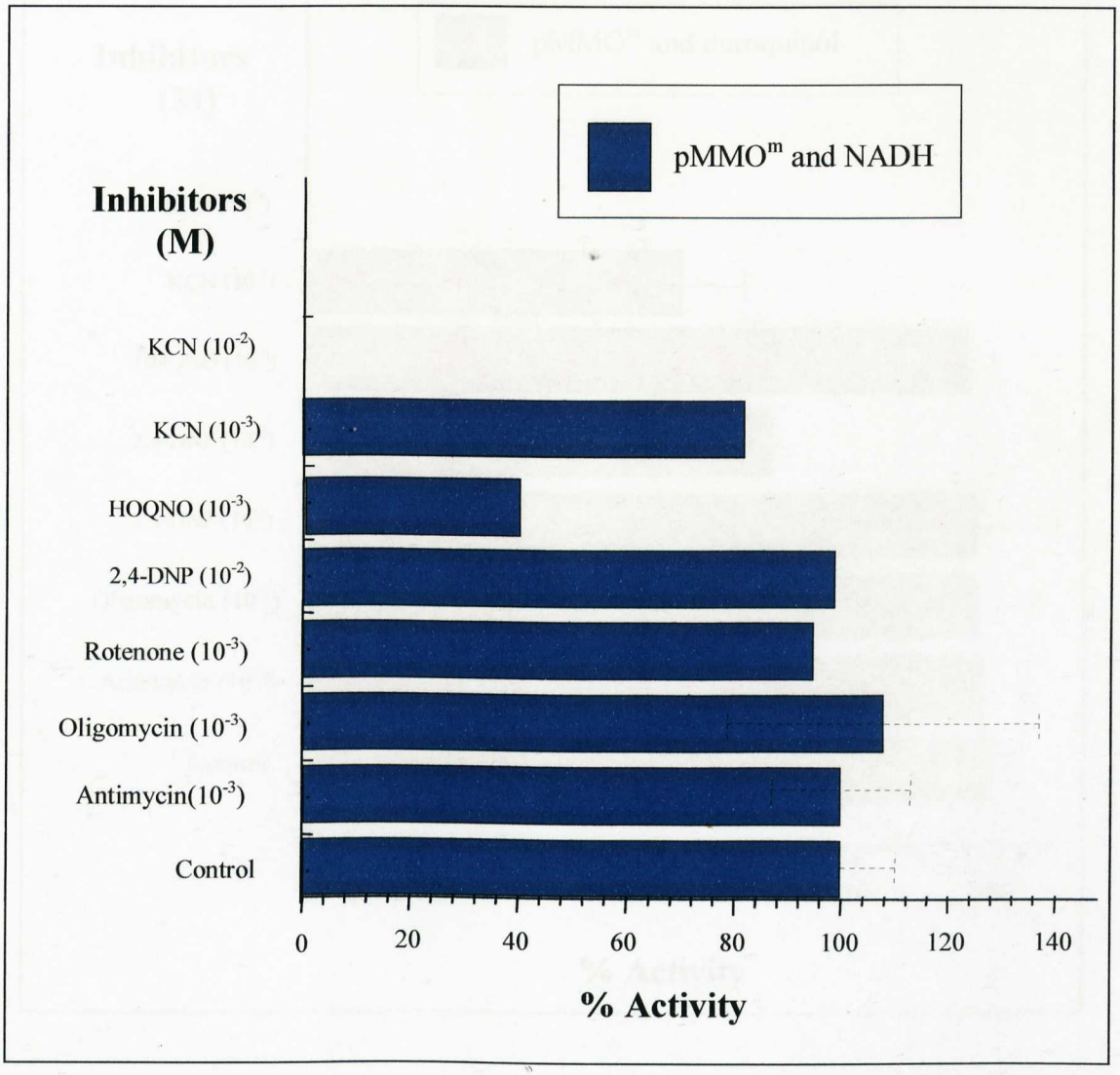

Figure 4.5 Relative pMMO activities of particulate extracts after incubation with various electron transport inhibitors using 5mM NADH as the reductant. The protein concentration for each assay was 5mg/ml. Assays were carried out as described in Chapter 2, Section 2.9.2. Inhibitors were dissolved at the appropriate concentration in 10mM PIPES buffer, pH 7.25. Particulate extract was preincubated for 1 minute with inhibitor prior to the assay. The control assay did not contain any inhibitor. Average NADH-linked activity was 70 nmoles of propylene oxide produced/min/mg of protein and was used as 100% pMMO activity.

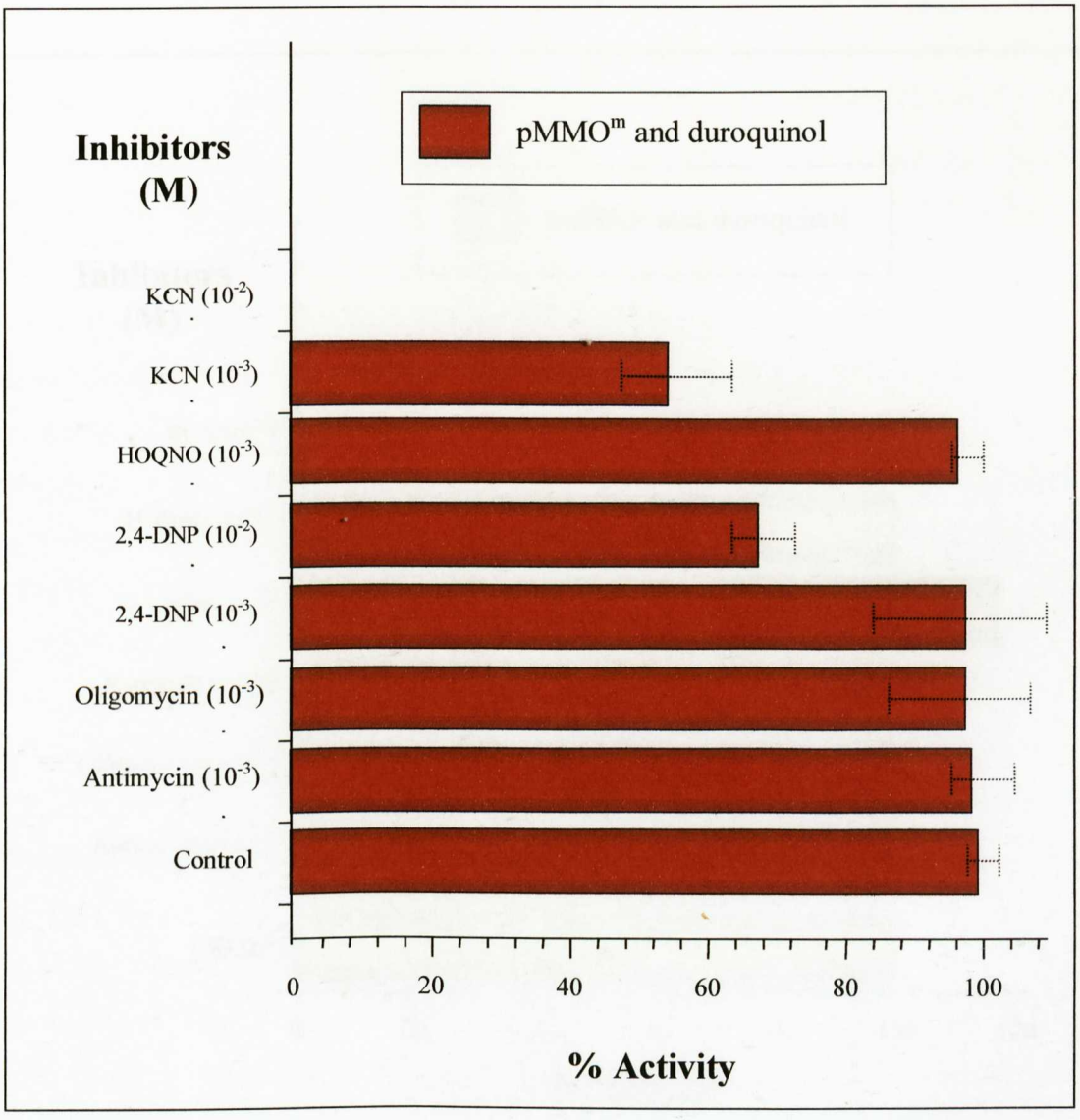

Figure 4.6 Relative pMMO activities of particulate extracts after incubation with various electron transport inhibitors using 5mM duroquinol as the reductant. The protein concentration for each assay was 5mg/ml. Assays were carried out as described in Chapter 2, section 2.9.2. Inhibitors were dissolved at the appropriate concentration in 10mM PIPES buffer, pH 7.25. Particulate extract was preincubated for 1 minute with inhibitor prior to the assay. The control assay did not contain any inhibitor. Average duroquinol-linked activity was 20 nmoles of propylene oxide produced/min/mg of protein and was taken as 100% pMMO activity.

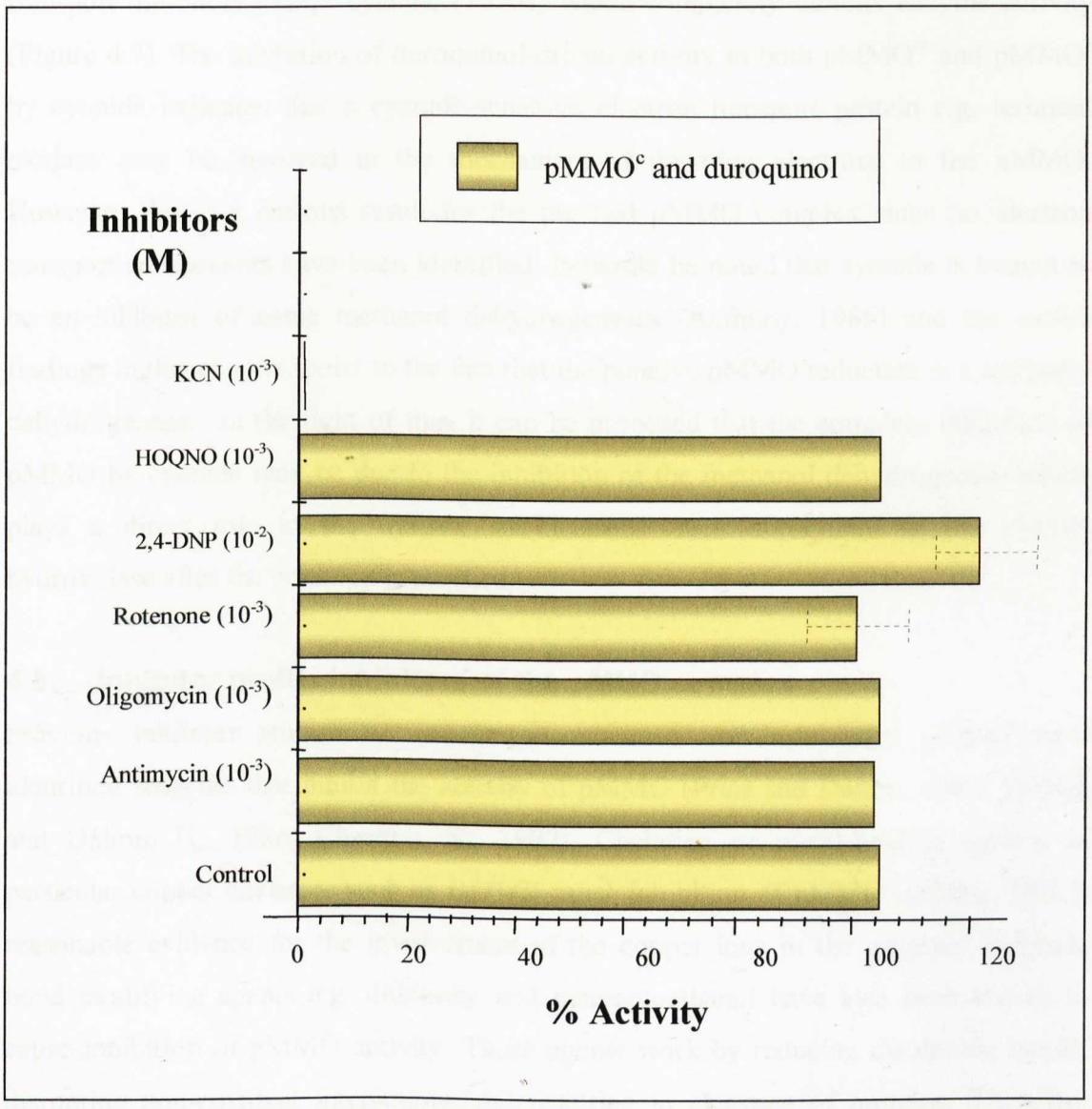

Figure 4.7 Relative activities of pMMO complex after incubation with various electron transport inhibitors using duroquinol as the reductant. The protein concentration for each assay was 1mg/ml. Assays were carried out as described in Chapter 2, section 2.9.3. Inhibitors were dissolved at the appropriate concentration in 10mM PIPES buffer, pH 7.25. The purified pMMO complex (as described in Section 3.6) was preincubated for 1 minute with inhibitor prior to the assay. The control assay did not contain any inhibitor. Average duroquinol-linked activity was 50 nmoles of propylene oxide produced/min/mg of protein and was taken as 100% activity.

The purified duroquinol-driven pMMO complex is unaffected by all the electron transport inhibitors except cyanide (10^{-3}M) which completely inhibits enzyme activity (Figure 4.7). The inhibition of duroquinol-driven activity in both $pMMO^{m}$ and $pMMO^{c}$ by cyanide indicates that a cyanide-sensitive electron transport protein e.g. terminal oxidase may be involved in the mechanism of donating electrons to the pMMO. However, this is a curious result for the purified pMMO complex since no electron transport components have been identified. It should be noted that cyanide is known to be an inhibitor of some methanol dehydrogenases (Anthony, 1986) and the earlier findings in this chapter, point to the fact that the putative pMMO reductase is a methanol dehydrogenase. In the light of this, it can be proposed that the complete inhibition of pMMO by cyanide may be due to the inhibition of the methanol dehydrogenase which plays a direct role in the transfer of electrons from duroquinol to the pMMO hydroxylase after the complex is purified.

4.5 Inhibitor profile inhibitors of the pMMO complex

Previous inhibitor studies on membrane-associated and solubilised pMMO have identified reagents that inhibit the activity of pMMO (Prior and Dalton, 1985, Stirling and Dalton, H., 1986, Charlton, S., 1997). Chelating or metal-binding agents, in particular copper chelators such as DDTC, cause inhibition of pMMO activity. This is reasonable evidence for the involvement of the copper ions in the enzyme. Sulphide bond modifying agents e.g. dithionite and mercaptoethanol have also been shown to cause inhibition of pMMO activity. These agents work by reducing disulphide bonds, disrupting non-covalent interactions and resulting in cleavage of proteins. Therefore these findings indicate the importance of sulphide bonds in the pMMO enzyme, although the exact significance of this is unclear. Acetylenic compounds are suicide substrates that bind irreversibly to the active site of the pMMO hydroxylase which then converts it to the unstable oxirene which is proposed to inactivate the pMMO by electrophilic attack of nucleophiles in the active site (Prior and Dalton, 1985).

Previous inhibitor studies were carried out on crude extracts of pMMO, which could lead to ambiguities as any number of proteins, which may be required for a functional

enzyme, could be inhibited. The following experiment was carried out to assess the sensitivity of pMMO^c to a variety of proposed inhibitors of pMMO. The inhibitors were made in the 10mM Pipes, pH 7.25 up to the final concentrations detailed in Table 4.3. The pMMO^c sample was used at a final concentration of 1mg/ml in the reaction mixture. pMMO^c was preincubated for 1 minute with the inhibitor prior to the addition of propylene to start the reaction. MMO activity was determined by measuring the epoxidation of propylene by gas chromatography. A control reaction was carried out in the absence of the inhibitor and its activity was taken as 100% activity.

Inhibitor	Mode	Final Concentration (mM)	Specific Activity (nmoles of propylene oxide produced/min/mg)	% Activity
None	None	0	56±3	100
Acetylene	Suicide substrate	Excess	0	0
Dithiothreitol	Sulphide bond Modifying agent	0.1	0	0
Mercapto-Ethanol	Sulphide bond Modifying agent	0.1	0	0
Imidazole	Copper chelator	0.1	9±1	16
EDTA	Divalent metal chelator	10	28 ±2	50
DDTC	Copper chelator	0.1	12±3	72

Table 4.3 Effect of inhibitors on pMMO^c activity at specified concentrations, using duroquinol as reductant. The results of the single dose experiment are an average of at least two experiments. A final pMMO^c concentration of 1mg/ml was preincubated for 1 minute with the inhibitor prior to the addition of propylene to start the reaction. MMO activity was determined by measuring the epoxidation of propylene by gas chromatography as described in Section 2.9.3. A control reaction was carried out in the absence of the inhibitor and its activity was taken as 100% activity.

The results shown in Table 4.3 are in good agreement with previously published results. Acetylene caused total inhibition of the pMMO complex indicating that it is a potent inhibitor of pMMO activity. This is in agreement with the previous findings of Prior and Dalton (1985).

Both the sulphide bond-modifying agents, dithiothreitol (DTT) and mercaptoethanol caused total inhibition of pMMO activity. There are only two cysteine residues present in the published protein sequence of the pMMO hydroxylase (Semrau *et al.*, 1995; Stolyar *et al.*, 2000) which could form a disulphide link, one which is present in *pmo*A (β subunit) and the other in the *pmo*C (γ subunit). Clearly the assumed disulphide link formed between these residues is vital for the functioning pMMO complex possibly because it maintains the structural integrity of the hydroxylase.

The metal binding agents imidazole, EDTA and DDTC caused partial inhibition of the pMMO which is consistent with the suggestion that certain divalent cations are necessary for pMMO activity. The exact role of metal ions in the pMMO is discussed in detail in the next chapter.

4.6 Kinetics of methane oxidation by the pMMO^c

The rationale behind the following experiment was to determine the kinetic constants for methane oxidation by the pMMO^c from *Methylococcus capsulatus* (Bath). Having defined these kinetic constants they can then be used to compare the efficiency of methane oxidation by different enzymes e.g. sMMO or pMMO from different methanotroph strains. The pMMO^c sample was used to generate initial velocity plots at increasing concentrations of methane. Methane concentrations were calculated using Henry's constant of 4.3 at 45°C as stated in chemical tables (Chapter 2 section 2.9.3). A double reciprocal Lineweaver-Burk plot was generated in order to calculate the kinetic constants V_{max} and K_m.

The kinetic constants V_{max} and K_m were calculated from the double Lineweaver-Burk plot (Figure 4.8).

y-axis intercept $\equiv 1/Vmax = 0.0075$

Therefore, V_{max} = 133 nmoles/min/mg

x-axis intercept $\equiv -1/K_m = -5$

Therefore, K_m = 0.2mM

Hence, the kinetic constants V_{max} and K_m were 133 nmoles/min/mg and 200μM, respectively. Low concentrations of methane were difficult to measure manually with accuracy and may have given rise to some misleading data. Ideally, this experiment should be carried out using cyclopropanol, a specific inhibitor of the methanol dehydrogenase (MDH) which is not available commercially. This would ensure that methanol production measurements were not being affected by methanol utilisation by MDH.

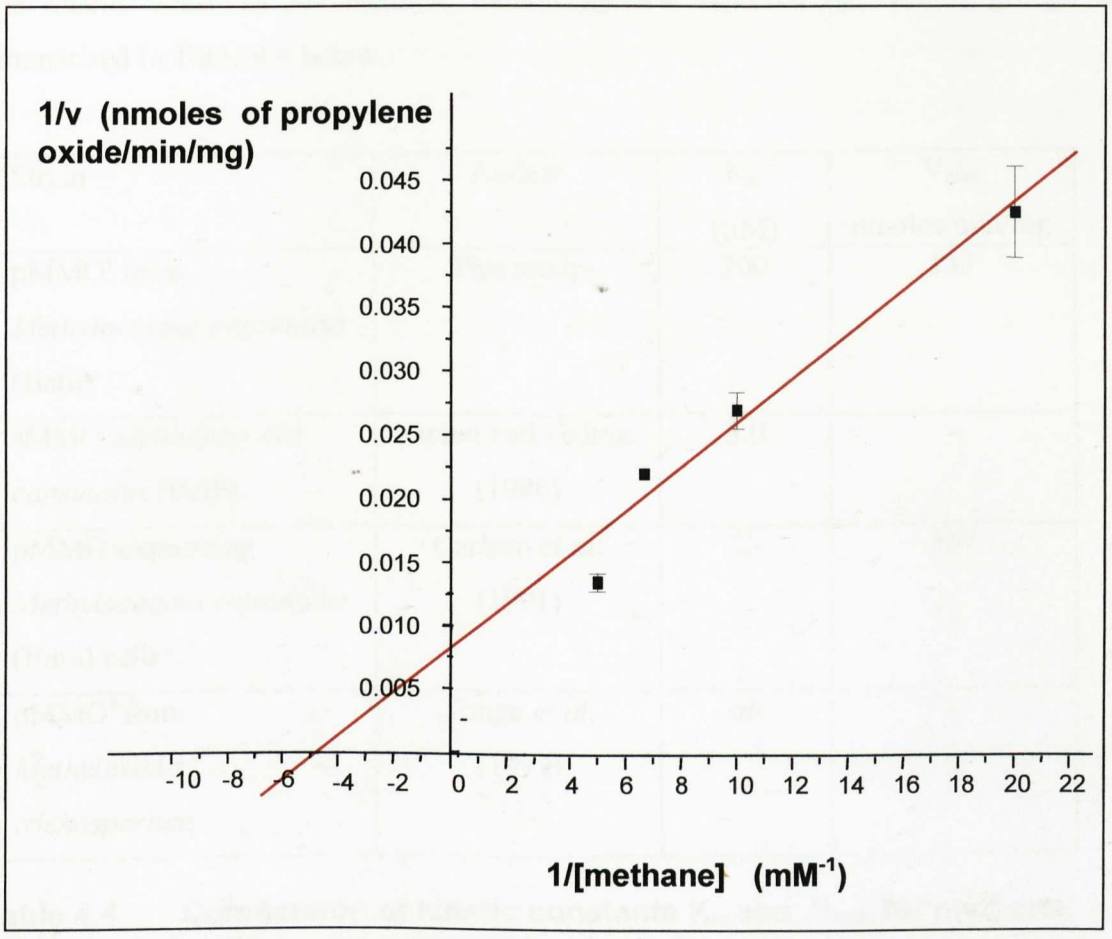

Figure 4.8 A double reciprocal Lineweaver-Burk plot of the pMMO complex using increasing concentrations of methane. 1mg/ml pMMO^{c} was used in the assay. The assays were carried out using 10mM Pipes pH7.25, 5mM duroquinol, 40μM copper sulphate and 1 mg/ml of purified pMMO complex. Assays were taken at 3 and 6 minutes intervals for each methane concentration. Results are the average of at least two assay.

The kinetic constants for methane monooxygenase reported by various groups is summarised in Table 4.4 below.

Strain	Author	K_m (μM)	V_{max} nmoles/min/mg
pMMO[c] from *Methylococcus capsulatus* (Bath)	This study	200	133
sMMO *Methylococcus capsulatus* (Bath)	Green and Dalton (1986)	3.0	-
pMMO-expressing *Methylococcus capsulatus* (Bath) cells	Carlsen *et al.* (1991)	23	457
pMMO[c] from *Methylosinus trichosporium*	Tonge *et al.* (1977)	66	-

Table 4.4 Comparison of kinetic constants K_m and V_{max} for methane oxidation by methane monooxygenase by various groups.

The K_m value for methane in this study is ~3-10 fold higher than the K_m values for pMMO found by other groups (Table 4.4). The soluble MMO appears generally more efficient than its counterpart pMMO as it has a much lower K_m for methane that pMMO i.e. lower concentration of methane are required to obtain maximal enzyme activity.

4.7 UV-visible spectral properties of pMMO^c and components

Neither Zahn and DiSpirito (1996) nor Nguyen *et al.* (1998) observed co-factors associated with their purified pMMO preparations. Both claim to have some haem contamination as previously discussed in Chapter 1. Co-factors e.g. haem groups, absorb at characteristic wavelengths, therefore pMMO^c and its individual components were examined to see if they contained any associated co-factors. The pMMO^c, pMMOH and pMMOR samples were prepared as described in Chapter 3, section 3.10. The UV-visible spectra were measured on a Hewlett Packard diode array spectrophotometer (Chapter 2, section 2.10.6)

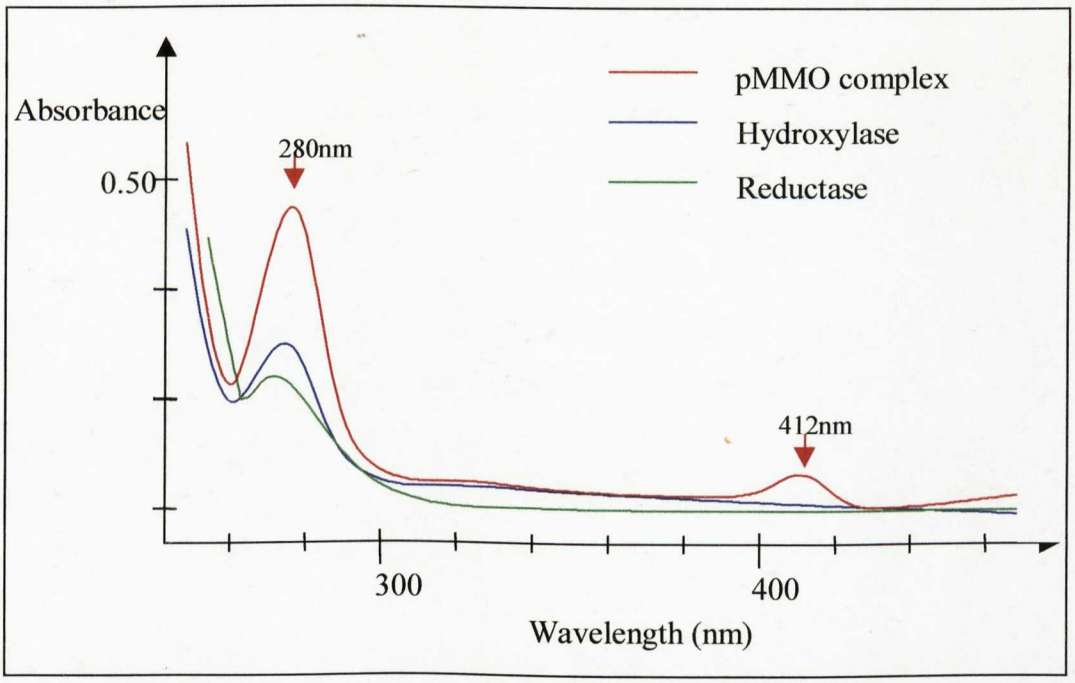

Figure 4.9 Absorption spectra of the pMMO complex, hydroxylase and reductase. Protein samples were diluted to give final concentrations of ~10μg/ml Peaks were observed at 280nm and 310nm which are characteristic of protein and haem constituents respectively.

The absorption spectrum of the pMMO complex in Figure 4.9 depicts an absorption band at 412nm that is indicative of the presence of haem. On dissociation of the complex i.e. when the components of the complex are purified, the haem component is removed. This suggests that the haem is non-covalently associated with the complex and could indicate the presence of a *b*-type haem (protohaem IX). The presence of haem is

consistent with the findings of Nguyen *et al.* (1998), where minor haem contamination with a weak absorption band at 410nm were also observed in purified pMMO samples.

Samples were boiled to 100°C for 5 minutes in order to release the methanol dehydrogenase co-factor PQQ, with a characteristic peak at 345nm and a shoulder at 400nm. Boiling had no significant effect on the spectra observed in Figure 4.9 suggesting that PQQ was not present in these samples. However, PQQ may be present at such low concentrations in the samples as to make it undetectable.

4.8 General Discussion and conclusions

In this chapter the putative pMMOR was identified as a probable methanol dehydrogenase (Section 4.3). This was an important finding which led to the subsequent reinvestigation of the proposal that *in vivo* electron transfer might occur via a mechanism in which methanol dehydrogenase (MDH) recycles electrons generated from methanol oxidation back to the pMMO without the involvement of NADH (Tonge *et. al.*, 1977). The findings in this study indicated that methanol can provide reducing power to the $pMMO^{m}$, albeit poorly at only 5% of NADH linked activity and was consistent with the earlier finding that primary alcohols could act as electron donors to *Methylococcus capsulatus* (Bath) cells (Leak and Dalton, 1983; Stanley *et al.*, 1983). The possibility of methane oxidation without the need for NADH would allow the cell to conserve energy. This is supported by the fact that cells expressing pMMO are energetically more efficient (in terms of g cells produced/g methane consumed) than cells expressing sMMO (Dalton and Leak, 1985).

The ability of methanol to act as reductant to the pMMO was lost upon purification of the enzyme which probably reflect the need to obtain a fully functioning methanol dehydrogenase with an intact cofactor, pyrrolo-quinoline quinone (PQQ). This is supported by the results of the UV-vis spectra (Figure 4.9) that indicate that the PQQ is not present in the purified MDH (pMMOR).

The findings in section 4.4.2 indicate that PQQ may compete with duroquinol for a quinone-binding site in the pMMO complex. This site could be like the quinone-binding sites found in the plant alternative oxidase (Moore *et al.*, 1995). Alternatively, the PQQ is known to exist in a hydrophobic site in the α subunit of the methanol dehydrogenase (Anthony *et al.*, 1994) and it may be possible that this is where duroquinol interacts with the MDH.

The electron transport inhibitor studies indicate that NADH provides electrons for the pMMO via other electron transport proteins possibly *b*- and *c*-type cytochromes. The fact that rotenone, a flavoprotein inhibitor, does not inhibit NADH-driven pMMO

activity does not rule out the possibility that a rotenone resistant flavoprotein similar to the type II NADH-quinone oxidoreductase (Yagi *et al.*, 1991) may be involved in electron transfer.

The electron transport proteins are probably removed during solubilisation and purification of the pMMO complex, as duroquinol-driven pMMO^c activity is only inhibited by cyanide, which is proposed to inhibit the pMMOR/MDH component of the pMMO complex. In summary, the results from this part of the study indicate that NADH donates electrons to the pMMO via a series of electron transport proteins and duroquinol directly provides electrons to the pMMO complex (Figure 4.10).

The inhibitor profile (Section 4.5) generated in this study has similar results as those found previously for the particulate enzyme (Prior and Dalton, 1985, Stirling and Dalton, 1986, Charlton, 1997). The sulphide bond modifying agents e.g. DTT have a profound effect on pMMO activity. This suggests that a covalent sulphide bridge may have an important role in the pMMO^c. The cysteine residue present in the *pmo*A (β) subunit, which is proposed to contain the active site (Semrau *et al.*, 1995), is conserved in the sequence of ammonia monooxygenase (AMO) from *Nitrosomonas europaea* which suggests that the cysteines may have an important role possibly in the active site of pMMO.

Inhibitor profiles of the pMMO complex confirm the importance of copper ions in the enzyme, possibly in the active site. However, it is as yet unclear what form this copper takes and whether there are any other metals involved in the active site. The next part of the study was to clarify the nature of metal ions in the active site of pMMO.

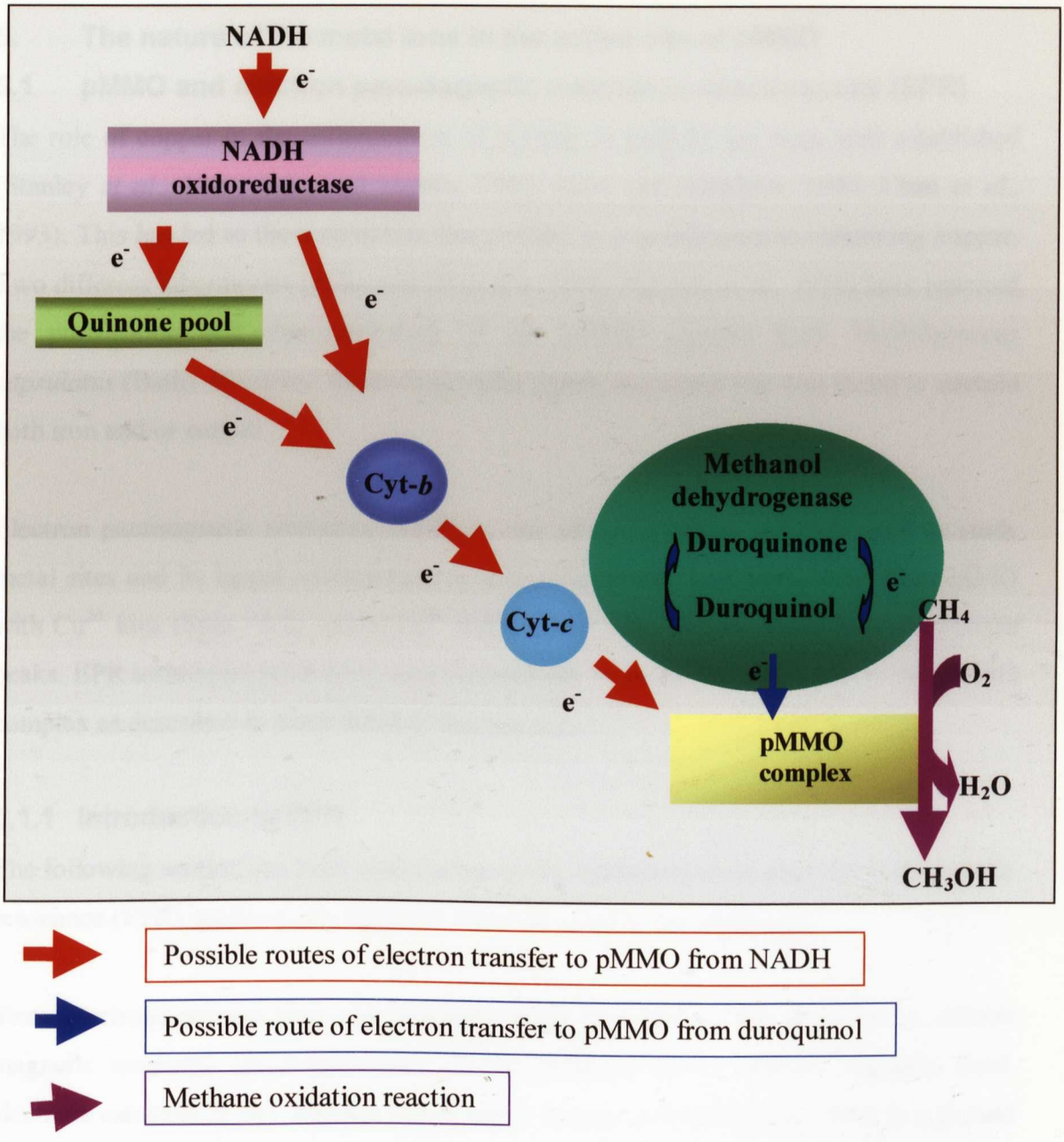

Figure 4.10 Proposed mechanism of electron transport routes to pMMO from NADH and duroquinol.

NADH transfers electrons to the pMMO via a possible rotenone-insensitive flavoprotein NADH oxidoreductase. The electrons could then be passed onto cytochromes-*b* and cytochromes-*c* and finally on to the pMMO. Alternatively, electrons may be passed from NADH to an unknown quinone pool and then on to the cytochromes and finally pMMO.

Duroquinol transfers electrons via the pMMOR/methanol dehydrogenase (MDH) to the pMMO hydroxylase.

5. The nature of the metal ions in the active site of pMMO

5.1 pMMO and electron paramagnetic resonance spectroscopy (EPR)

The role of copper in the enhancement of activity in pMMO has been well established (Stanley *et al.*, 1983; Prior and Dalton, 1985; Zahn and DiSpirito, 1996; Chan *et al.*, 1993). This has led to the assumption that pMMO is a metalloprotein containing copper. Two different laboratories (Zahn and DiSpirito, 1996; Nguyen *et al.*, 1998) have reported the purification and characterisation of the pMMO enzyme from *Methylococcus capsulatus* (Bath). However, depending on the report, the active site was found to contain both iron and/or copper.

Electron paramagnetic resonance (EPR) is one of the principal methods used to study metal sites and its ligand environment in a metalloprotein. Metalloproteins like pMMO with Cu^{2+} ions (Spin =1/2) and/or Fe^{3+} ions (Spin = 5/2, 1/2) etc. have EPR absorbance peaks. EPR techniques have been used successfully to probe the metal site of the pMMO complex as described in more detail in Section 5.2.

5.1.1 Introduction to EPR

The following section is a brief introduction to the fundamentals of electron paramagnetic resonance (EPR) spectroscopy for those unaccustomed to the technique.

Since electrons possess both spin (S) and charge they behave like magnets i.e. exhibit magnetic moments (paramagnetism). In the presence of an applied magnetic field, electrons can exist in two different states, either aligned parallel with the field in a ground state (low energy) or antiparallel to the field in an excited state (high energy). Transition of the electron from a low to a high-energy state is induced when an electromagnetic radiation of appropriate frequency is applied to make resonance occur (as depicted in Figure 5.1).

The resonance condition is defined as

$$h\nu = g\beta B_0$$

where

h = Planck constant
ν = frequency of applied radiation
g = constant, electronic splitting-factor (free electron=2.0023)
β= magnetic moment of the electron - Bohr magneton (0.92×10^{-23} J.T)
B_0= applied magnetic field

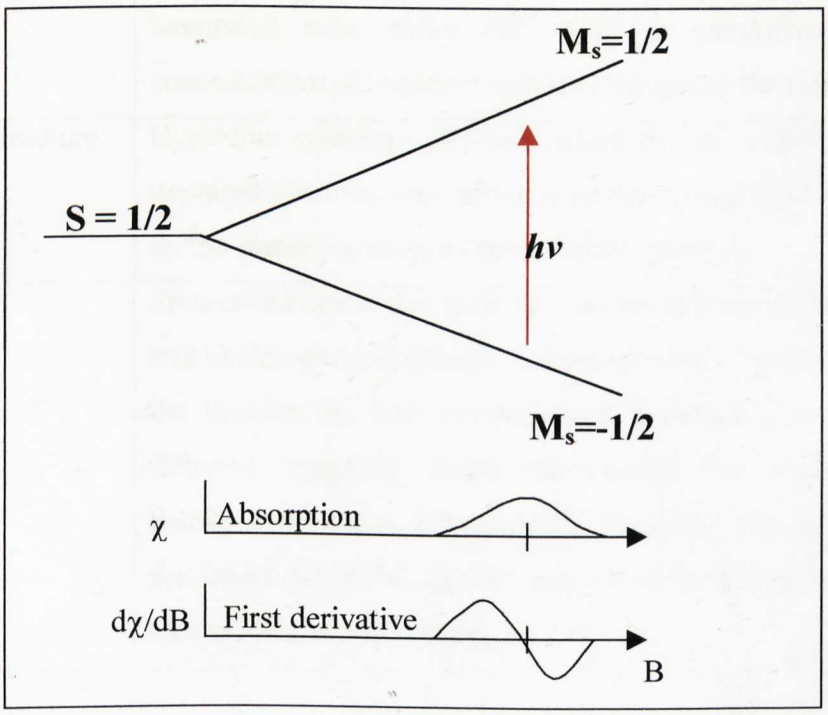

Figure 5.1 Schematic diagram of resonance (*hν*) in a two-level system giving rise to EPR absorption peaks. When the sample is placed in a magnetic field, B and an electromagnetic radiation of appropriate frequency is applied, electron transition gives rise to EPR absorption peaks (χ) and subsequent derivative spectra. The two levels are described by the magnetic quantum number M_s=±1/2.

Figure 5.1 depicts what happens when an experimental sample is placed in a magnetic field and an electromagnetic radiation of appropriate frequency is applied. The resulting

electron transition gives rise to EPR absorption peaks. The EPR spectra are displayed as the first derivative of the absorption spectra and can be characterised by four main parameters:

Parameter	Description
g-value	This is a measure of the local magnetic field of an electron giving information on the nature of bonding and the immediate environment of the unpaired electron.
Intensity	This gives information on the concentration of the radical. The integrated area under the signal is proportional to the concentration of unpaired spins giving rise to the signal.
Multiplet structure	Hyperfine splittings (A) are caused by the interaction of the unpaired electron with adjacent nuclei (I) and give information on the spatial location of atoms in the molecule
Linewidth	Spin-lattice relaxation time (T_1) is the measure of the recovery rate of the spin population after perturbation. The shorter the T_1 the broader the line. Homogenous broadening occurs due to different magnetic fields experienced by each molecule therefore, spreading the resonance frequency. Useful linewidths for observing EPR signals can be obtained by altering the temperature of the sample.

Table 5.1 Definition of the parameters associated with EPR spectra. The parameters are listed in the left-hand column and a brief definition of these parameters is given in the right -hand column.

5.1.2 Copper and EPR

It is has been established that copper is an integral element at the active site of pMMO. However, the type of copper in pMMO is still a matter of controversy and is discussed in brief here and in more detail in section 5.2. The cupric ion, Cu^{2+} ($3d^9$) is EPR detectable because of its unpaired electron whereas the cuprous ion, Cu^{+} is EPR silent. Figure 5.2 depicts the electron configuration of copper and its ions.

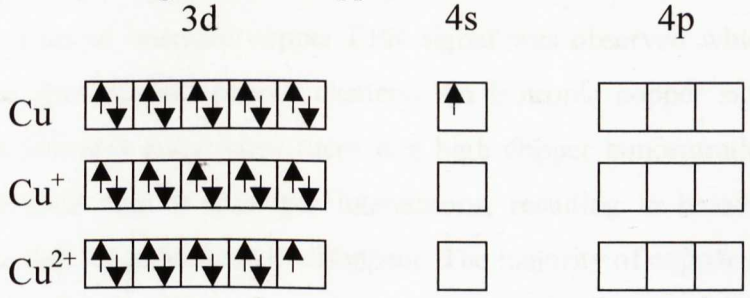

Figure 5.2 Electron configuration of copper and its ions. The 3d, 42 and 4p atomic orbitals are depicted in the schematic diagram.

Copper (II) ions use four bonds in complex formation. A type 2 Cu^{2+} centre is formed when the copper is ligated by three ligands, either 3 nitrogen atoms, 2 nitrogen and 1 oxygen atom or 2 nitrogens and 1 methionine. The fourth co-ordination site may remain free in which case the copper usually has a catalytic (C) role. If the fourth coordination site is taken then only a fifth apical site is free and therefore there is no co-ordination site available for interaction with oxygen etc. In this instance the copper will usually be involved in electron transfer (E).

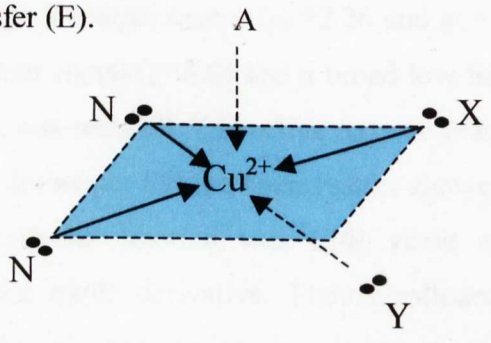

Figure 5.3 Copper (II) ions use four bound in complex formation. The spatial arrangement of a square planar complex. **A**=apical site; **N**=nitrogen; **X**=nitrogen , oxygen or methionine; **Y**=N or free.

5.2 Background to EPR studies on pMMO

Chan and coworkers (Chan *et al.*, 1993; Nguyen *et al.*, 1994, 1996a, 1996b, 1998) suggested that the copper in the active site of pMMO exists as trinuclear copper clusters. This model was based on correlating spectral (EPR) changes in the membrane fraction and purified pMMO to methane oxidation activity and to changes in copper composition of the membrane fraction. Although the as-isolated pMMO samples exhibited EPR spectrum typical of a type 2 copper signal, when the samples were oxidised with ferricyanide, a broad isotropic copper EPR signal was observed which was thought to correspond to spin-coupled copper clusters. An isotropic copper signal is an unusual signal and is normally seen when there is a high copper concentration (>1.5mM) in a sample. This gives rise to spin-spin interactions, resulting in broadening of the EPR signal and causing the $g_{\|}$ features to disappear. The majority of copper was shown to exist in Cu^{+} form by K-edge X-ray absorption spectra of membranes (Nguyen *et al.*, 1996). However, this 'broad isotropic copper signal ' was not detected in purified preparations of pMMO by Zahn and DiSpirito (1996) who claimed that this signal originated from membrane-associated copper-binding cofactors (CBCs). They claimed that this small (618Da) co-factor could bind to 2 to 3 copper atoms and exhibited a complex EPR spectrum, which could account for the previously observed copper EPR signals in the membrane fraction of Nguyen *et al.* (1996).

The EPR spectrum of the purified enzyme observed by Zahn and DiSpirito (1996) showed evidence for a type 2 copper centre ($g_{\|}$=2.26 and $g_{\perp}$= 2.06, $A_{\|}^{Cu}$ = 180 G, A^{N} = 15G), a weak high spin iron signal (g=6.0) and a broad low field signal at g=12.5 which was lost when the sample was reduced. The active enzyme complex was found to contain 2.5 iron and 14.5 copper atoms per 99kDa.Their results showed that the majority of iron associated with the membrane fraction was EPR silent and only detectable after formation of an iron-nitric oxide derivative. They concluded that the non-haem iron existed as a single ferrous iron centre, an iron-iron centre or an iron-copper. The presence of iron in the enzyme was also supported by the observation of copper-induced iron uptake into the membranes, activation of pMMO by ferric ions in purified preparations of

Methylococcus capsulatus (Bath) and inhibition of the formation of the nitric oxide-ferrous iron complex by preincubation of membrane samples with nitrapyrin.

There is some confusion over the exact nature of the copper ions and whether iron plays any role in the active site of pMMO. Antholine and coworkers (Yuan *et al.* 1997, 1998, 1999; Lemos *et al.*, 2000) have carried out X band and S band EPR studies on whole cells from *Methylococcus capsulatus* (Bath) of *Methylomicrobium albus* BG8, which were grown in media enriched with ^{63}Cu and ^{15}N. They observed two nearly identical type 2 copper signals in both *Methylococcus capsulatus* (Bath) and *Methylomicrobium album* BG8 cells. The second signal found in membrane fractions was attributed to the oxidation of cupric sites. The S-band EPR spectra gave resolved N hyperfines in the $g_{\perp}$ region and established unambiguously that one copper was ligated to 4 nitrogens. They have not as yet carried out investigations on the purified pMMO enzyme.

The reproducible isolation of a duroquinol-driven pMMO complex has allowed investigations to be carried out in order to clarify the nature of metal ions in the active site of the pMMO.

5.3 EPR spectra of as-isolated protein samples

As previously discussed in this chapter, EPR signals corresponding to a ferric iron and a type 2 copper ions were observed in purified pMMO samples obtained by Zahn and DiSpirito (1996) from *Methylococcus capsulatus* (Bath). These findings were disputed by the Nguyen *et al.* (1998), who claimed that the iron associated with the pMMO was due to iron-containing contaminants. In addition to this, they proposed that the copper ions existed as trinuclear copper clusters (Chan *et al.*, 1993; Nguyen *et al.*, 1994, 1996a, 1996b, 1998). Although, Yuan and co-workers (Yuan *et al.* 1997, 1998, 1999; Lemos *et al.*, 2000) found no evidence for iron in pMMO from *Methylomicrobium albus* BG8 cells. They observed copper signals corresponding to a Cu^{2+} ion ligated to 4 nitrogens.

The first stage of metal analysis by EPR spectroscopy was to examine as-isolated pMMO samples for copper and iron signals. Samples of membrane-associated, solubilised and purified pMMO were prepared *Methylococcus capsulatus* (Bath) as described in Section 2.7 and Section 3.3. The X-band EPR spectra were recorded on a Bruker ESP 300 spectrometer.

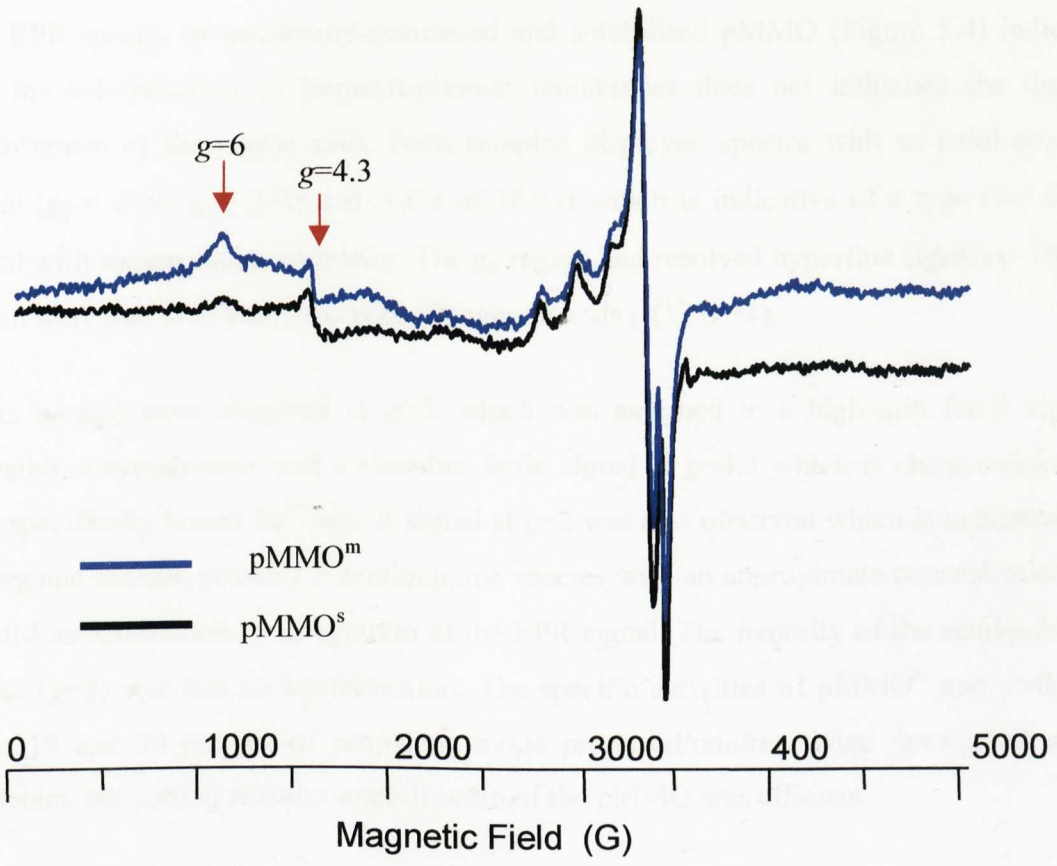

Figure 5.4 EPR spectra of the membrane fraction and the solubilised membrane of *Methylococcus capsulatus* (Bath). 200μl of membrane sample (27mg/ml) and solubilised membrane sample (15mg/ml) were prepared for analysis as described in Section 2.8. Both spectra ($pMMO^m$ and $pMMO^s$) had an axial copper signal with EPR parameters of $g_{||}$= 2.24 and $g_{\perp}$= 2.06, $A_{||}^{Cu}$=185G, A^N=15G (see Figure 5.8). Spectra were recorded at a microwave power of 10mW, a temperature of 10K and a modulation amplitude of 5G.

The EPR spectra of membrane-associated and solubilised pMMO (Figure 5.4) indicate that the solubilisation of intracytoplasmic membranes does not influence the ligand environment of the cupric sites. Both samples displayed spectra with an axial copper signal ($g_{\|}$ = 2.24, $g_{\perp}$= 2.06 and $A_{\|}Cu$ of 185G) which is indicative of a type two Cu^{2+} signal with square planar geometry. The $g_{\perp}$ region had resolved hyperfine signals (~15G), which were due to interactions with nitrogen ligands ($I(^{14}N)$ =1).

Other signals were observed at g=6, which was assigned to a high-spin ferric signal (possibly a cytochrome) and a rhombic ferric signal at g=4.3 which is characteristic of non-specifically bound Fe^{3+} ion. A signal at g=2 was also observed which is indicative of an organic radical, possibly a semiquinone species with an approximate concentration of < 3μM as determined by integration of the EPR signal. The majority of the semiquinone signal (g=2) was lost on solubilisation. The specific activities of $pMMO^{m}$ and $pMMO^{s}$ were 19 and 30 nmoles of propylene oxide produced/min/mg using duroquinol as a reductant, suggesting that the solubilisation of the pMMO was efficient.

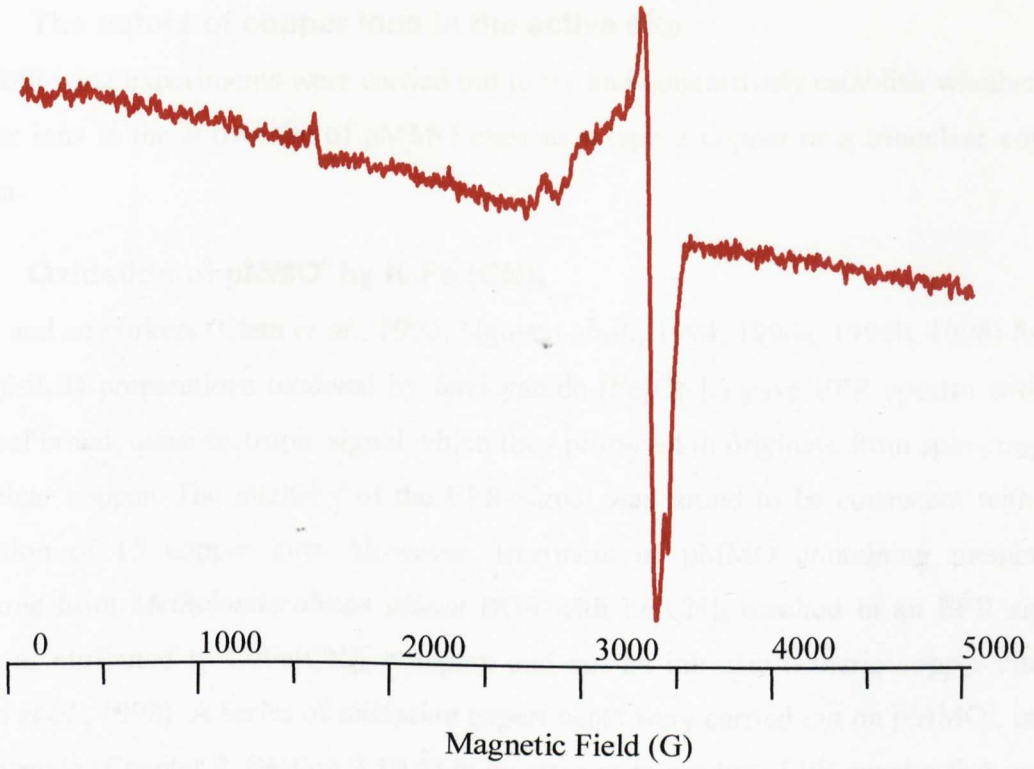

Figure 5.5 EPR spectrum of purified pMMO complex from *Methylococcus capsulatus* (Bath). 200µl of pMMO^c (5mg/ml) was prepared for analysis as described in Section 2.8. The cupric signal had EPR parameters of $g_{||}$ = 2.24, $g_{\perp}$=2.06 and $A_{||}^{Cu}$ =185G. Spectra were recorded at a microwave power of 10mW, a temperature of 10K and a modulation amplitude of 5G.

The purified pMMO complex (Figure 5.5) also displayed a type 2 copper EPR signal (~30-40µM Cu^{2+}ions) and a signal at g=4.3 corresponding to 'junk iron' similar to the signal seen in Figure 5.4. This suggests that the purification process does not affect the EPR cupric signal. The signals at g=2 and g=6 were not observed suggesting these signals which may be contaminants (cytochromes and semiquinone species), had been removed during the purification process. The specific activity of pMMO^c using duroquinol as a reductant was ~50nmoles of propylene oxide produced/min/mg. The g=12.5 signal observed by Zahn and DiSpirito (1996), possibly corresponding to a diferric cluster, was not observed in this study.

The preliminary EPR data of pMMO supports a type 2 copper site and provides no evidence for a trinuclear copper cluster or an iron in the active site.

5.4 The nature of copper ions in the active site

The following experiments were carried out to try and conclusively establish whether the copper ions in the active site of pMMO exist as a type 2 copper or a trinuclear copper cluster.

5.4.1 Oxidation of pMMO^c by $K_3Fe(CN)_6$

Chan and coworkers (Chan *et al.*, 1993; Nguyen *et al.*, 1994, 1996a, 1996b, 1998) found that pMMO preparations oxidised by ferricyanide ($Fe[CN]_6$) gave EPR spectra with an unusual broad, quasi-isotropic signal which they proposed to originate from spin-coupled trinuclear copper. The intensity of the EPR signal was found to be consistent with the oxidation of 15 copper ions. However, treatment of pMMO containing membrane fractions from *Methylomicrobium album* BG8 with $Fe[CN]_6$ resulted in an EPR signal that was attributed to $CuFe[CN]_6$ complex and not an intrinsic trimeric copper cluster (Yuan *et al.*, 1998). A series of oxidation experiments were carried out on pMMO^c, using ferricyanide (Chapter 2, Section 2.10.5) in an attempt to produce EPR spectra that would indicate whether a trinuclear copper cluster was present as observed by Chan and coworkers.

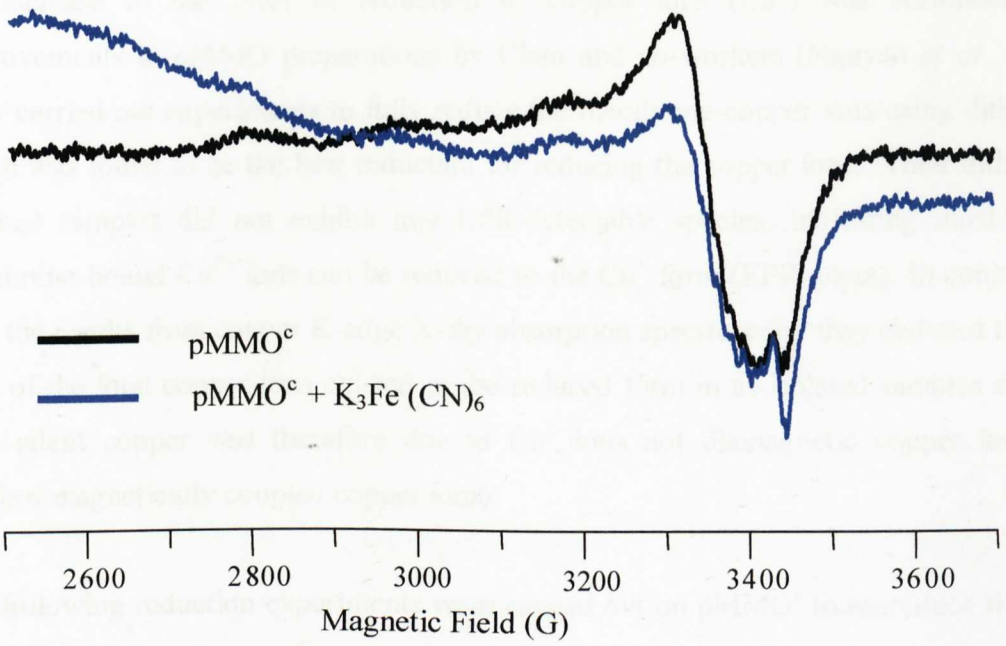

Figure 5.6: X-band EPR spectra of the purified pMMO complex before and after oxidation. 170μl purified pMMO complex was incubated with 1mM $K_3Fe[CN]_6$ as described in Section 2.8. Spectra were recorded at a microwave power of 100μW, a temperature of 9K and a modulation amplitude of 5G.

Neither, the broad, quasi-isotropic EPR signals (Nguyen *et al.*, 1996) nor the $CuFe[CN]_6^{2-}$ complex (Yuan *et al.*, 1998) were observed in the oxidised spectra of pMMO (Figure 5.6) in this study. Oxidation of $pMMO^c$ resulted in a slight increase in the intensity of the Cu^{2+} EPR signal but the concentration did not increase by a factor of 2 to 3 as reported by Chan and coworkers (Nguyen *et al.*, 1996, 1998). The broad peak around 2500G is due to $CuFe[CN]_6^{2-}$ and prevents an exact determination of the Cu^{2+} concentration. These results indicate that there are some oxidisable Cu^+ ions present in as-isolated pMMO complex.

5.4.2 Reduction of pMMO^c

An increase in the level of reduction of copper ions (Cu^+) was correlated with improvements in pMMO preparations by Chan and co-workers (Nguyen *et al.*, 1996). They carried out experiments to fully reduce the membrane-copper ions using dithionite, which was found to be the best reductant for reducing the copper ions. Their dithionite-reduced samples did not exhibit any EPR-detectable species, indicating most of the membrane-bound Cu^{2+} ions can be reduced to the Cu^+ form (EPR silent). In conjunction with the results from copper K-edge X-ray absorption spectroscopy they deduced that 70-80% of the total copper ions existed in the reduced form in as-isolated samples and any EPR silent copper was therefore due to Cu^+ ions not diamagnetic copper ions e.g. antiferromagnetically coupled copper ions).

The following reduction experiments were carried out on pMMO^c to reproduce the EPR spectra of Chan and coworkers and therefore supporting the theory that the majority of copper ions may exist in the Cu^+ form. pMMO^c was placed in an EPR tube, evacuated and then flushed with argon several times to obtain anaerobic conditions. Anaerobic solutions of the reductant and the mediator phenyl methyl sulphate (PMS) were then added and the sample was incubated for 10 minutes prior to EPR measurements Chapter 2, section 2.10.5).

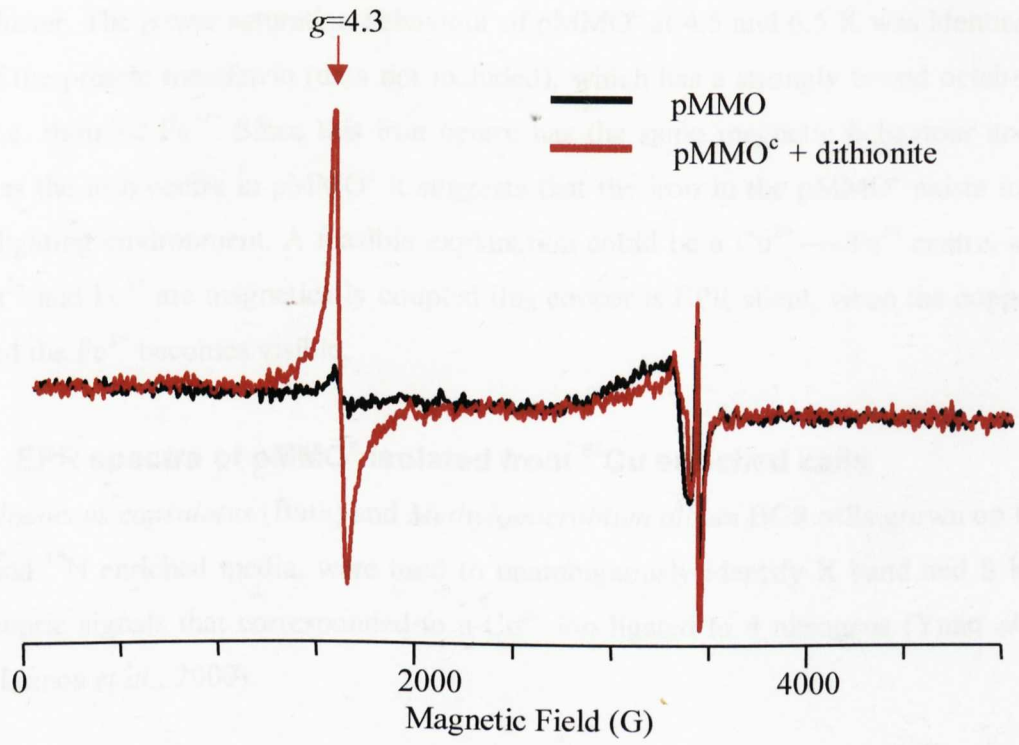

Figure 5.7 X band EPR spectra of ferric site of pMMO^c after reduction by dithionite. The anaerobic sample pMMO^c was reduced with 1mM sodium dithionite in presence of the mediator 100μM phenyl-methyl sulphate (PMS). The spectra were recorded at temperature 4K, modulation frequency 100kHz, modulation amplitude 5G and power 1mW. The radical signal at g=2 is due to PMS.

The reduction of pMMO^c by dithionite/PMS (figure 5.7) resulted in a decrease in the Cu^{2+} EPR signal, but not complete reduction of the Cu^{2+} ions as observed by Nguyen *et al.* (1996). The spectrum of the reduced pMMO^c gave an unexpected, dramatic increase in a symmetrical signal at g=4.3, which is usually characteristic of non-specifically bound Fe^{3+} ions. The concentration of Fe^{3+} ions in pMMO^c was estimated to be approximately 33 μM by integration of the Fe^{3+} EPR signal.

However, this is a curious result as the reduction of Fe^{3+} to Fe^{2+} (EPR silent) ions by dithionite, would result in a decrease not an increase of the iron signal (g=4.3). This effect has also been seen in *Methylococcus capsulatus*, strain M (Dr B. Katterle. pers.com.). Therefore, the increase in the Fe^{3+} signal (g=4.3) was thought to be due to an iron cluster. The power saturation behaviour of $pMMO^c$ at 4.5 and 6.5 K was identical to that of the protein transferrin (data not included), which has a strongly bound octahedral iron, i.e. rhombic Fe^{3+}. Since this iron centre has the same magnetic behaviour and g-value as the iron centre in $pMMO^c$ it suggests that the iron in the $pMMO^c$ exists in the same ligating environment. A feasible explanation could be a Cu^{2+}-----Fe^{3+} centre, since the Cu^{2+} and Fe^{3+} are magnetically coupled this copper is EPR silent, when the copper is reduced the Fe^{3+} becomes visible.

5.5 EPR spectra of $pMMO^c$ isolated from ^{63}Cu enriched cells

Methylococcus capsulatus (Bath) and *Methylomicrobium album* BG8 cells grown on both ^{63}Cu and ^{15}N enriched media, were used to unambiguously identify X band and S band EPR cupric signals that corresponded to a Cu^{2+} ion ligated to 4 nitrogens (Yuan *et al.*, 1996; Lemos *et al.*, 2000)

The following experiment was carried out to try and establish whether the superhyperfine splittings (A^N) observed in the EPR visible cupric site of pMMO were consistent with spectrum for a type 2 copper and to identify the ligand environment. The copper isotopes have a natural abundance of 69% ^{63}Cu and 31% ^{65}Cu, both have nuclear spins of I=3/2 and the ratio of the nuclear moments of ^{63}Cu and ^{65}Cu is 1.07. Therefore, *Methylococcus capsulatus* (Bath) cells were grown in ^{63}Cu enriched media to avoid superposition of signals from ^{63}Cu and ^{65}Cu.

Methylococcus capsulatus (Bath) cells grown in ^{63}Cu enriched media were kindly donated by Dr S. Charlton (Charlton, 1997) and the $pMMO^c$ was isolated as described in Chapter 3.

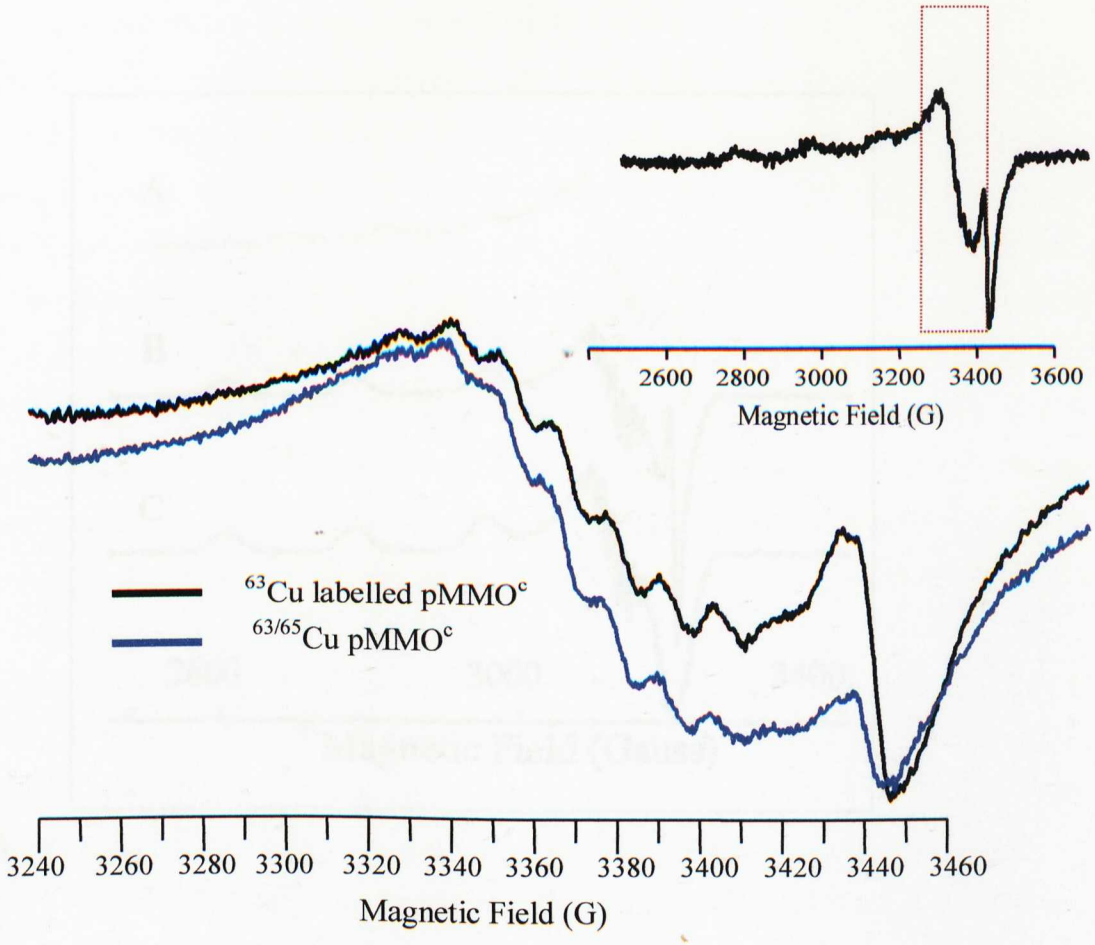

Figure 5.8 X-band EPR spectra of pMMO complex isolated from *Methylococcus capsulatus* (Bath) cells grown in ^{63}Cu-enriched and non-enriched media. pMMO^{c} samples were purified and prepared for EPR analysis as described in Section 2.7. Spectra were recorded at a microwave power of 100 μW, a modulation frequency of 100 kHz, a temperature of 10K and a modulation amplitude of 5 G.

As expected, the N-hyperfines were better resolved in the spectra of pMMO^{c} from *Methylococcus capsulatus* (Bath) cells grown in ^{63}Cu enriched media than spectra of pMMO^{c} from *Methylococcus capsulatus* (Bath) cells grown in non-enriched copper media (see Figure 5.8). The N-hyperfines were not as pronounced as expected suggesting the copper exchange may not be complete. There are some traces of the radical signal (g=2) in this sample.

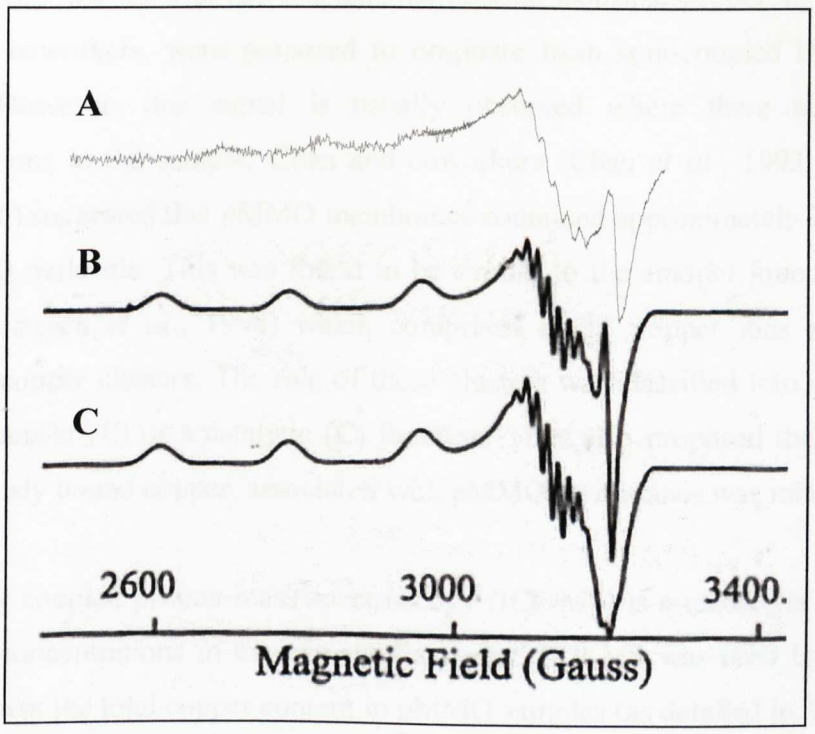

Figure 5.9 A comparison of the experimental cupric signal from *Methylococcus capsulatus* (Bath) with a simulation consistent of type 2 copper spectrum by Yuan and coworkers (adapted from Yuan *et al.* 1996). **(A)** copper EPR signal ($g_{||}$=2.24) of pMMO^c from *Methylococcus capsulatus* (Bath) from this study **(B)** simulation of type 2 copper signal ($g_{||}$=2.24) with simulated free radical at g=2.007 **(C)** simulation of type 2 copper signal without simulated free radical.

The experimental spectrum of ^{63}Cu labeled pMMO^c were compared to simulations of a type 2 copper spectrum (Figure 5.9). It could be concluded from this that the seven-line pattern observed in the $g_{\perp}$ region in EPR spectra of pMMO^c is consistent with spectra arising from an unpaired electron spin on a copper coupled to three or four nitrogens. It is not reasonable to suggest that the spectra consists of a ten-line pattern arising from three equivalent I=3/2 copper nuclei as observed for a trinuclear copper cluster model as proposed by Chan and coworkers (Chan *et al.*, 1993; Nguyen *et al.*, 1994, 1996 and 1998).

5.6 Concentration of copper in the pMMO

As previously discussed in this chapter, the unusual isotropic copper signal observed by Chan and coworkers, were proposed to originate from spin-coupled trinuclear copper clusters. However, this signal is usually observed where there are high copper concentrations in the sample. Chan and coworkers (Chan *et al.*, 1993; Nguyen *et al.*, 1994, 1996) suggested that pMMO membranes contained approximately 20 copper atoms per pMMO molecule. This was found to be similar to the amount found in the purified pMMO (Nguyen *et al.*, 1998) which comprised of 15 copper ions arranged into 5 trinuclear copper clusters. The role of these clusters was classified into either having an electron transfer (E) or a catalytic (C) function. They also proposed that the amount of adventitiously bound copper, associated with pMMO membranes was minimal.

Inductively coupled plasma-mass spectroscopy (ICP-MS) is a technique used to analyse the metal concentrations in experimental samples. ICP-MS was used by Nguyen *et al.* (1998) to give the total copper content in pMMO samples (as detailed in Table 5.2). Zahn and DiSpirito (1996) found as-isolated pMMO to contain approximately 14 nmoles of copper atoms per nmole of purified pMMO. They suggested that the EPR spectra which were proposed to correspond to trinuclear copper (Chan *et al.*, 1993; Nguyen *et al.*, 1994, 1996 and 1998) may be due to the copper ions associated with the copper binding cofactor (CBC).

The following ICP-MS analysis was carried out to obtain the total concentration of metal ions in the pMMO complex. ICP-MS was performed by the Warwick analytical service, University of Warwick. Protein samples were prepared as described in Chapter 2, section 2.10.5..

	Copper/ Protein (μmoles/mg)	Iron/ Protein (μmoles/mg)	Specific Activity (nmoles of propylene oxide produced/min/mg)
pMMO Nguyen et al. (1998)	0.133-0.141 (15)	0	2.6-5.1
$pMMO^c$ (as isolated) * This study	0.025 (3)	0.011 (1)	30
$pMMO^c$ +10mM EDTA This study	0.010 (1)	0.009 (1)	15

Table 5.2 Copper and iron metal analysis of purified pMMO complex
*Metal ion analysis was performed on buffer alone and deducted from sample values. Values in parentheses show the approximate number of copper atoms per protein molecule assuming a molecular mass of 104kDa as estimated from protein sequences available on the NCBI database (http://www.ncbi.nim.nih.gov) under accession number L40804.

After $pMMO^c$ was treated with 10mM EDTA, the ICP-MS measurements (Table 5.2) shows that the total concentration of copper ions decreased by approximately 2 fold to 0.01μmoles/mg. The concentration of total iron did not notably decrease after EDTA-treatment. The specific activity of the $pMMO^c$ decreased by 50% suggesting that the copper ions removed were essential for activity. When the EDTA-treated $pMMO^c$ sample was analysed by EPR (Figure 5.10) there was no drastic change in the cupric signal although the N-superhyperfines were slightly better resolved indicating that very little of the Cu^{2+} ions were removed. This indicates that the copper ions removed do not contribute to the cupric signal but are still necessary for the enzyme i.e. EPR silent copper ions.

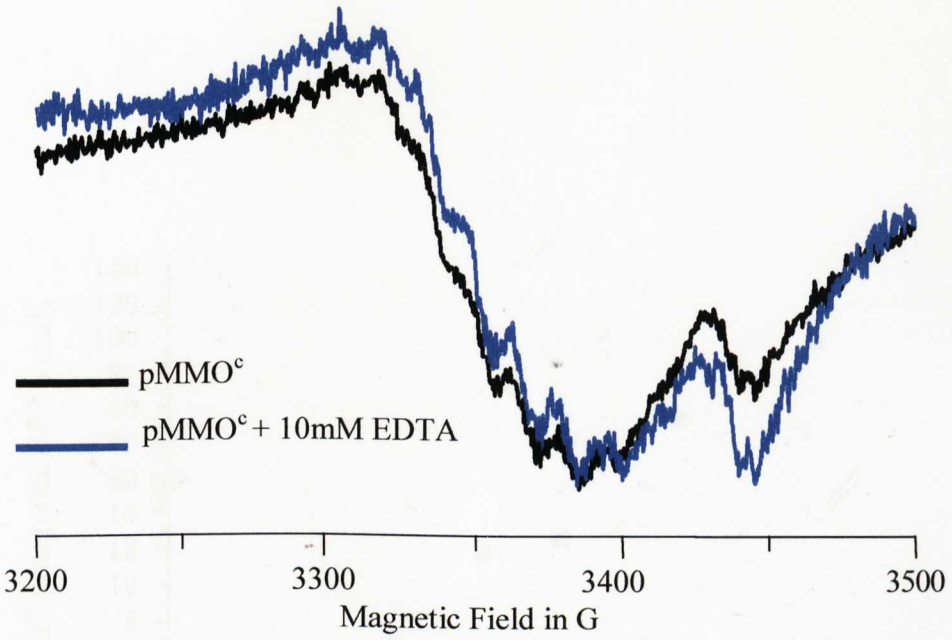

Figure 5.10 Spectra of purified pMMO complex before and after EDTA-treament. 10mM EDTA was added to 200μl of purified pMMO^c and then removed by washing as described in Section 2.8. The spectra were recorded at The blue curve is pMMO^c washed with EDTA. Recording conditions are: temperature 10K, modulation frequency of 100kHz, modulation amplitude of 5G, power 100 μW.

Having ascertained that extra coppers were required for enzyme activity, the following experiment was carried out to investigate the effect of copper addition to the EDTA-treated pMMO^c to see if the added copper ions would undergo magnetic interaction therefore supporting the trinuclear copper cluster proposal by Chan and coworkers (Chan *et al.*, 1993; Nguyen *et al.* 1994, 1996, 1998). The EDTA-treated pMMO^c sample was estimated to have approximately 14μM Cu^{2+} ions, by integration of the copper signal and was the value for $[Cu]_0$ in the following copper titration experiment. The addition of Cu^{2+} ions was correlated with the concentration of Cu^{2+} ions that could be calculated by integration of the corresponding signal. Any magnetic interaction of the copper ions would result in a lower intensity cupric signal than expected for the corresponding concentration of Cu^{2+} ions added.

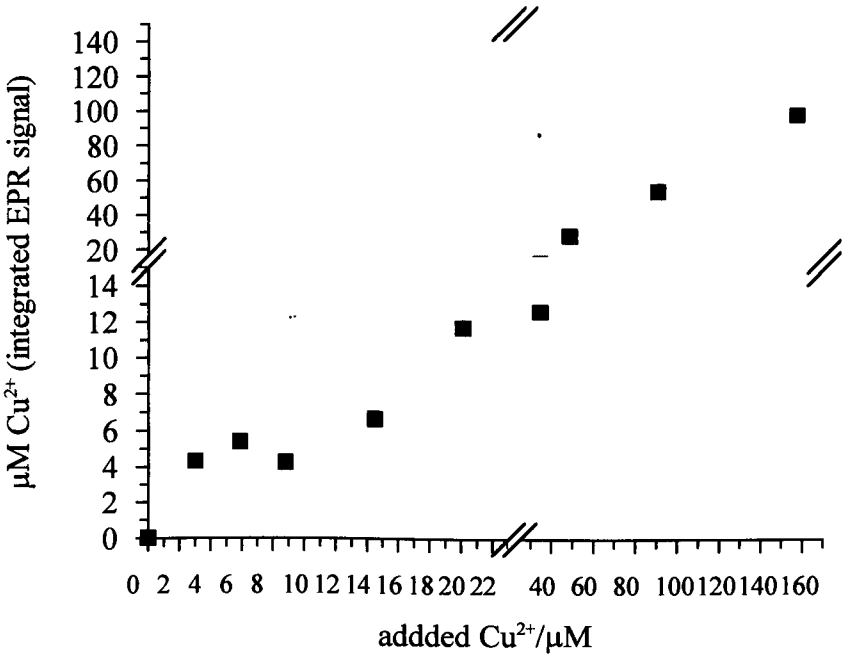

Figure 5.11 Graph of copper titration against concentration of copper deduced by corresponding signal in pMMO complex. $CuSO_4$ was sequentially added to 200µl of as-isolated pMMO^c (5mg/ml), to give the final concentrations detailed in x-axis above (Chapter 2, Section 2.10.5). Corrected by $[Cu]_0$ = 14µM.

Figure 5.11 demonstrates that the addition of copper was reflected by the same increase in Cu^{2+} detection. This infers that there is no magnetic interaction between the added coppers i.e. there was no copper cluster formation, and is evidence (though not conclusive) that does not support the trinuclear copper cluster hypotheses suggested by Chan and coworkers (Chan *et al.*, 1993; Nguyen et al., 1994, 1996 and1998).

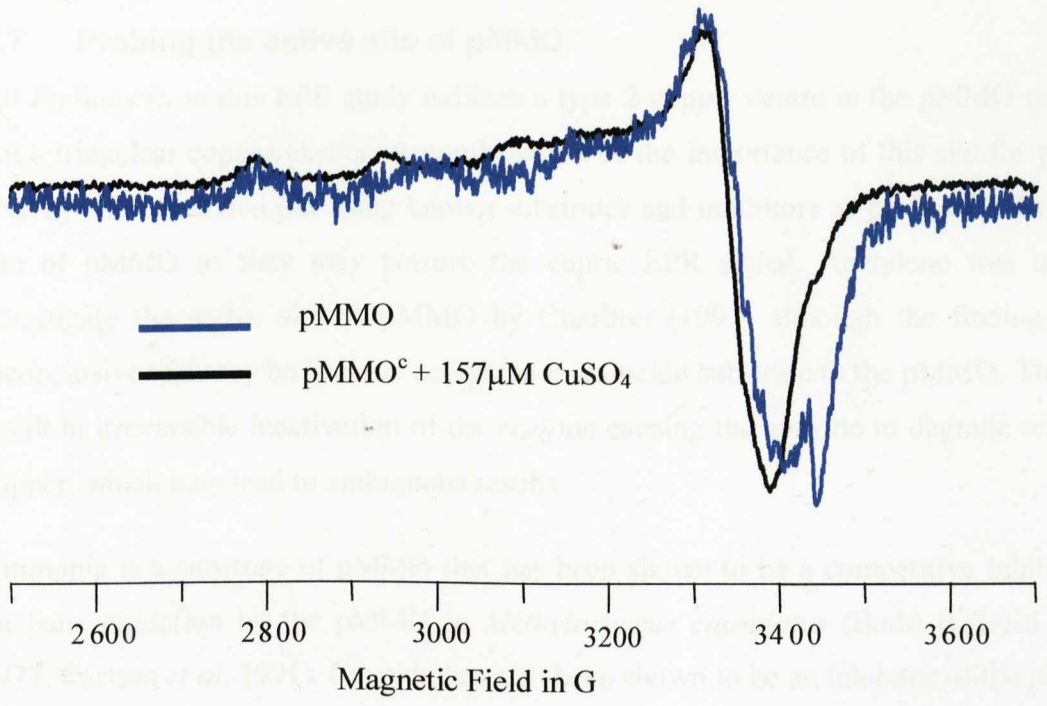

Figure 5.12 EPR spectra of the pMMO complex before and after addition of 157μM copper. The blue curve represents untreated pMMO^c and the black curve represents pMMO^c + 157 μM Cu^{2+}. The spectra were recording using conditions: temperature 10 K, modulation frequency 100 kHz, modulation amplitude 5 G, power 100 μW.

The EPR parameters of the cupric site shifted slightly with the addition of 157μM copper and there was no resolution of the N hyperfines (Figure 5.12). The extra adventitiously bound copper superimposed the pMMO^c cupric site making it difficult to distinguish the environment of the coppers based on analysis of the copper hyperfines and *g*-values. Interestingly, this spectrum was similar to the oxidised pMMO sample spectra observed by Chan and co-workers (Nguyen *et al.*, 1996 and 1998). This indicates that the concentration of copper is unusually high in the sample and may contribute to the broad isotropic signal thought to correspond to trinuclear copper clusters by Chan and co-workers. This is in agreement with the proposal by Zahn and DiSpirito (1996) although

they suggest that the signal may be due to the association of copper ions to copper binding cofactors (CBCs).

5.7 Probing the active site of pMMO

All findings from this EPR study indicate a type 2 copper centre in the pMMO complex not a trinuclear copper cluster. A confirmation of the importance of this site for pMMO activity can be carried out using known substrates and inhibitors as probes for the active site of pMMO as they may perturb the cupric EPR signal. Acetylene was used to investigate the active site of pMMO by Charlton (1997) although the findings were inconclusive and may be because acetylene is a suicide substrate to the pMMO. This may result in irreversible inactivation of the enzyme causing the enzyme to degrade releasing copper, which may lead to ambiguous results.

Ammonia is a substrate of pMMO that has been shown to be a competitive inhibitor of methane oxidation by the pMMO in *Methylococcus capsulatus* (Bath) (O'Neill *et al.*, 1977; Carlsen *et al.* 1991). Cyanide has also been shown to be an inhibitor of the pMMO^c although its mode of inhibition is still unclear (Prior and Dalton, 1985; This study).

pMMO^c samples were treated with ammonia and cyanide to determine whether there were any changes in the copper superhyperfines and *g*-values, due to binding of the copper active site (Chapter 2, section 2.10.5).

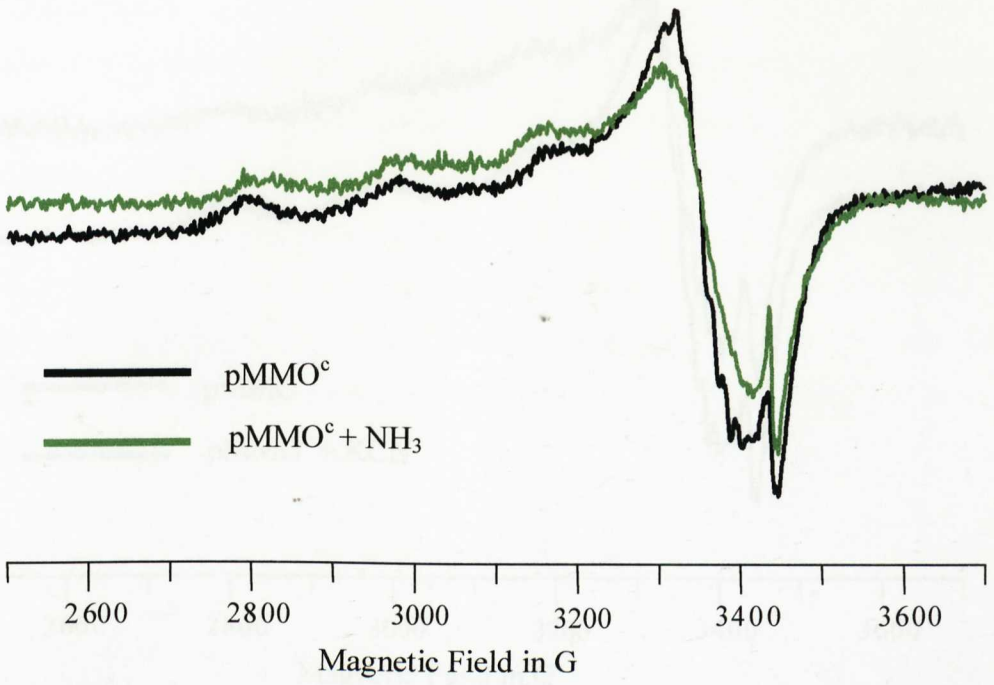

Figure 5.13 EPR spectrum of pMMO complex before and after the addition of ammonia solution. 500μM ammonia solution (adjusted to pH 8 with HCl) was added to 200μl pMMO (5mg/ml) (Final concentration of reaction mixture was pH 7.5) as described in Section 2.8. Spectra were recorded at a microwave power of 5mW, a temperature of 10K and a modulation amplitude of 5G.

There is no change in the overall spectra (Figure 5.13) when $pMMO^c$ is treated with ammonia solution but the N superhyperfines of the cupric site have disappeared. This result indicates that there is some interaction of ammonia with cupric site of pMMO which is in agreement with the proposal that ammonia is a competitive inhibitor of methane oxidation.

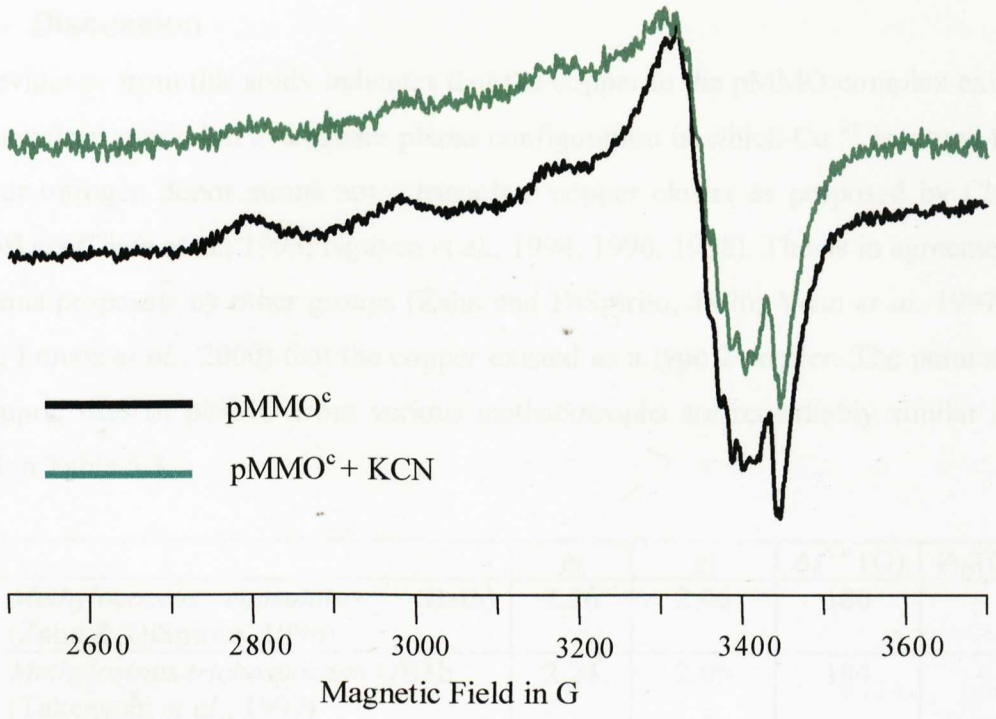

Figure 5.14 EPR spectrum of pMMO complex before and after the addition of cyanide. 500μM potassium cyanide (KCN) was added to 200μl pMMO (5mg/ml) as described in Section 2.8. Spectra were recorded at a microwave power of 5mW, a temperature of 10°K and a modulation amplitude of 5G.

There was no change observed in the overall spectrum and the N hyperfines (Figure 5.14) when the pMMO^c was treated with KCN indicating that KCN does not bind to the cupric site of pMMO. There is a slight decrease in the amount of visible copper, which infers that some Cu^{2+} ions were reduced to Cu^{+} ions. The reason for the reduction of Cu^{2+} ions by KCN is not clearly understood.

5.8 Discussion

The evidence from this study indicates that the copper in the pMMO complex exists as a mononuclear cupric ion in a square planar configuration in which Cu^{2+} is bound to three or four nitrogen donor atoms not a trinuclear copper cluster as proposed by Chan and coworkers (Chan et al., 1993; Nguyen et al., 1994, 1996, 1998). This is in agreement with previous proposals by other groups (Zahn and DiSpirito, 1996; Yuan *et al.* 1997, 1998, 1999; Lemos *et al.*, 2000) that the copper existed as a type 2 copper. The parameters of the cupric sites of pMMO from various methanotrophs are remarkably similar and are listed in Table 5.3.

	$g_{\|}$	$g_{\|}$	$A_{\|}^{Cu}$ (G)	A_N(G)
Methylococcus capsulatus (Bath) (Zahn & DiSpirito, 1996)	2.26	2.06	180	-
Methylosinus trichosporium OB3b (Takeguchi *et al.*, 1997)	2.24	2.06	184	-
Methylococcus capsulatus (Bath) (Nguyen *et al.*, 1998)	2.25	2.06	181	-
Methylomicrobium album BG81 *Methylomicrobium album* BG8 2 *Methylococcus capsulatus* (Bath) 1 *Methylococcus capsulatus* (Bath) 2 (Lemos *et al.*, 2000)	2.243 2.251 2.244 2.246	2.067	180 180 185 180	18 18 19 19
Methylococcus capsulatus (Bath) (This study, 2000)	2.24	2.06	185	15

Table 5.3 EPR parameters for type 2 copper from various methanotrophs by various groups.

The following evidence indicates that the cupric site of pMMO exists as a type 2 **not** a trinuclear cluster copper:-

1)The samples from *Methylococcus capsulatus* (Bath) cells grown in ^{63}Cu enriched media had EPR parameters (g =2.24) which are consistent with a cupric ion with 3 or 4 equivalent nitrogen donor atoms as determined from Peisach-Blumberg plots simulated by Yuan *et al.* (1997). Whether a seven-line or nine-line pattern corresponding to 3 nitrogens or 4 nitrogens respectively was obtained could not be resolved, which is perhaps unsurprising from natural abundance samples. Lemos *et al.* (2000) found that the

resolution of EPR spectra was considerably improved in cells grown in ^{15}N enriched media. If one delocalised electron over three approximately equivalent coppers a 10-line pattern with one-third of the coupling expected from monomeric copper should be observed. This signal was not observed in this study.

2) Ferricyanide-oxidised samples (Figure 5.6) did not produce the unusual isotropic EPR spectrum observed by Chan and coworkers (Nguyen *et al.*, 1996 and 1998). Possible reasons for their signal have been suggested to be due to copper binding cofactors (Zahn and DiSpirito, 1996), a $CuFe[CN]_6$ complex (Yuan *et al.*), or adventitiously bound copper ions.

The latter proposal is substantiated by the fact that when 157 μM Cu^{2+} ions was added to $pMMO^c$, the resultant spectrum (figure 5.12) was similar to the oxidised spectra of pMMO samples observed by Chan and coworkers (Chan *et al.*, 1993; Nguyen *et al.*, 1994, 1996, 1998). This indicates that the concentration of copper in the pMMO samples purified by Chan and coworkers was very high. If this is so, the excess coppers may be kept reduced (Cu^+) by the chemicals used to maintain anaerobic conditions e.g. dithionite, during protein purification and on oxidation may give rise to the broad isotropic EPR signal observed. Indeed, the copper concentrations of the $pMMO^c$ samples calculated by ICP-MS in this study (0.025μmoles/mg of protein) were ~5 times lower than the concentrations observed by Nguyen *et al.*, 1998 (0.141μmoles/mg of protein). A control experiment (this study, data not shown) carried out with mixed lipid/detergent micelles shows that the micelles strongly bind Cu^{2+} ions.

In the EDTA-treated $pMMO^c$ sample, the copper concentration deduced by integration of the cupric EPR signal (0.003 μmoles/mg of protein) was ~3 fold lower than the concentration of copper as calculated by ICP-MS (0.01μmoles/mg of protein). This indicates that for every EPR detectable Cu^{2+} there is ~3 EPR silent copper ions. These could exist as Cu^+ ions or as a magnetically coupled Cu^{2+}--Fe^{3+} centre. This is in agreement with proposal that there are two or three EPR silent Cu^+ ions for every EPR detectable Cu^{2+} ion in *Methylomicrobium album* BG8 (Lemos *et al.*, 1998). They also

conclude that the enzyme (47, 27 and 25 kDa) comprises of four coppers which is a more reasonable suggestion than the 15 coppers since they propose that it is difficult to place even 3-5 copper ions in copper binding sites based on the pMMO amino acid sequences.

There is also mounting evidence that the functioning pMMO complex contains Fe^{3+}, possibly as a Cu^{+}------Fe^{3+} cluster. This proposal is supported by the findings of magnetic susceptibility measurements on as-isolated membranes by Nguyen *et al.* (1994). Their results indicate notable levels of diamagnetic copper ions, which could arise from antiferromagnetically-coupled copper ions.

The presence of iron has also been observed in purified pMMO from *Methylococcus capsulatus* (Bath) by Zahn and DiSpirito (1996), although it is largely EPR silent and can only be observed after the formation of a ferrous-nitric oxide derivative (g=4.03). Our preliminary experiments have not successfully reproduced this iron-NO complex as yet. Neither has the broad EPR signal at g=12.5 been observed which has been proposed by Nguyen *et al.* (1998) to be due to iron-containing contaminants. The presence of iron was also observed in purified pMMO from *Methylosinus trichosporium* OB3b (Takeguchi *et al.*, 1997).

Clearly, the presence of any iron-containing protein, found in $pMMO^{c}$ from this study, is vital for the efficient functioning of the duroquinol-driven pMMO complex as protein contamination has been minimised during purification.

When pMMO is treated with ammonia, the N superhyperfines disappear from the spectra (Figure 5.13) indicating that ammonia perturbs to the cupric site of pMMO as would be expected for a competitive inhibitor. However, recent studies by Lemos *et al.* (2000) suggest that there is a second type 2 copper signal with unresolved N hyperfines, which can not be distinguished from the normal type 2 copper signal in *Methylococcus capsulatus* (Bath) cells grown in natural abundance media. If this is the case, the findings may point to the binding of ammonia to the usual cupric site thus giving rise to a clearer second cupric signal with no N hyperfines.

Inhibition profiles have shown KCN to be an inhibitor to pMMO[c] although the exact mode of inhibition is unknown. The spectra of KCN-treated pMMO indicates that KCN does not directly inhibit pMMO by binding to the cupric site. A possible explanation could be that KCN inhibits the reductase component of the pMMO complex, which may have an indirect role in the oxidation of copper ions.

5.7 Summary

The results of this study indicate that the copper in the active site of pMMO exists as a type 2 copper, that is a cupric ion bound to three or four nitrogen donor atoms, not as trinuclear copper clusters. In addition to this, there is evidence to suggest that there may be an iron cluster in the pMMO complex, possibly a Cu^{2+}--Fe^{3+} centre, which is EPR silent in as-isolated pMMO samples. The role of this iron centre for pMMO activity is still unclear.

Having ascertained the nature of metal ions in the active site of pMMO it was thought necessary to try and elucidate a gross structure for the complex in order to place possible binding sites for the type 2 Cu^{2+} in pMMO.

6. Structural determination of the pMMO complex

6. 1 Introduction

The structural information of the pMMO complex has been hindered by the small amount of purified active protein available. To date, any structural information of the protein has been deduced from hydrophobicity plots of the pMMOH protein sequences, as previously discussed in Chapter 1 (Semrau *et al.*, 1995 and Elliott, *et al.*, 1998). X-ray crystallography is a technique that offers high-resolution structures of proteins but is often not practical for use on membrane proteins as these preparations usually contain detergents, which can hinder the crystallisation process. Alternative techniques such as electron microscopy and electron crystallography combined with particle analysis can be used to generate low-resolution structural models and are discussed in more detail later in this chapter.

An early electron microscopy study was carried out by Suzina *et al.* (1985) to determine the supramolecular organisation in intracytoplasmic membranes (ICMs) of various methanotrophs such as *Methylomonas methanica, Methylosinus trichosporium, Methylocystis echinoides* and *Methylocystis pyreformis*. Globular structures were observed and proposed to consist of seven symmetrically arranged subunits in hexagonal arrays. Differences in structure were observed between membrane-bound and membrane- free states of the structures. Low-resolution structural information was obtained but it is not clear how micrographs were analysed, although it is implied that observations were made purely 'by eye' alone which made have led to inaccuracies in interpretation.

The following experiments were carried out in order to generate a structural model of the pMMO complex using various techniques such as hydropathy plot analysis and electron microscopy techniques.

6.2 Molecular mass, purity and subunit association analysis

The pMMO complex from *Methylococcus capsulatus* (Bath) is proposed to consist of at least the hydroxylase. The pMMO hydroxylase purified by Zahn and DiSpirito (1996) was comprised of three subunits of approximate molecular mass 47, 27 and 25 kDa. Nguyen *et al.* (1998) proposed the pMMOH to comprise of α, β and γ subunits of approximate molecular mass 47, 26 and 23 kDa. They also observed a modified, proteolytically-cleaved, α subunit (α') of molecular mass of ~ 35kDa.

6.2.1 Molecular mass and polypeptide profile of the pMMO complex

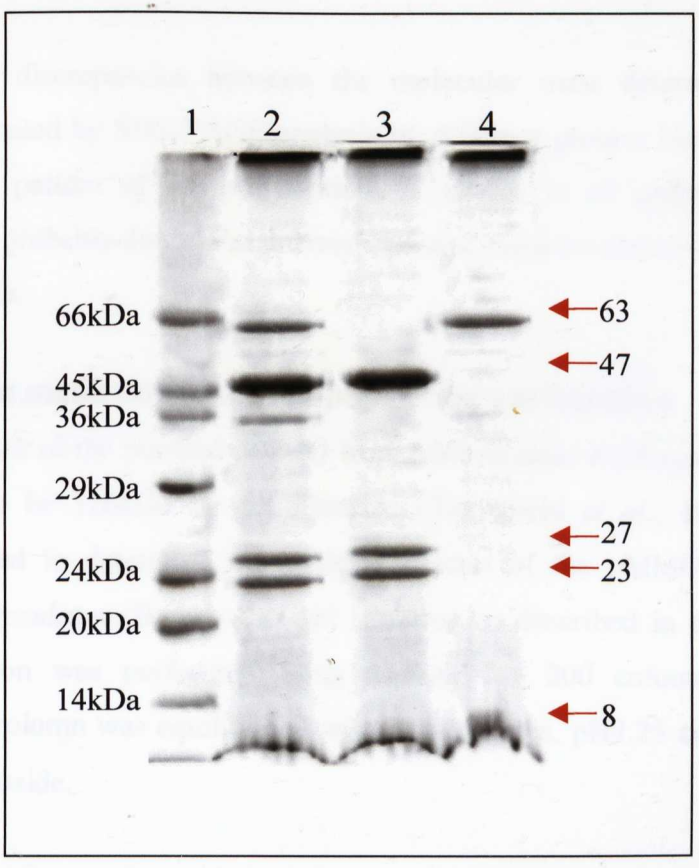

Figure 6.1 12% SDS PAGE gel of the pMMO complex and components
The pMMO components were purified as previously described in Chapter 3, Section 3.6.
Lane 1- Molecular weight markers
Lane 2 - pMMO complex off Superdex 200 column (5μg loaded)
Lane 3 - pMMO Hydroxylase off DEAE cellulose column (5μg loaded)
Lane 4-pMMO Reductase off DEAE cellulose column (5μg loaded)

The pMMO hydroxylase (Lane 3) is comprised of three subunits (α, β and γ) of approximate molecular mass 47, 26 and 23 kDa as estimated by the 12% SDS PAGE gel of the pMMO complex. (Figure 6.1). These polypeptide masses are comparable to those associated with the purified pMMO of both Zahn and DiSpirito (1996) and Nguyen *et al.* (1998). The putative duroquinol-dependent reductase (Lane 4) consisted of a large 63kDa subunit and a smaller 8kDa subunit, which often ran with the dye-front of the gel. The pMMO complex consisted of the total polypeptides for both the hydroxylase and the reductase. In addition to this a proteolytically-cleaved α' subunit was also identified of molecular mass of around 35kDa as observed by Nguyen *et al.* (1998).

There are slight discrepancies between the molecular mass determinations of the pMMOH as estimated by SDS-PAGE analysis by different groups. However, it is clear that the banding pattern of the polypeptides is similar in all preparations and the discrepancies are probably due to the different gel and sample conditions that were used by different groups.

6.2.2 Molecular mass estimation of pMMO^{c} by gel filtration

The molecular mass of the purified pMMO from *Methylosinus trichosporium* OB3b has been estimated to be 326kDa by gel filtration (Takeguchi *et al.*, 1997). The same approach was used to determine the molecular mass of the pMMO complex from *Methylococcus capsulatus* (Bath) using gel filtration as described in detail in Section 2.10. Gel filtration was performed using a Superdex 200 column (15x 984cm, Pharmacia). The column was equilibrated with 10mM Pipes, pH7.25 containing 0.01% dodecyl-β-D-maltoside.

The molecular mass determination of pMMO was made by comparing the elution volume of pMMO with that of five proteins of known molecular mass (BIORAD calibration kit) as described in detail in Chapter 2, Section 2.7. The resultant values were plotted to generate a calibration curve (Figure 6.2). In this way the molecular weight of pMMO could be deduced by reading off the calibration curve.

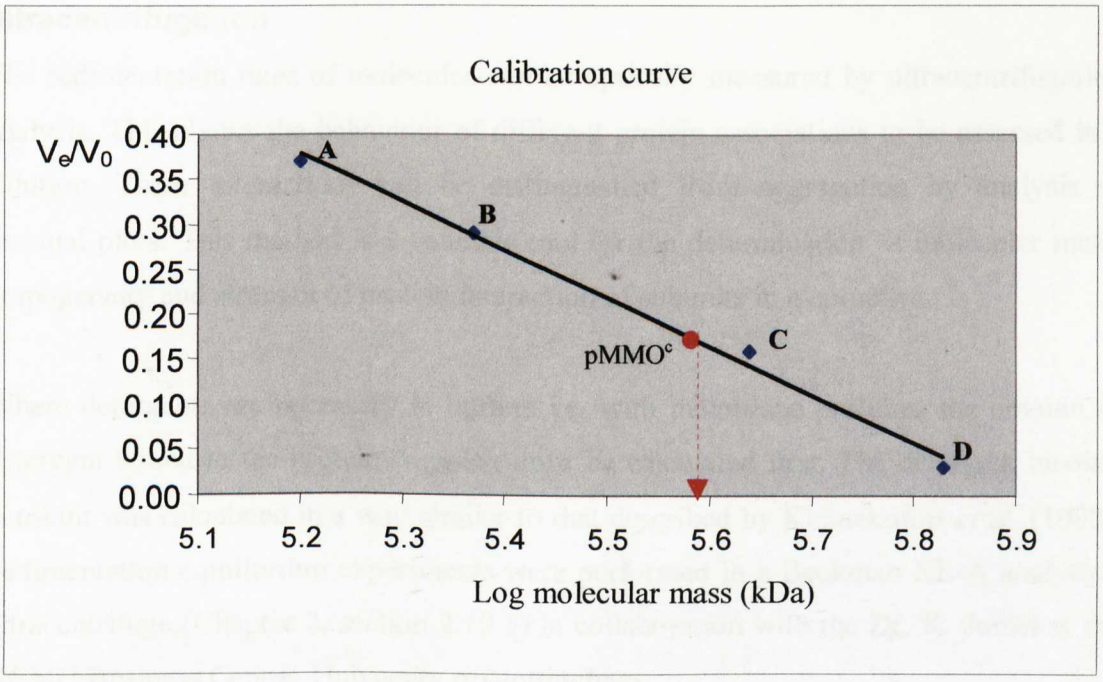

Figure 6.2 Estimation of molecular mass of pMMO from *Methylococcus capsulatus* (Bath) by gel filtration on Superdex 200 column. Column size, 1.5 by 98cm: Flow rate, 2 ml/min. Molecular weight standards . **A)** aldolase (M_r 158kDa); **B)** catalase (M_r 232kDa) ; **C)** ferritin (M_r 440kDa); **D)** thyroglobulin (M_r 669kDa);

The approximate molecular mass of the complex was estimated to be 390kDa by this technique. This method offers a rough molecular mass value and does not account for the mass of detergent bound to the complex.

6.2.3 Sedimentation equilibrium analysis of pMMO by analytical ultracentrifugation

The sedimentation rates of molecules can be optically measured by ultracentrifugation analysis. This allows the behaviour of different protein associations to be assessed in a solution. These interactions can be distinguished from aggregation by analysis of residual plots. This method is a valuable tool for the determination of molecular mass, homogeneity and strength of protein interaction of subunits in a complex.

Where detergents are necessary in buffers i.e. with membrane proteins, the amount of detergent bound to the protein complex must be calculated first. The detergent binding constant was calculated in a way similar to that described by Kleinekofort *et al.* (1992). Sedimentation equilibrium experiments were performed in a Beckman XL-A analytical ultracentrifuge (Chapter 2, section 2.10.3) in collaboration with the Dr. K. Jumel at the NCMH Business Centre, University of Nottingham.

The molecular weights of $pMMO^c$ and pMMOH in different D_2O/H_2O ratios and buffer density measurements were determined as described in Chapter 2, section 2.10.3. Data from one speed only ($pMMO^c$=6000rpm) and (pMMOH=10000rpm) were used for analysis as these proved to be the best conditions. The buoyant molecular weights of different protein samples were calculated using: -

$$M_b = M[1-\bar{\nu}\rho]$$

where default values of partial specific volume, $\bar{\nu}$ = 0.73 and density of solution, ρ =1.00

The buoyant molecular weights, M_b were then plotted against the buffer density measurements (Figure 6.3 and 6.4).

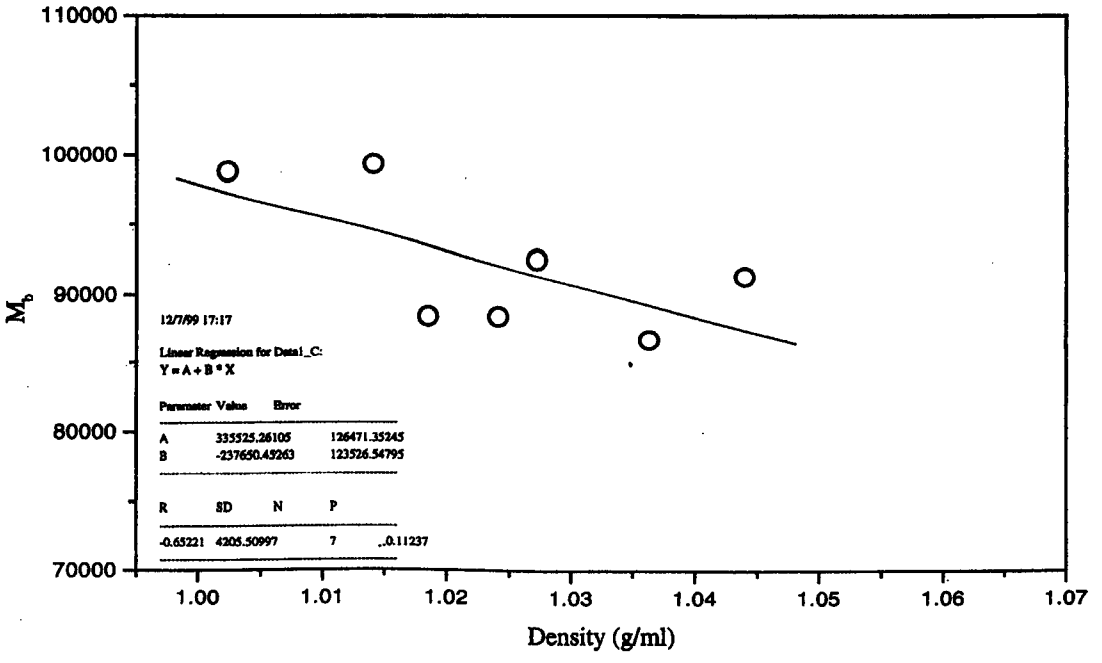

Figure 6.3 Determination of molecular weight of the pMMO complex Buoyant molecular weights, M_b were plotted against the buffer density measurements.

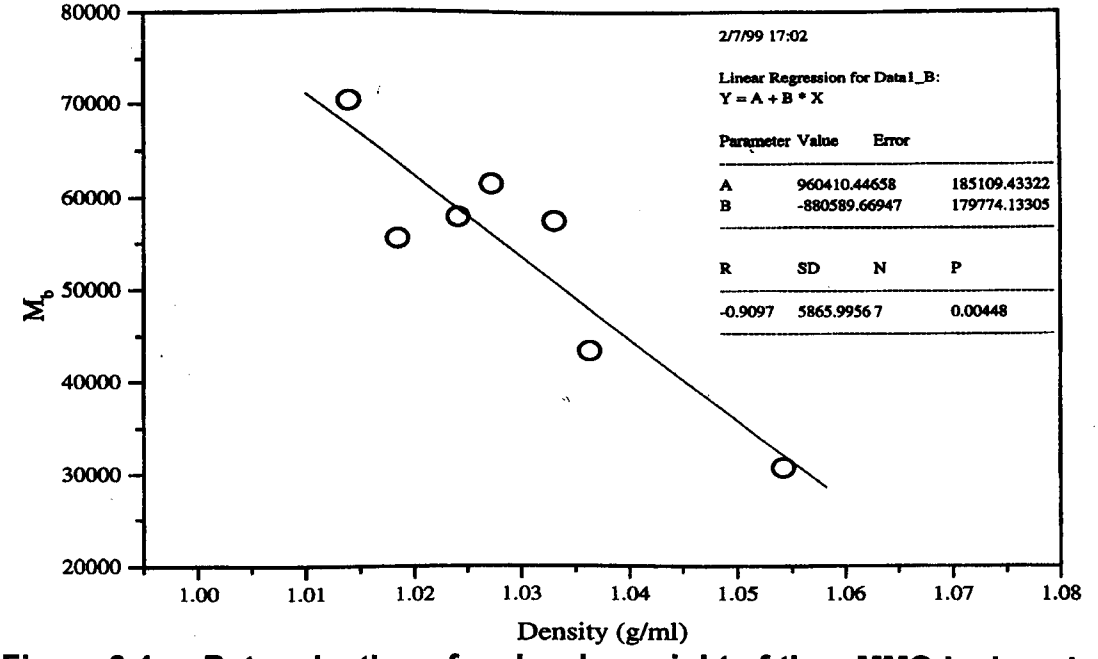

Figure 6.4 Determination of molecular weight of the pMMO hydroxylase. Buoyant molecular weights, M_b were plotted against the buffer density measurements.

i) The partial specific volume ($\bar{v}$) for the complexes were obtained from the point of intersection of M_b with the abscissa ($\bar{v} = 1/\rho$) from Figure 6.3 and 6.4.

$\bar{v}$pMMO complex = 0.7083 ml/g

$\bar{v}$hydroxylase = 0.9169 ml/g

ii) The buoyant molecular weight at a density of 1.0000mg/ml was found to be 97,600 Da for the pMMO complex and 78900 Da for the hydroxylase. In order to obtain the molecular weight for the protein detergent complexes at this density, the $\bar{v}$ values calculated above (i) were used giving

$M_{pMMO/detergent}$ = 334,590 Da

$M_{hydroxylase/detergent}$ = 949,460 Da

iii) Extrapolation of the buoyant molecular weight to the density of the detergent results directly in the molecular weight of the protein without bound detergent.

ρdetergent =1.00106716 g/ml (determined in the same way as other buffer densities)

M_b, pMMO = 97,621Da

M_b, hydroxylase = 78,881Da

iv) The molecular weights of the proteins were calculated from the M_b values using: -

$$M = \frac{M_b}{1 - \bar{v}\rho}$$

Therefore, M_{pMMO} = 387,100Da and $M_{hydroxylase}$ = 312,800Da.

The molecular weights of the pMMO complex and the hydroxylase were determined to be approximately 387,100 Da and 312,800 Da respectively which leaves a component(s) of molecular weight ~ 74kDa unaccounted for. If the pMMOH has a molecular weight of M=104, 309 Da as calculated from the published sequences available from the NCBI database (http://www.ncbi.nim.nih.gov) under accession number L40804, the hydroxylase may exist as a trimer (n=2.98).

6.3 Structural prediction of the pMMOH using hydrophobicity plots

Hydropathy plot analysis of amino acid sequences can be used for predicting models of the folding topology of membrane proteins. This approach has been used for the pMMOH from *Methylococcus capsulatus* (Bath) by Semrau *et al.* (1995). A Kyte-Doolittle algorithm was used to predict that the pmoB (47kDa) subunit had two potential membrane-spanning regions and a leader sequence. The hydropathy plot of the pmoA (27kDa) subunit predicted four potential membrane-spanning helices with no leader sequence.

A transmembrane helices model of the pMMO hydroxylase (pMMOH) was proposed (Figure 6.5) based on predicted hydrophobicity plots using the TMPred package (http://www.isrec.isb-sib.ch/software/TMPredfom.html). The published protein sequences of the pMMO hydroxylase from *Methylococcus capsulatus* (Bath) were available from the NCBI database (http://www.ncbi.nim.nih.gov) under accession number L40804.

Using TMPred prediction package, both the β (27kDa) and γ (23kDa) subunits of the pMMOH were predicted to have six potential membrane spanning helices each. A large portion of the α (47kDa) subunit appears to be situated outside the membrane. Histidine residues, which have been proposed to be responsible for the ligation of coppers in the active site, are predicted to be located on the periplasmic side of the membranes as previously proposed by Elliott *et al.* (1998). This would support the interaction of the pMMO hydroxylase with a periplasmic protein e.g. methanol dehydrogenase (MDH), as suggested by earlier findings in this study.

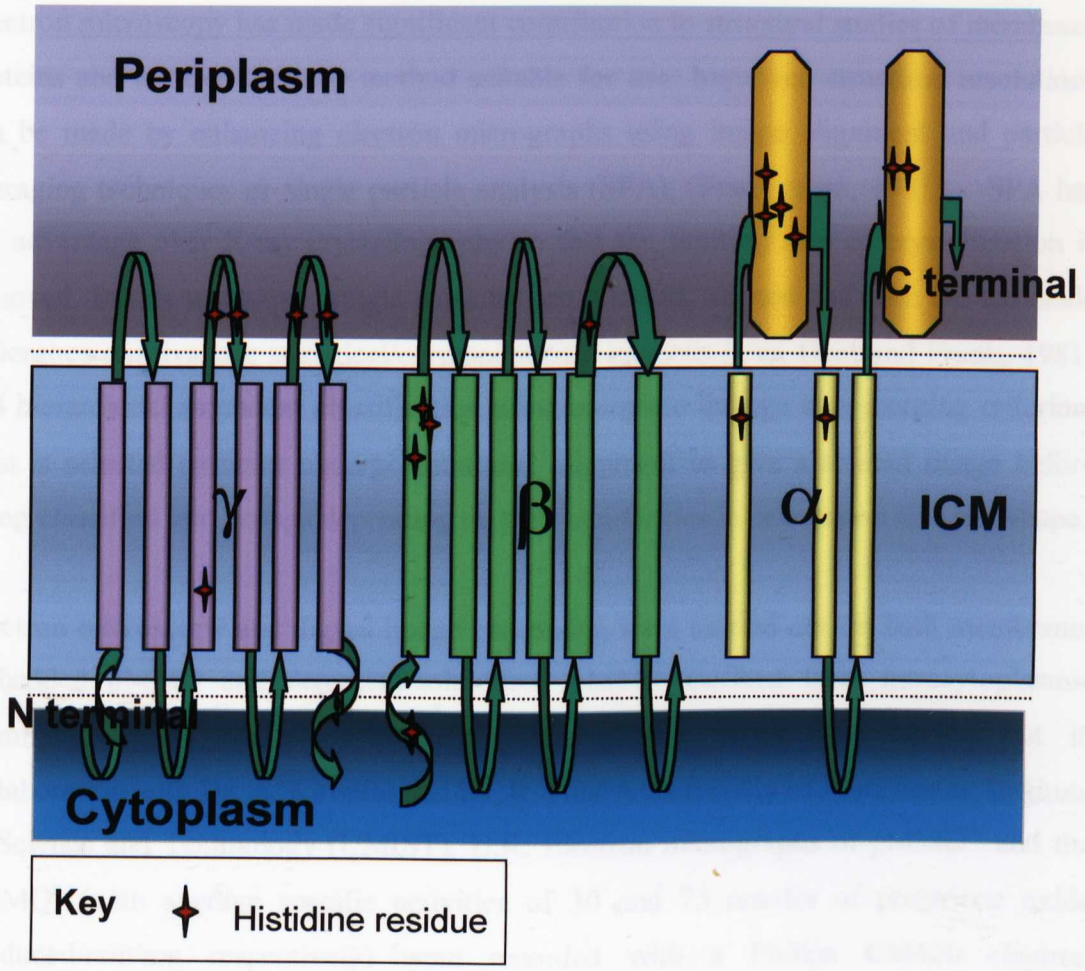

Figure 6.5 Transmembrane helices model of α,β and γ subunits of the pMMO Hydroxylase (pMMOH). Based on predicted hydropathy plots of the pMMOH protein sequences available from the NCBI database (http://www.ncbi.nim.nih.gov) under accession number L40804.

6.4 Electron microscopy and Single Particle Analysis of the pMMO^c

Electron microscopy has made significant contribution to structural studies of membrane proteins and is often the only method suitable for use. Improved structural resolutions can be made by enhancing electron micrographs using image alignment and particle averaging techniques or single particle analysis (SPA), (Frank *et al.*, 1981). SPA has the advantage over X-ray crystallography in that the limiting step of crystallisation is removed. In this technique, single particles are selected, aligned and then the molecule undergoes multivariate statistical/correspondence analysis (Van Heel and Frank, 1981) and hierarchical ascendant classification using complete linkage as a merging criterion. That is selected particles undergo rotational alignment to give a refined image before being classified into groups depending on their similarities in orientation size and shape.

Electron microscopy and digital image processing were carried out on both membrane-embedded pMMO and detergent-solubilised pMMO isolated from intracytoplasmic membranes from *Methylococcus capsulatus* (Bath). Work was carried out in collaboration with Dr. A. Kitmitto and Dr. R. Ford at University of Manchester, Institute of Science and Technology (UMIST), U.K. Electron micrographs of pMMO^m and the pMMO^c (with average specific activities of 30 and 75 nmoles of propylene oxide produced/min/mg respectively) were recorded with a Philips CM420 electron microscope and analysed as described in Materials and Methods (Chapter 2, Section 2.10.4). SPIDER and WEB image processing packages were used for single particle analysis. Either reference–free or reference-based algorithms were applied to rotationally and translationally align the particles. During reference-based algorithms a particle in the data-set is selected as a reference on the basis of its similarity to the majority of the other particles in the data-set in terms of size and shape.

6.4.1 Single particle analysis of membrane-associated pMMO ($pMMO^m$)

Electron microscopy and single particle analysis were carried out on $pMMO^m$ and $pMMO^c$ to allow a comparative study to be made between membrane-embedded and membrane-free pMMO complexes.

pMMO membrane samples (100-150μg/ml) were prepared as described in Chapter 2, section 2.5. Samples were negatively stained and examined in a Phillips 400 transmission electron microscope as described in Chapter2, section 2.10.4. Micrographs were originally recorded at a calibrated magnification of x 43,600. Electron micrographs were digitised (Zeiss Scanner) resulting in a pixel size of 6.4Å at the specimen level.

A typical electron micrograph of negatively stained membrane-embedded pMMO is presented in Figure 6.6. The membrane appears densely packed with proteins (white/lighter regions). Since, >75% of the total protein appeared to exist as 'doughnut' shapes of similar size (as seen in red section, X), they were anticipated to be the pMMO complex as >60% of the polypeptides in intracytoplasmic membranes (ICMs) are associated with the pMMO.

Patches of ordered membrane-embedded complexes (green section, Y) and membrane-associated 2D arrays (blue section, Z) were also observed and are discussed later in Section 6.5).

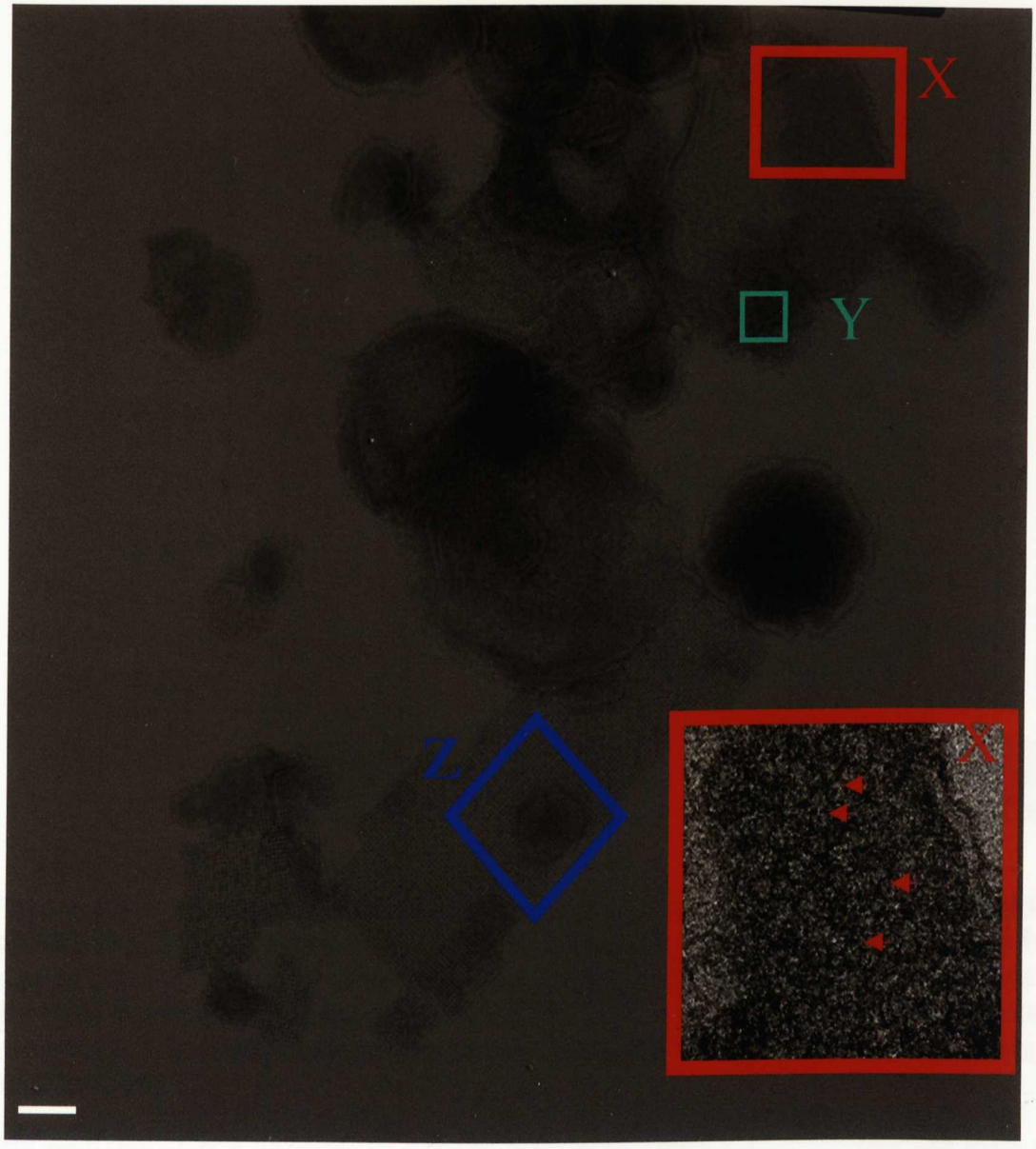

Figure 6.6 Typical electron micrograph of negatively stained intracytoplasmic membranes (ICMs) from *Methylococcus capsulatus* (Bath). Micrographs were taken at x43,600 and scanned to 6.4Å /pixel. Red section X depicts an enhanced image of the 'doughnut' shaped proteins. The red arrows designate typical particles for selection. Green section, Y and blue section Z are areas of ordered membrane-embedded and membrane-associated complexes respectively. Enhanced images of section Y and Z are shown in Figure 6.12 and 6.14, respectively. Scale bar = 0.1μm

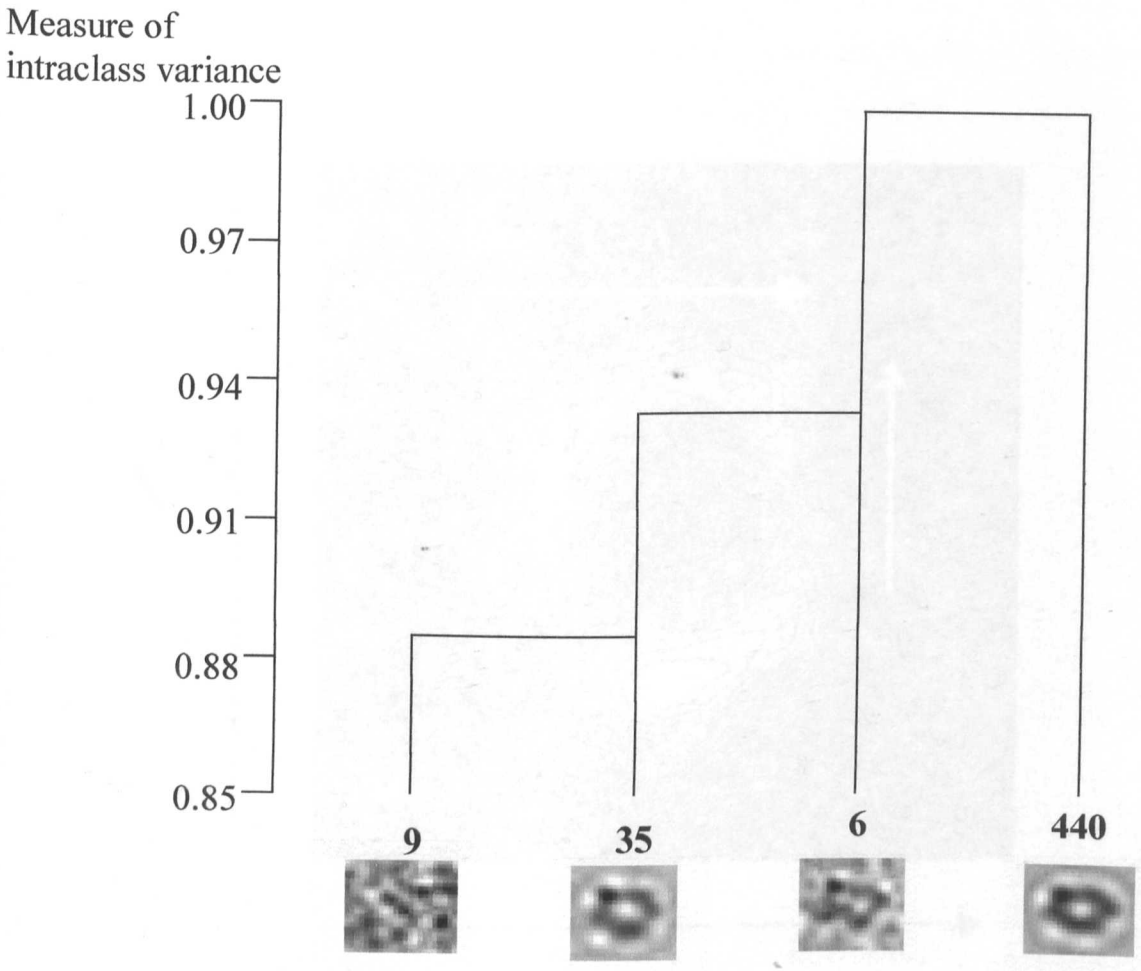

Figure 6.7 Hierarchical ascendant classification of membrane-embedded pMMO (X). 500 particles of complex X were individually selected using a box size of 23 x 23 pixels (6.4Å/pixel). The vertical axis represents the measure of the gain in intraclass variance obtained through merging (measure of intraclass variance). The main classes are shown here with their population numbers in bold (n=500).

500 particles of non-ordered, membrane embedded complexes were selected from the digitised micrograph of the ICMs (Figure 6.6) and subjected to translational and rotational alignment followed by hierarchical clustering as depicted in Figure 6.7. As would be expected the data set was very homogenous since the membrane-embedded complexes are restricted in their orientation with respect to the membrane. A major class of 440 particles (88%) was identified, Class A and an average projection map was generated as shown in Figure 6.8.

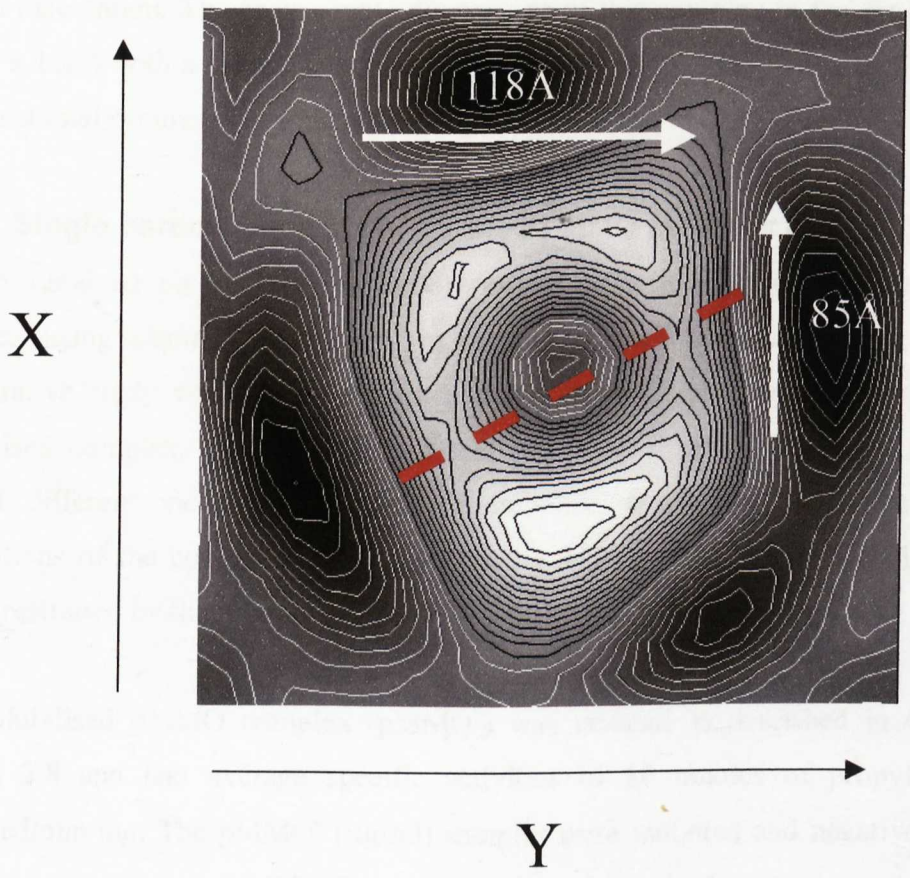

Figure 6.8 Average projection map of major class of membrane-embedded complexes (A). Box size, X = Y = 192 Å. The proteins domains are depicted as the white regions of the map and the black areas are the applied stain. The dimensions of the complex are approximately 85 x 118Å with a central indentation of about 39 x 47Å. The red dashed line indicates possible 2-fold symmetry.

The averaged projection map of the major class of membrane-embedded (Class A) particles (Figure 6.8) depicts a complex where the protein domains surround a large central indentation. The approximate dimensions of this complex in the projection map are 85 x 118Å with a central indentation of about 39 x 47Å. The complex may have 2-fold rotational symmetry as indicated in Figure 6.8.

6.4.2 Single particle analysis of purified pMMO complex (pMMO^c)

Having obtained an average projection map of the membrane-embedded pMMO complex using electron microscopy in conjunction with single particle analysis, a comparative study was carried out on pMMO^c to generate a projection map of the solubilised complex. It was expected that after solubilisation from the membrane, several different views of the pMMO complex would be visible i.e. different orientations of the complex with respect to the support film, as the complex was no longer restricted by the membrane in orientation.

The solubilised pMMO complex (pMMO^c) was isolated as described in Chapter 2, section 2.8 and had average specific activities of 50 nmoles of propylene oxide produced/min/mg. The pMMO^c (μg/ml) samples were mounted and negatively stained for examination using a Phillips 400 transmission electron microscope (as described in Chapter 2, section 2.10.4). Electron micrographs were digitised (Zeiss Scanner) resulting in a pixel size of 6.4Å at the specimen level.

The particles seen in the typical electron micrograph of negatively stained pMMO^c (Figure 6.9) appeared to be homogenous in terms of size. 1631 particles were selected for single particle analysis (reference-free) using a box size of 30 x 30 pixels (6.4Å/ pixel).

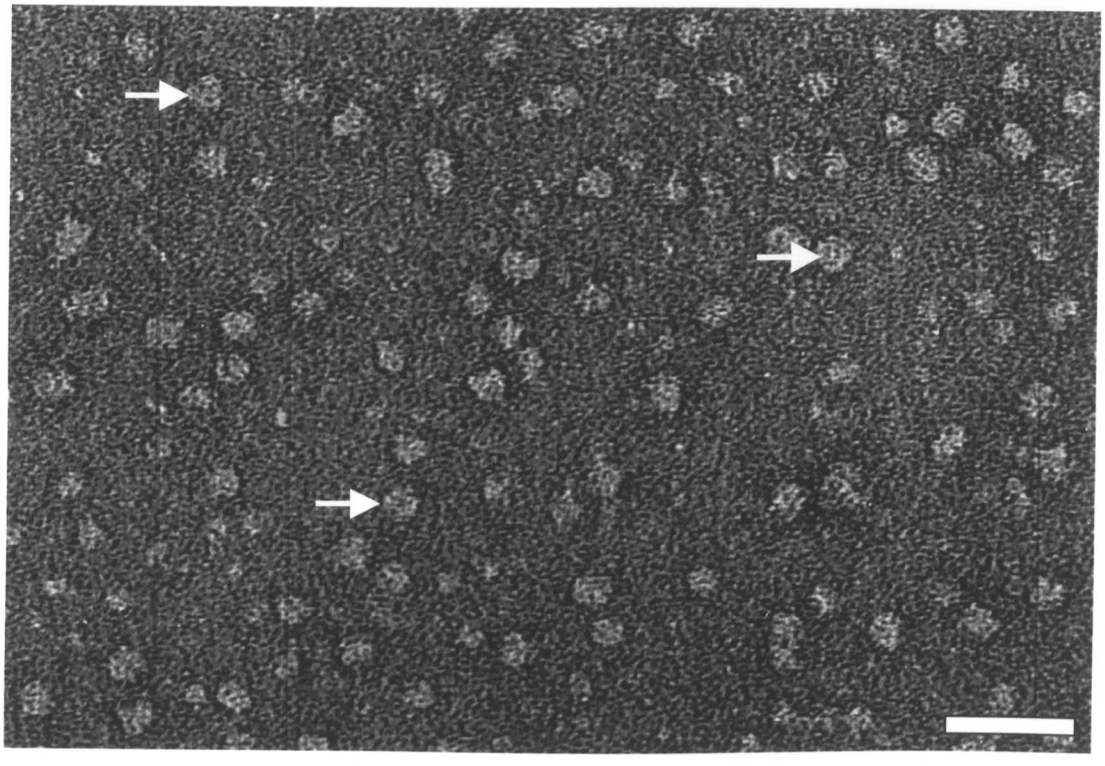

Figure 6.9 A typical electron micrograph of negatively stained purified pMMO complex (pMMO^c). Typical particles for selection are designated by the white arrows. The micrograph was originally taken at a magnification of x 43,600 and scanned to 6.4Å/pixel. Scale bar =50nm

Correspondence analysis and hierarchical ascendant classification was carried out on the pMMO^c particles in a similar manner to that described previously for the membrane-embedded complex. Three main classes were identified, class 1 (30%), 2 (27%), 3 (10%). The average projection maps of each of the main groups of particles are shown in Figure 6.10.

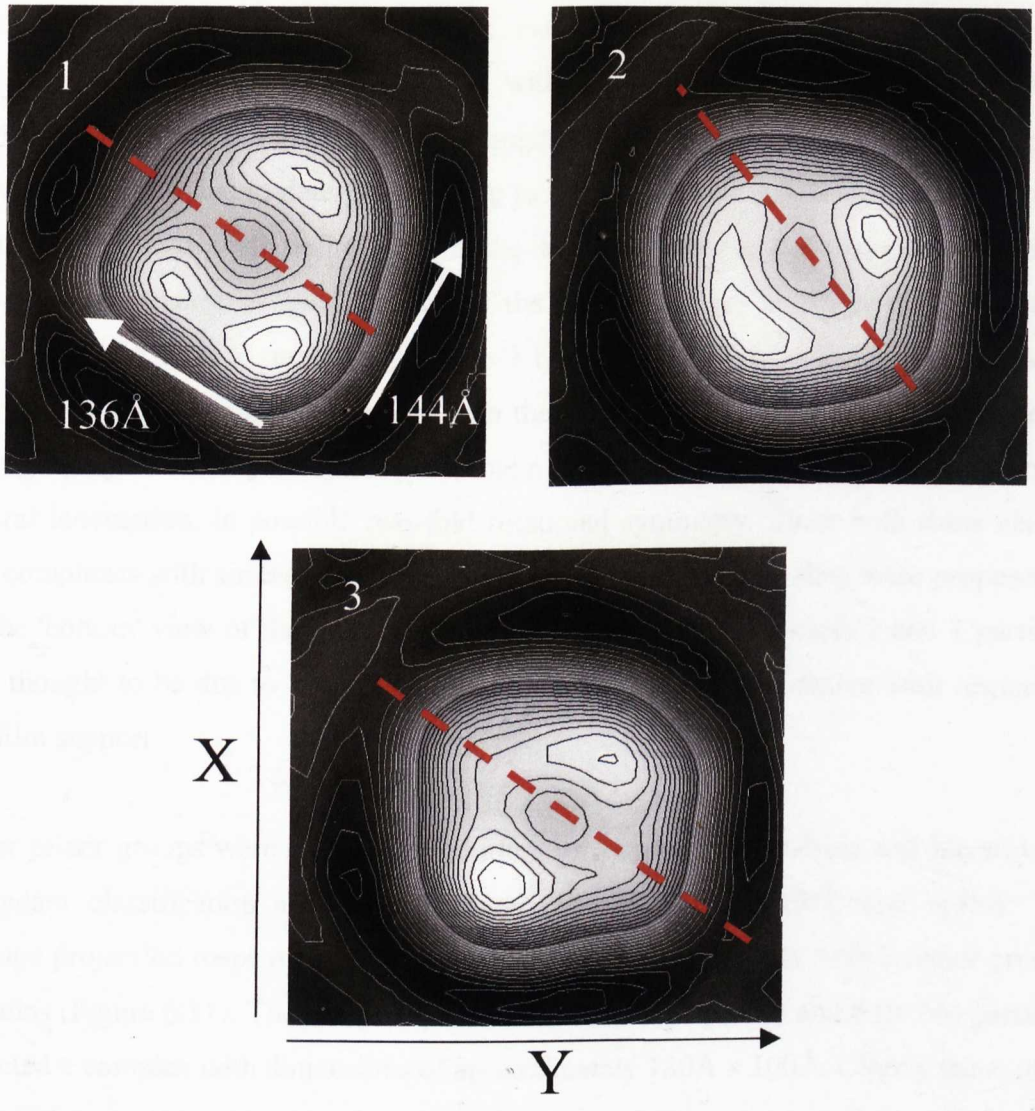

Figure 6.10 Average projection maps of three main classes of pMMO complex. Class 1(n=488), Class 2(n=440) and Class 3(n=163) after selection of 1631 particles. Particles were selected from digitised micrograph of pMMO^{c} (figure 6.9) and subjected to correspondence analysis and hierarchical ascendant classification. Maps were generated for each class and depicted two protein domains (white areas) surrounded by applied stain (black). The approximate dimensions of the complex (1) are 136 x 144Å. The red dashed line indicates possible 2-fold mirror symmetry. Box size, X = Y = 192 Å.

489 particles of class 1 were selected and found to have almost identical features to the membrane-embedded complex depicted in Figure 6.8, if the map was rotated by 90° and was therefore likely to offer the 'top face' view of the complex'. The complex appears flattened with possibly 4 protein domains, with approximate dimensions of 136 x 144Å. This membrane-free complex is slightly larger than the membrane-embedded complex, which is probably due to detergent binding to the complex on solubilisation. The central cavity was not as well defined as in the membrane-embedded complexes. This is perhaps unsurprising, as solubilisation of the complexes may result in some structural variation. Both class 2 (n=440) and class 3 (n=163) particles present a different view (Figure 6.10) of the pMMO complex than the class 1 particles. Both the class 2 and 3 average projection maps depict two protein domains (white regions) surrounding a central indentation, in possible two-fold rotational symmetry. Since both these classes had complexes with similar dimensions to the class 1 complexes, they were proposed to be the 'bottom' view of the complex. The slight variation of the class 2 and 3 particles was thought to be due to slightly different orientations of the complex with respect to the film support.

Other minor groups were also identified after correspondence analysis and hierarchical ascendant classification and were assigned class 4 (7.5%), 5(5%) and 6(4%). The average projection maps of the minor classes illustrated a complex with 2 major protein domains (Figure 6.11). The complexes observed in class 5 (n=85) and 6 (n=66) particles depicted a complex with dimensions of approximately 130Å x 100Å. Clearly these three averaged projection maps are closely related and probably represent the same 'face' of the complex but at slightly different orientations with respect to the support film. The complexes were assigned as 'side views' as they appeared to have possible two-fold symmetry, which would be expected in the side-view of a homopolymeric complex. The class 4 (n=122) particles were thought to represent an extended side-view of the complex i.e. tilted top view (seen in class 1 particle). From the dimensions of the class 5 and 6 particles, the length of a membrane spanning helix was estimated at approximately 130Å.

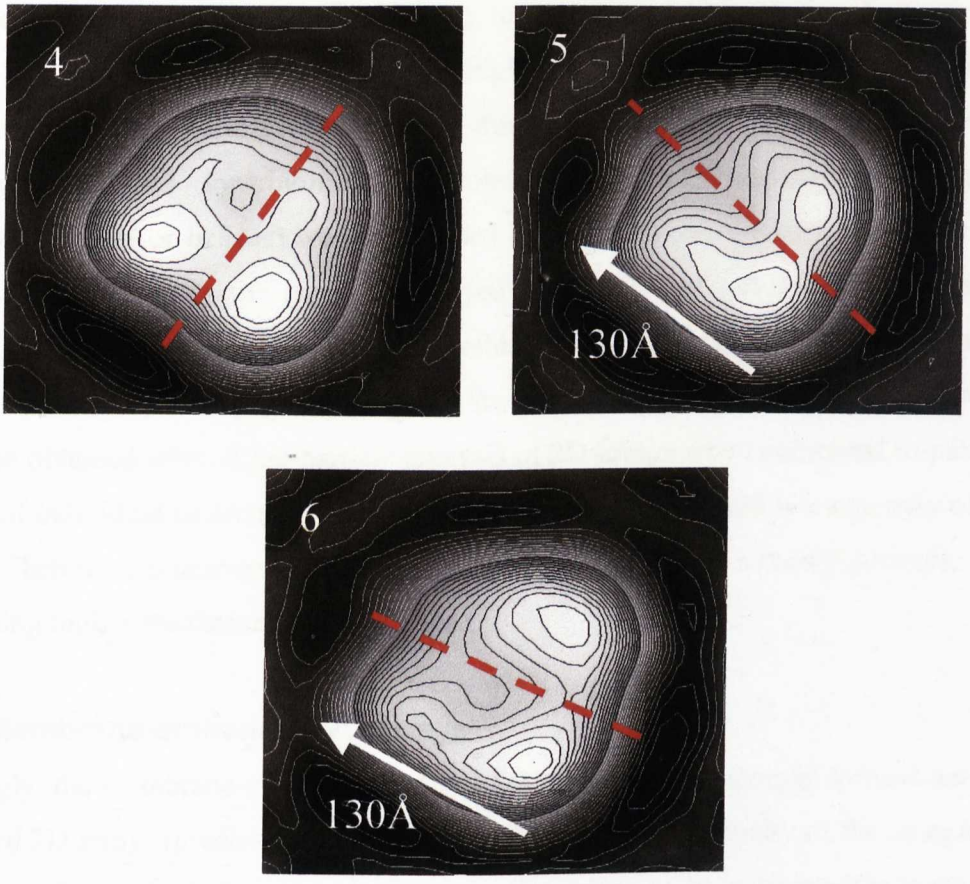

Figure 6.11 Average projection maps of three minor classes of pMMO complex, Class 4 (n=122) Class 5 (n=85) and Class 6 (n=66). Box size, X = Y = 192 Å. Particles were selected from digitised micrograph of pMMO^c (Figure 6.9) and subjected to correspondence analysis and hierarchical ascendant classification. Maps were generated for each class of particle. Two protein domains were observed (white areas) surrounded by applied stain (black areas). The approximate dimension of the complex shown in (4) and (5) are 130Å x130Å. The red dashed line indicates possible 2-fold mirror symmetry.

There is a clear correlation between the membrane-embedded complexes and the purified pMMO complexes suggesting they are essentially the same entity. The solubilisation and purification of the pMMO^c has allowed different views of the pMMO complex to become accessible and the resulting projection maps have portrayed top, bottom and side views of the complex at low resolution. These projection maps may serve as blueprints for the eventual generation of an overall model of the pMMO complex.

6.5 Electron Crystallography of the pMMO complex

The major obstacle in the advancement of tertiary structure analysis of membrane proteins has been the difficulty to produce high amounts of pure protein required for investigations and the presence of detergent during the crystallisation process. Particle averaging techniques for biomacromolecules arranged in regular arrays (two-dimensional crystal or helices) were developed by Klug and co-workers (DeRosier and Klug, 1968). This technique has been proved successful for membrane proteins, as three-dimensional structures with reproducible resolutions down to approximately 0.7nm have been achieved (Henderson and Unwin, 1975). Higher resolution images can usually be obtained when using particle analysis of 2D-arrays when compared to particle analysis of individual molecules. This is largely due to the increased homogeneity of the data set. Therefore, acquiring 2D arrays of the pMMO complex is a highly desirable step in obtaining higher resolution structural data.

6.5.1 Membrane-embedded 2D arrays

Intrestingly, the membrane-embedded pMMO complexes spontaneously formed patches of ordered 2D arrays (green section, Y in figure 6.6). The homogeneity of the complexes in the crystalline areas allowed average projection maps to be generated in a manner similar to that previously described. Digital image processing of the crystalline areas was carried out using the PC based CRISP and TRIMERGE image-processing software packages as described in Chapter 2, section 2.10.4.

The membrane-embedded 2D arrays exhibited hexagonal packing (Figure 6.12). Approximately 20 molecules were selected from areas of membrane-embedded 2D arrays from the digitised micrograph of ICMs (Figure 6.6). The resultant average projection map (Figure 6.13) depicted a complex with the unit cell dimensions of a = 119Å, b= 120Å. In addition to this, the complex exhibited similar gross features as that calculated by single particle analysis of non-ordered membrane-embedded pMMO complexes (Figure 6.8) and purified pMMO (Figure 6.10). That is, the ordered membrane-embedded pMMO complex is comprised of approximately two distinct domains surrounding a central cleft.

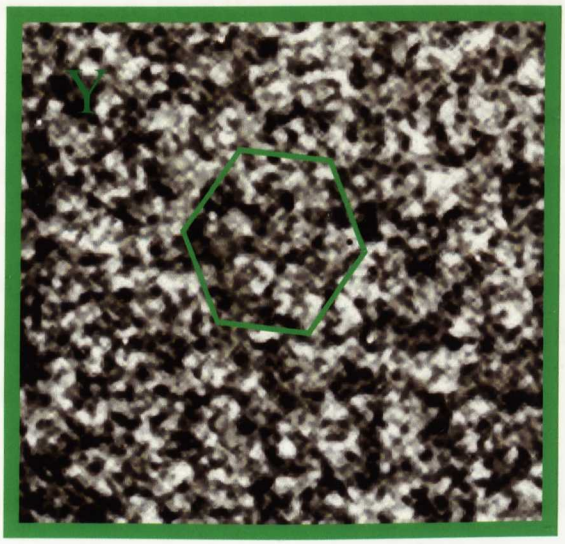

Figure 6.12 Typical enhanced section depicting ordered membrane-embedded complexes. The section was taken from the digitised micrograph (Figure 6.6) of intracytoplasmic membranes from *Methylococcus capsulatus* (Bath). The complexes exhibited hexagonal packing as indicated by green hexagon.

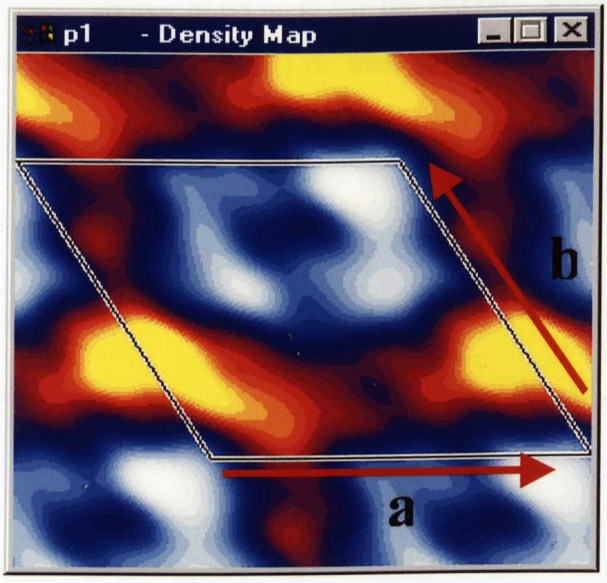

Figure 6.13 Density map of membrane-embedded complexes. Unit cell dimensions a=119 Å, b=120Å. Approximately, 4 protein domains are depicted by the white regions and surround a central cleft. The orange areas represent applied stain. Approximately 20 molecules were selected from the digitised micrograph (Figure 6.6)

Both the protein domains are similar in shape and size, except that the right hand domain appears to protrude more from the membrane than the left hand domain

6.5.2 Average projection map of membrane-associated complexes

Crystalline areas were also found associated with, but not embedded in the membrane (Figure 6.14). The source of these 2D arrays could not be readily identified and therefore particle analysis was carried out to try and determined the identity of the arrays. 15 areas of the membrane-associated 2D arrays were selected and subjected to translational and rotational alignment.

Digital image processing of 15 crystalline areas generated a projection map of the unit cell ($a=b=12.2\pm0.2$nm; $\gamma=90^{o}$) as depicted in Figure 6.15. The unit cell is composed of four similar complexes, rotated 90° with respect to each other.

The exact nature of these crystals is still unclear since the average projection map bears no resemblance to the maps shown previously for the pMMO. Attempts to remove the arrays from the membrane using salt (2M) or urea (5M) washing were unsuccessful (data not shown).

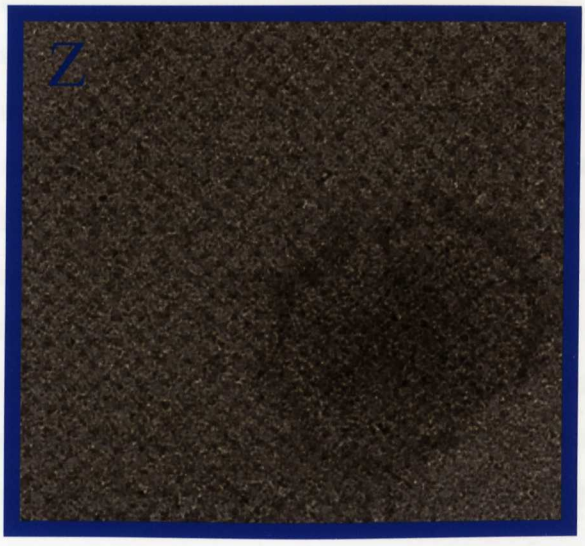

Figure 6.14 Typical enhanced section of electron micrograph (Figure 6.6) portraying membrane-associated 2D arrays. 15 crystalline areas were selected for particle analysis.

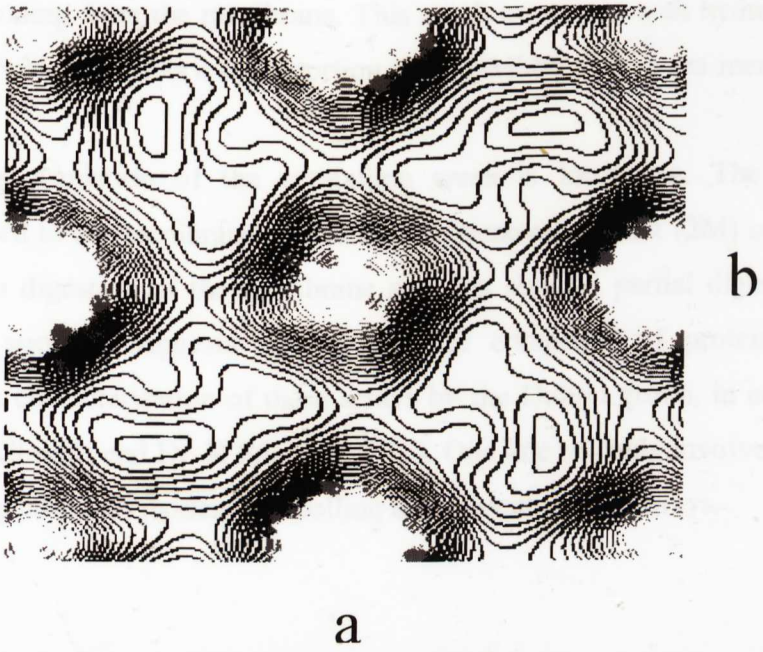

Figure 6.15 Final contour projection map of the unit cell of the membrane-associated 2D arrays.
15 crystalline areas were selected. The unit cell dimensions are a=b=12.2±0.2nm; γ=90°. The unit cell is comprised of four complexes, rotated 90° with respect to each other.

6.6 Discussion

Preliminary electron microscopy studies indicates that the pMMO complex exists as at least a dimer, possibly a tetramer. The sedimentation equilibrium analysis confirms that pMMO exists as an oligomer but the molecular weight of the complex suggests it exists as a trimer. It should be noted that the techniques are fundamentally different in that the subunit association takes place in solution during sedimentation equilibrium and out of solution during electron microscopy. As expected the solubilised complexes are slightly larger than those from the membrane, which was also seen by Suzina (1985) in various methanotrophs. This was thought to be due to the structural variation when the complex is released from the membrane or may be due to detergent binding to the complex.

The membrane-spanning dimension of the complex was calculated to be approximately 130Å as inferred from the 'side view' of the complex. If the 'thickness' of a bacterial membrane is estimated to be approximately 60Å, this suggests that a large portion of the complex is protruding from the membrane. This result correlates with hydropathy plots of the pMMOH, which predicts a large portion of the pMMO to be extra-membraneous.

The spontaneous formation of the crystalline areas is intriguing. The arrays are physically attached to the membrane and cannot be removed by salt (2M) or urea (5M) washing. Trypsin digestion of the membrane samples showed partial digestion of the crystals, which strongly suggests the crystals are composed of protein. Work is continuing in the characterisation of these arrays by the Dalton group, in collaboration with the Dr. A. Kitmitto and Dr. R Ford (UMIST). One line of study involves the use of gold-conjugated pMMO antibodies in labelling experiments of the arrays.

Various projection maps from this study were used to generate a schematic model for the different views of the pMMO complex (Figure 6.16 a,b and c). The average projection maps of both the membrane-associated and membrane-free pMMO suggest the complex is comprised of 2 distinct protein domains (monomers or dimers), which are related by rotational symmetry when viewed from the top of the complex. These two distinct protein domains surround a closed cavity as inferred by the assumed 'bottom views' of the complex (Figure 6. 11). The role of this central depression is not clear but it may allow hydrophillic substrates accessibility to the active site.

Using electron microscopy and single particle analysis techniques has given us an insight into the structure of the pMMO. Higher resolution structures may be obtained from reconstituting the purified pMMO complex into lipids. If protein:lipid concentrations are high enough, crystal formation can be induced, which will enhance the quality of subsequent data. This method has been successfully used for other membrane proteins to obtain reproducible resolutions of down to 0.7nm. (Henderson and Unwin, 1968).

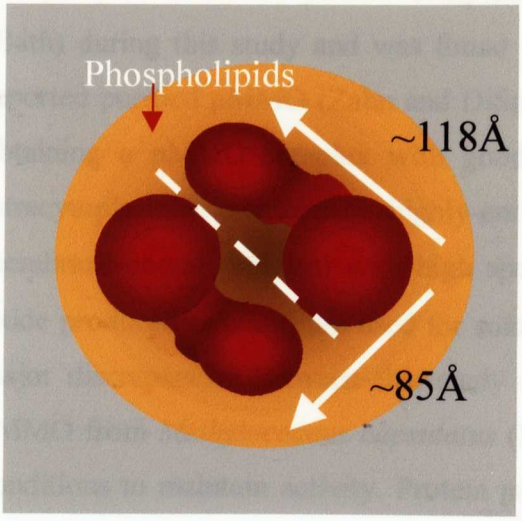

Figure 6.16a Top view of pMMO model Model depicts two pMMO monomers surrounding a central cavity. White line represents two-fold symmetry

Figure 6.16b Bottom view of pMMO model. Model depicts two associated pMMO monomers. White line represents two-fold symmetry

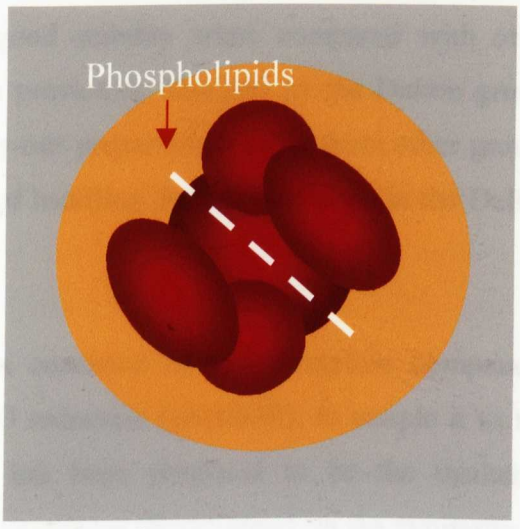

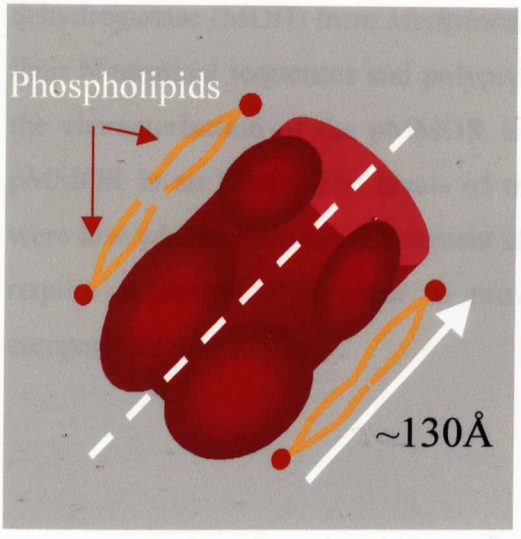

Figure 6.16c Side view of pMMO model Model depicts the side view of two pMMO monomers . White line represents mirror symmetry

7. General Discussion

A high specific activity pMMO complex was purified from *Methylococcus capsulatus* (Bath) during this study and was found to have 5-10 times the activity of previously reported purified pMMO (Zahn and DiSpirito, 1996; Nguyen *et al.*, 1998). The key to obtaining a pMMO complex with good specific activity, lies in precept that only intracytoplasmic membranes highly-enriched with pMMO (60-80% of the total membrane-bound proteins) with high specific activities (≥50-75 nmoles of propylene oxide produced/min/mg) are used for solubilisation and further purification. One of the major discrepancies between this study and published reports on the purification of pMMO from *Methylococcus capsulatus* (Bath) by other groups is the use of anaerobic conditions to maintain activity. Protein preparations maintained aerobically during this study were of high specific activity and good stability when compared with other groups. These findings are similar to results previously obtained by the Dalton group, University of Warwick. It is still unclear why our preparations differ from other groups and may be due to the extensive experience of handling the methanotroph in the Dalton group.

In this study, the purified pMMO complex consisted of a hydroxylase component (pMMOH), which required a putative pMMO reductase (pMMOR), to couple it to the electron donor, duroquinol. The pMMOR has been proposed to be the methanol dehydrogenase (MDH) from *Methylococcus capsulatus* (Bath) based on the similarity of their N-terminal sequences and polypeptide profiles (Adeosun, 2000). Further work on the characterisation of the pMMOR is required to conclusively establish the putative pMMOR is an MDH. The levels of the purified pMMOH and pMMOR components were low which restricted subsequent characterisation so the purification procedure will require optimisation in order to provide large-scale purification of the individual components.

The results from this study indicate that the methanol dehydrogenase (MDH) may be at least partially membrane-bound as has been suggested previously (Patel and Felix, 1976; Grosse, *et al.*, 1997 Anthony, 1986). It is unclear how MDH associates and interacts with pMMO hydroxylase in the membrane, although it is thought that the ionic washes used in the isolation procedure stabilise interactions between the two. MDH remains associated with the membrane despite washing and sonication, and can only be removed with harsh conditions i.e. urea, which causes complete denaturation of the enzyme complex. The pMMO samples prepared by Zahn and DiSpirito (1996) and Nguyen *et al.* (1998) do not contain significant amounts of MDH and this may be reflected in the low activities they obtain.

7.1 Properties of the pMMO

The EPR analysis of the pMMO complex indicates that the copper in the active site of pMMO exits as a type 2 copper not a trinuclear copper cluster as proposed by Chan and coworkers (Chan *et al.*, 1993; Nguyen *et al.*, 1994, 1996, 1998). This finding is in agreement with other groups who also found that the copper in pMMO existed as a cupric ion ligated to three or four nitrogens atoms (Zahn and DiSpirito, 1996; Yuan *et al.* 1997, 1998, 1999; Lemos *et al.*, 2000). However, it is not clear whether the copper ion is ligated to three or four nitrogens atoms. This could only be conclusively established by EPR analysis of the pMMO complex and its individual components from *Methylococcus capsulatus* (Bath) cells grown in either ^{15}N enriched media as carried out from *Methylomicrobium albus* BG8 cells by Lemos *et al.* (2000).

There is also mounting evidence that the functioning pMMO complex contain some iron atoms as proposed by Zahn and DiSpirito (1996). The exact nature of these iron atoms ions is not known although the majority of iron is EPR silent and could be part of a Cu+---Fe^{3+} centre. The presence of iron in three preparations of purified pMMO (Zahn and DiSpirito, 1996; Takeguchi *et al.*, 1997; This study) does suggest there must be some iron component in pMMO which is contradictory to the findings of Nguyen et al., (1998). Future EPR analysis will be required to further elucidate the nature and role of the iron centre in pMMO.

The results of this study offer the first real structural insight into the pMMO. The complex was found to be comprised of 2 distinct protein domains (where one domain =monomer or dimer) surrounding a closed cavity of unknown function, although it may allow hydrophillic substrates accessibility to the active site. Whether the complex exists as a dimer or a tetramer requires investigation which will be considerably aided by mass spectrometry analysis to find out the accurate molecular mass of the complex and its components. The individual components could not be assigned in this study and may be identified using antibody labelling techniques with antibodies raised to the pMMO. Higher resolution structures may be obtained by using cryo-conditions where samples are embedded in vitreous ice and can be sectionalised to collate data to generate 3-D models. However, this is technically far more difficult.

The apparent spontaneous formation of the membrane-attached 2D crystals is an intriguing phenomenon. It is possible that the arrays are formed from membrane-dissociated subunits of pMMO e.g. the large 47kDa subunit (α) which is proposed to be mainly extramembraneous. Alternatively, the 2D arrays could offer an insight into membrane protein processing, where the crystals are the storage form of pMMO before the complex has completely inserted itself into the membrane. A concerted effort to characterise these crystals is still underway by the Dalton group (University of Warwick) in collaboration with the E.M group (UMIST). It is hoped that these experiments will help to elucidate the nature of these 2D crystals.

The results of the kinetic analysis of the pMMO complex indicate that the complex has a low affinity for methane when compared to sMMO values. This finding is not in accordance with previous observations that pMMO-expressing cells have a greater affinity for methane than sMMO-expressing cells (Leak, 1992; Leak and Dalton, 1986a and b; Leak *et al.*, 1985) and may be due to the absence of the *in vivo* electron donor of pMMO.

7.2 *In vivo* electron donors for the pMMO complex

It is now becoming apparent that the *in vivo* mechanism for methane oxidation is a complex and ingenious system. The possible role of the methanol dehydrogenase (MDH) in donating electrons generated from methanol oxidation back to the pMMO independent of NADH, as previously suggested by Tonge and co-workers (1977), now seems plausible with the demonstration of methanol as a reductant to the membrane-bound pMMO in this study. This would suggest an energy efficient mechanism of methane oxidation in pMMO expressing methanotrophs which is supported by the fact that cells expressing pMMO are energetically more efficient (in terms of g cells/g methane consumed) than cells expressing sMMO (Dalton and Leak, 1985).

However, the subsequent loss of the ability for methanol to act as a reductant for the purified pMMO complex may be due to a couple of factors. It may reflect the need to obtain a fully functional MDH cofactor $PQQH_2$ or it may indicate that the physiological electron acceptor for MDH, the cytochrome c_L, which may be associated to the MDH in membrane samples but removed during the purification process, is necessary to maintain methanol-linked pMMO activity. If this is the case, it may be inferred that cytochrome c_L is the true *in vivo* electron donor for pMMO and this is supported by electron transport inhibitor studies that indicate that a cytochrome *c* is involved in electron transfer to the pMMO.

However, it can be postulated that in the absence of a functional PQQH and its true physiological electron acceptor, MDH may aid an efficient transfer of electrons from duroquinol to the pMMO, possibly due to it locational attributes. That is for rapid electron transfer to take place between duroquinol and the active site of the pMMO they need to be as close together as possible. This proposal is supported by the findings that the pyrrolo-quinoline quinol and duroquinol could be competing for a binding site in the pMMO complex, possibly in the reductase/MDH component i.e. the vacation of the PQQH from its binding site (as indicated from uv/vis spectrophotometry) may allow duroquinol to bind. It may also explain the findings of other groups (Shiemke *et al*, 1985; Zahn and DiSpirito, 1996) where the presence of the reductase/MDH has not been

noted but minimal pMMO activity is obtained using duroquinol as an electron donor, due to inefficient electron transfer from duroquinol to pMMO.

7.3 The pMMO complex, an oxygenase and an oxidase?

There have been reports that pMMO samples with no MMO activity e.g. by acetylene inhibition, have stable rates of oxygen consumption, indicating that the oxygen reducing activity may be due to a terminal oxidase. (Dalton and Whittenbury, 1976; Stirling and Dalton, 1979; Prior and Dalton, 1985a; DiSpirito *et al.*, 1994).

A terminal oxidase was purified from *Methylococcus capsulatus* (Bath) (Zahn *et al.*, 1994) and could be purified with or without a cytochrome *c*-557 (now referred to as the cytochrome *c* peroxidase, Zahn *et al.*, 1997) which was proposed to be the probable initial electron donor to the oxidase. Interestingly, this enzyme was found to consist of 7-10 copper atoms (an unusually high level for an oxidase) and iron atoms and had a polypeptide profile (~46, 28 and 20kDa) which is remarkably similar to that of the pMMO hydroxylase (47, 27 and 23kDa). These findings led Nguyen *et al.*, (1998) to propose that the oxidase preparation was heavily contaminated with the pMMO polypeptides although no other polypeptides (except for the accounted for cytochrome *c*-557 polypeptide) were apparent in the cytochrome preparation. The explanation does not account for the terminal oxidase activity detected in preparations lacking pMMO activity

Therefore, a proposal has been suggested based on a number of observations made in this study and previous literature. Electron transport inhibitor studies on the pMMO from *Methylococcus capsulatus* (Bath) (Prior and Dalton, 1985, Charlton, 1997 and this study) led to the proposal that NADH passes electrons to pMMO via a chain of electron transfer proteins, involving a possible NADH oxireductase and/or quinol pool, cytochrome *b* and cytochrome *c*, in a manner similar to the mitochondrial electron transport chain. Whether ATP is generated is not clear, as 2,4-DNP (uncoupling agent) and oligomycin (prevents final step in ATP formation) have little effect on NADH-mediated $pMMO^{m}$ activity. The role of final electron acceptor in an electron transport

chain with subsequent reduction of O_2 to H_2O, by pMMO, is also reminiscent of a terminal oxidase. Therefore it is tentatively proposed that the native membrane-bound pMMO complex i.e. with haem components present, is also the terminal oxidase responsible for the oxidase activity observed in membrane and solubilised preparations in the absence of pMMO activity. If this is true, a number of conclusions can be inferred.

The cytochrome c_L is known to interact with cytochrome aa_3 (Nunn and Anthony, 1988) which supports the earlier proposal that cytochrome c_L is the true *in vivo* electron donor to pMMO. This logistically facilitates and optimises any electron transfer from methanol dehydrogenase to pMMO via the cytochrome c_L. This is in agreement with the findings of a CO-binding cytochrome c_{co}, which was identified as the immediate donor to pMMO from *Methylosinus trichosporium* OB3b (Tonge *et al.*, 1975). Complete cyanide-inhibition of activity in the pMMO is consistent with the proposal of a terminal oxidase being involved.

From these conclusions, a mechanism of *in vivo* pMMO electron transfer could be proposed based on the same principles as those proposed by Tonge *et al.*, 1995 and 1977). If the model (Figure 7.1) is correct then there would probably be two ranks of cytochromes in the electron transfer pathway since NADH is a two-electron donor and each cytochrome can only carry one electron. Therefore, electron transfer would be more efficient (logistically-speaking) if the final electron acceptor (pMMO) was present in at least two copies as well. This would be consistent with the structural model of the pMMO complex which exists as, at least a dimer. The presence of multiple copies of the *pmo* hydroxylase genes (Semrau *et al.*, 1995; Costello *et al.*, 1995; Stolyar *et al.*, 1999) a phenomenon rarely found in prokaryotes, lends credence to the fact that the pMMO may exist in a polymeric state or even in different forms.

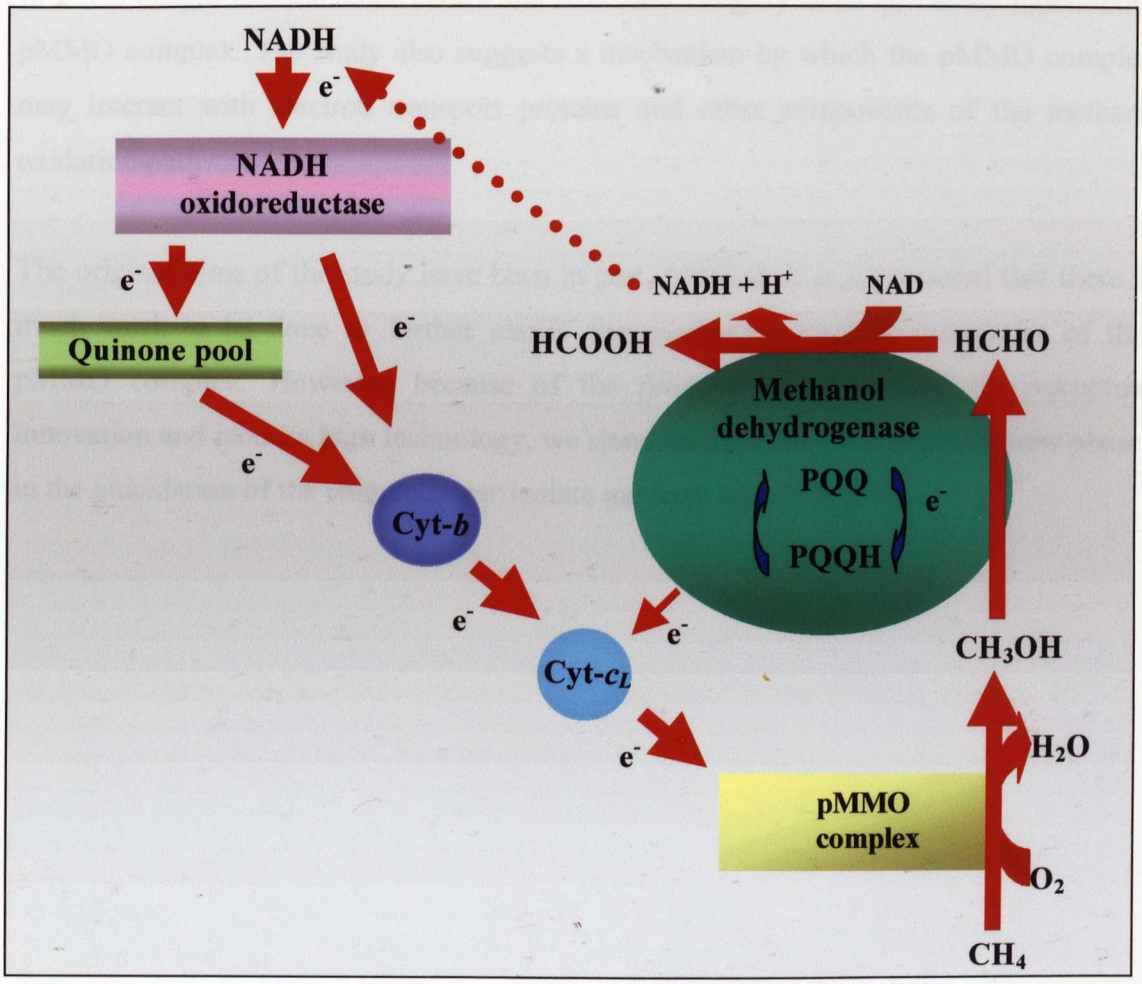

Figure 7.1 Schematic diagram for the tentative mechanism of *in vivo* electron transfer to pMMO. Electrons are recycled back to the monooxygenase from the methanol oxidation reaction by methanol dehydrogenase, via cytochrome c_L. NADH generated by the oxidation of formaldehyde and formate (not shown here) could be channelled back into the electron transport system.

The aims of this study were to find a reproducible method of purification of the pMMO and to subsequently characterise the enzyme. During this study a duroquinol-driven particulate methane oxidising complex was isolated reproducibly from *Methylococcus capsulatus* (Bath), with good specific activity. Various methods were used to give the first real insight into the metal centre and structural integrity of an *efficiently* functioning pMMO complex. The study also suggests a mechanism by which the pMMO complex may interact with electron transport proteins and other components of the methane oxidation pathway.

The original aims of the study have been in part, fulfilled. It is appreciated that there is much work to be done to further clarify the mechanism and characteristics of this pMMO complex. However, because of the promising combination of conceptual innovation and modern high technology, we stand on the brink of an exciting new phase, in the elucidation of the enigmatic particulate methane monooxygenase.

8. References

Adeosun, E. (2000). 'Formaldehyde Oxidation in *Methylococcus capsulatus* (Bath)'. *PhD. Thesis, University of Warwick.*

Akent'eva, N.F. and Gvozdev, R.I. (1988). Purification and physicochemical properties of methane monooxygenase from membrane structures of *Methylococcus capsulatus. Biokhimiya* **53:***91-96.*

Anthony, C. (1982). The biochemistry of methylotrophs. Academic Press Ltd., London.

Anthony, C. (1986). Bacterial oxidation of methane and methanol. *Advances in Microbial Physiology* **27:**113-209.

Anthony, C. (1992). The *c*-type cytochromes of methylotrophic bacteria. *Biochim. Biophys. Acta* **1099**: 1-15.

Anthony, C. and Ghosh, M. (1998). The structure and function of the PQQ-containing quinoprotein dehydrogenases. *Progress in Biophysics and Molecular Biology.* **69:**1-21

Anthony, C. and Zatman, L.J. (1964b). The microbial oxidation of methanol. II. The methanol-oxidising enzyme of *Pseudomonas M27. Biochemical Journal* **92:**614-621.

Anthony, C. and Zatman,L.J. (1964a). The microbial oxidation of methanol. 1. Isolation and properties of *Pseudomonas* sp M27. *Biochemical Journal* **92:**606-614.

Anthony, C., Ghosh, M., and Blake, C.C.F. (1994). The structure and function of methanol dehydrogenase and related PQQ-containing quinoproteins. *Biochemical Journal* **304:**665-674.

Arumugam, S., Pascal, S., North, C.L., Hu, W., Lee, K.-C., Cotten, M., Ketchem., R.R., Xu, F., Brenneman, M., Kovacs, F., Tian, F., Wang, A., Huo, S. and Cross, T.A. (1996). Conformational trapping in a membrane environment: A regulatory mechanism for protein activity? *Proc. Natl. Acad Sci. USA.* **93:**58725876.

Avezoux, A, Goodwin M.G and Anthony C. (1995). The role of the novel disulphide ring in the active site of the quinoprotein methanol dehydrogenase from *Methylobacterium extorquens. Biochem. J.* **307:** 735-741

Bergmann, D.J. and Hooper, A.B. (1994). Sequence of the gene, *amo* B, for the 43kDa polypeptide of ammonia monooxygenase of *Nitrosomonas europaea. Biochem. Biophys. Res. Commun.* **204:**759-762.

Bhambra, A (1996). 'The regulatory protein of sMMO'. *Thesis, University of Warwick.*

Bowman, J.P., Sly, L.I., Nichols, P.D. and Hayward, A.C. (1993). Revised taxonomy of the methanotrophs: description of *Methylobacter* gen. nov., emendation *of Methylococcus,* validation of *Methylosinus and Methylocystis* species, and a proposal that the family *Methylococcaceae* includes only the group I methanotrophs. *Int. J Syst. Bacteriol.* 43:735-743.

Bradford, M.M. (1976). A rapid and sensitive method for the quantitation of microgram quantities of protein utilising the principle of protein-dye binding. *Anal* Biochem. **72:**248-254.

Brusseau, G.A., Tsien, H.-C., Hanson, R.S. and Wackett, L.P. (1990). Optimization of trichloroethylene oxidation by methanotrophs and the use of a calorimetric assay to detect soluble methane monooxygenase activity. *Biodegradation* **1:** 19-29.

Burbaev, D.S., Moroz, I.A., Gvozdev, R.I. and Korshunov, L.A. (1994). Copper containing protein from the membranes of methane oxidising bacterium *Methylococcus capsulatus* (Strain M) containing methane monooxygenase. *Doklady Biochemistry* **339:**150-152.

Burch, R. and Parkyns, N. (1992) "New uses for natural gas" *Chemistry in Britain* November, 1013.

Burrows, K.D., Cornish, A., Scott, D. and Higgins, I.J. (1984). Substrate specificities of soluble and particulate methane monooxygenase of *Methylosinus trichosporium* OB3b. *J. Gen. Microbiol.* **130:**3327-3333.

Carlsen H.N., Joergensen L. and Degn, H., (1991). Inhibition by ammonia of methane utilisation in *Methylococcus capsulatus* (Bath). *Appl. Microbiol. Biotechnol.* **35:**1224-127.

Chan, S.I., Nguyen, H-H.T., Shiemke, A.K. and Lidstrom, M.E. (1993). Biochemical and biophysical studies towards characterisation of the membrane-associated methane monooxygenase. *In*: *Microbial Growth on C_1 Compounds pp* 107. Eds: Murrell, J.C. and Kelly, D.P. Intercept, Andover.

Charlton, S (1997). The Particulate Form of the Enzyme Methane Monooxygenase'. *PhD. Thesis, University of Warwick.*

Chistoserdova, L., Vorholt, J.A., Thauer, R.K. and Lidstrom, M.E. (1998). C_1 transfer enzymes and coenzymes linking methylotrophic bacteria and methanogenic Archaea. *Science* **281:** 99-102.

Chistoserdova, L.V. and Lidstrom, M.E. (1994). Genetics of the serine cycle in *Methylobacterium extorquens* AMI: identification of *sgaA and mtdA* and sequences of *sgaA, hprA, and mtdA. Journal of Bacteriology* **176:**1957-1968.

Colby, J. and Dalton, H. (1976). Some properties of a soluble methane monooxygenase from *Methylococcus capsulatus* Strain Bath. *Biochem. J.* **157:**495-49.

Colby, J. and Dalton, H. (1978). Resolution of the methane monooxygenase of *Methylococcus capsulatus* (Bath) into three components. *Biochem. J.* **171:**461-468

Colby, J. and Dalton, H. (1979). Characterisation of the second prosthetic group of the flavoenzyme NADH-acceptor reductase (component C) of the methane monooxygenase of *Methylococcus capsulatus* (Bath). *Biochem. J.* **177:**903-908.

Colby, J., Dalton, H. and Whittenbury, R. (1975). An improved assay for bacterial methane monooxygenase: some properties of the enzyme from *Methylomonas methanica. Biochemical Journal.* **151:**459-462.

Colby, J., Stirling, D. and Dalton, H. (1977). The soluble methane monooxygenase *of Methylococcus capsulatus* (Bath): its ability to oxygenate n-alkanes, n-alkene ethers, and acyclic, aromatic and heterocyclic compounds. *Biochem. J.* **165:**395-402

Cook, S.A. and Shiemke, A.K. (1996). Evidence that copper is a required cofactor for the membrane-bound form of methane monooxygenase. *J. Inorganic Biochem.* **63:**273-284.

Cook, S. A.; Shiemke, A. K. (1997)."Isolation and Characterization of a NADH:Quinone Reductase Capable of Reducing Membrane-Bound MMO from *Methylococcus capsulatus2".* Poster presentation.

Costello, A.M., Peeples, T.L., and Lidstrom, M.E., (1995). Duplicate methane monooxygenase genes in methanotrophs. Poster presentation at 8th International Symposium on Microbial Growth on C_1 Compounds. San Diego, California.

Crutzen, P.J. (1991). Methane's sinks and sources. *Nature* (London) **350:**380-381.

Dalton, H. (1977). Ammonia oxidation by the methane oxidising bacterium *Methylococcus capsulatus* strain Bath. *Arch. Microbiol.* **114:**273-279.

Dalton, H. and Leak, D.J. (1985). *In: Gas Enzymology,* Ed. Degn, H., Cox, R.P. and Toftlund, H., D. Reidel. Publishing Co. Dordrecht, Netherlands, ppl69-186.

Dalton, H., Prior, S.D., Leak, D.J. and Stanley, S.H. (1984). Regulation and control of methane monooxygenase, *In*: Microbial Growth on C_1 Compounds, 82. (Eds) Crawford, R.L. and Hanson, R.S. The American society for Microbiology Washington D.C.

Dalton, H., Smith, D.D.S. and Pilkington, S.J. (1990). Towards a unified mechanism of biological methane oxidation. *FEMS Microbiol. Reviews* **87:**201-208.

Dalton, H., Wilkins, P., and Jiang, Y. (1993). Structure and mechanism of action of the hydroxylase of soluble methane monooxygenase. *In:* Microbial Growth On C_1 Compounds. (Eds) J.C. Murrell and D.P. Kelly. Andover:lntercept press. pp. 65-80.

De Rosier, D.J. and Klug, A. (1968) Image averaging techniques for macromolecules arranged in regular arrays. *Nature.* **217:**130-134.

DiSpirito, A. A., Gulledge, J., Shiemke, A. K., Murrell, J. C., Lidstrom, M. E., and Krema, C. L. (1992). Trichloroethylene oxidation by the membrane-associated Methane Monooxygenase in Type I, Type II, and Type X Methanotrophs. *Biodegradation.* **2:**151-164.

DiSpirito, A.A., Shiemke, A.K., Jordan, S.W., Zahn, J.A. and Krema, C.L. (1994). Cytochrome aa_3 from *Methylococcus capsulatus* (Bath). *Arch Microbiol.* **161:**258-265.

Duine J.A. Frank J. Verwiel P.E. (1980). Structure and activity of the prosthetic group of methanol dehydrogenase. *European Journal of Biochemistry.* **108(1):**187-92.

Duine, J.A. and Frank, J (1980). The prosthetic group of methanol dehydrogenase. Purification and some of its properties. *Biochemical Journal.* **187:**221-226.

Dunstan, P.M.C., Anthony, C., and Drabble, W.T. (1972). Microbial metabolism of Cl and C2 compounds. The role of glyoxylate, glycollate and acetate in the growth of *Pseudomonas* AM1 on ethanol and on Cl compounds. *Biochemical Journal* **128:**107115.

Elliott S.J., Randall D.W., Britt, R.D. and Chan, S.I. (1998). Pulsed EPR studies of particulate methane monooxygenase from *Methylococcus capsulatus* (Bath): Evidence for Histidine Ligation. *J. Am. Chem. Soc.* **120**: 3247-3248.

Elliott, S. J., M. Zhu, L. Tso, H.-H. T. Nguyen, J. H.-K. Yip, and S. 1. Chan. (1997). Regio- and stereoselectivity of particulate methane monooxygenase from *Methylococcus capsulatus* (Bath). *J. Am. Chem. Soc.* **119**: 9949-9955.

Ensign, S.A., Hyman, M.R. and Arp, D.J. (1993). *In vitro* activation of ammonia monooxygenase from *Nitrosomonas europaea* by copper. *J.Bacteriol.* **175:**1971 - 1980.

Ferenci, T. (1974). Carbon monoxide-stimulated respiration in methane-utilising bacteria. *FEBS Letts.* **41:**94-98.

Ferenci, T., Strøm, T. and Quayle, J.R. (1975). Oxidation of carbon monoxide and methane by *Pseudomonas methanica. Journal of General Microbiology* **91:**79-91.

Finch, R. (1997). The molecular genetics and regulation of methane monooxygenase in *Methylosinus trichosporium* OB3b. *PhD. Thesis*, University of Warwick.

Fjellbirkeland, A., Kleivdal, H., Joergsen, C., Thestrup, H., and Jensen, H.B. (1997). Outer membrane proteins of *Methylococcus capsulatus* (Bath). *Arch. Microbiol.* **168:**128-135.

Fox, B.G., Borneman, J.G., Wackett, L.P. and Lipscomb, J.D. (1990). Haloalkene oxidation by soluble methane monooxygenase from *Methylosinus trichosporium* OB3b: mechanistic and environmental implications. *Biochemistry* **29:**6419-6427.

Fox, B.G., Froland, W.A., Dege, J.E. and Lipscomb, J.D. (1989). Methane monooxygenase from *Methylosinus trichosporium* OB3b. *J. Biol. Chem.* **264:**10023-10033.

Frank, J., Radermacher, M. , Pemczek, P., Zhn, J., Li, Y., Ladjadj, M. and Leith, A. (1996). Spider and WEB: Processing and visualisation of images in 3-D electron microscopy and related fields. *Journal of Structural Biology.* **116:**190-199.

Fuse *et al.*, (1998). Oxidation of trichloroethylene and dimethyl sulfide by a marine *Methylomicrobium* strain containing soluble methane monooxygenase. *Biosci. Biotechnol. Biochem.* **62:**1925-1931.

Gilbert, B., McDonald, I.R., Finch, R. Stafford, G.P., Nielsen, A.K. and Murrell, J.C. (2000). Molecular analysis of the *pmo* (Particulate Methane Monooxygenase) operons from two type II methanotrophs. *Appl. and Environ. Microbiol.* **66(3):**966-975.

Green, J. and Dalton, H. (1985). Protein B of soluble methane monooxygenase from *Methylococcus capsulatus* (Bath): a novel regulatory protein of enzyme activity. *J. Biol. Chem.* **260:**15795-15801.

Green, J. and Dalton, H. (1988). The biosynthesis and assembly of protein A of soluble methane monooxygenase from *Methylococcus capsulatus* (Bath). *J.Biol.Chem.* **263:**17561-17565.

Green, J. and Dalton, H. (1989). Substrate specificity of soluble methane monooxygenase: mechanistic implications. *J Biol. Chem.* **264:**17698-17703.

Green, J., Prior, S.D. and Dalton, H. (1985). Copper ions as inhibitors of protein C of soluble methane monooxygenase of *Methylococcus capsulatus* (Bath). *Eur. J. Biochem.* **153:**137-144.

Green, P.N. (1992). Taxonomy of methylotrophic bacteria. *In*: *Methane and methanol utilisers.* pp23-83. (Eds) Murrell, J.C. and Dalton, H. Plenum Press, New York.

Grosse, S., Wenlandt, K.D. and Kleber, H.P. (1997). Purification and properties of methanol dehydrogenase from *Methylocystis sp.* GB 25. *Journal of Basic Microbiology* **37:**269-279.

Gvozdev, R.I., Shushenacheva, E.V., Pylyashenko-Novochatnii, A.I. and Belova, V.S. (1984). Investigation of enzymatic oxidation by methane monooxygenase of *Methylococcus capsulatus,* strain M, membrane structure. *Oxidation Communications.* 7:249-266.

Haber, C.L., Allen, L.N., Zhao, S. and Hanson, R.S. (1983) Methylotrophic bacteria: biochemical diversity and genetics. *Science* **221:**1147

Hanson, R.S. (1992) *In*: *Methane and methanol utilisers,* ppl-21. Eds Murrell, J.C. and Dalton, H. Plenum Press, New York.

Hanson, R.S. and Hanson, T.E. (1996). Methanotrophic bacteria. *Microbiological Reviews* **60(2):**439-471.

Hartshorne, R.P. and Catterall, W.A. (1984). The sodium channel from rat brain. Purification and subunit composition. *J Biol. Chem.* **259:**1667-1675

Henderson, R. and Unwin, P.N.T. (1975) Bacteriorhodopsin. *Nature.* **257:**28-32.

Heptinstall, J. and Quayle, J.R. (1970). Pathways leading to and from serine during growth of *Pseudomonas* AMI on C_1 compounds or succinate. *Biochemical Journal* **117:**563-572.

Higgins, I.J. and Quayle, J.R. (1970). Oxygenation of methane by methane-grown *Pseudomonas methanica* and *Methanomonas methanooxidans. Biochemical Journal* **118:**201-208.

Higgins, I.J., Best, D.J. and Hammond, R.C. (1980). New findings in methane utilising bacteria highlight their importance in the biosphere and their commercial potential. *Nature* **286:**561-564.

Higgins, I.J., Best, D.J., Hammond, R.C. and Scott, D. (1981a). Methane oxidising microorganisms. *Microbiol Rev.* **45:**556-590.

Higgins, I.J., Best, D.J., and Scott, D. (1981b). *In: Microbial growth on C_1 compounds.* (Ed) H. Dalton. Heyden and Son Ltd., London. pp11-20.

Higgins, I.J., Knowles, C.J. and Tonge, G.M. (1976). Enzymic mechanisms of methane and methanol oxidation in relation to electron transport systems in methylotrophs; purification and properties of methane oxygenase. *In: "Proceedings of the symposium on Microbial Production and utilisation of gases"* (Ed) H.G. Schlegel, G. Gottschalk and N. Pfennig. E. Goltze, Göttingen.pp389-392

Hogan, K.B., Hoffman, J.S and Thompson, A.M. (1991). Methane on the greenhouse agenda. *Nature* (London). **354:**131-132.

Holm, R.H., Kennenpohl, P. and Solomon, E.I. (1996). Structural and functional aspects of metal sites in biology. *Chemical Reviews,* **96:**2239-2314.

Holmes, A.J., Costello, A., Lidstrom, M.E. and Murrell, J.C. (1995). Evidence that particulate methane monooxygenase and ammonia monooxygenase may be evolutionarily related. *FEMS Microbiol. Letts.* **132:**203-208.

Hooper, A.B. and Terry, K.R. (1973). Specific inhibitors of ammonia oxidation in *Nitrosomonas. J. Bacteriology* **115:**480-485.

Hubley, J.H., Thomson, A.W. and Wilkinson, J.F. (1975). Specific inhibitors of methane oxidation in *Methylosinus trichosporium. Archives of Microbiology* **102:**199-202.

Hyman, M.R. and Arp, D.J. (1992). $^{14}C_2H_2$- and $^{14}CO_2$-labelling studies of the *de novo* synthesis of polypeptides by *Nitrosomonas europaea* during recovery from acetylene and light inactivation of ammonia monooxygenase. *J. Biol. Chem.* **267:**1534-1445.

Hynes and Knowles (1982). Effect of acetylene on autotrophic and heterotrophic nitrification. *Can. J. Microbiol.* **28:**334-340.

Ingram, D.J.E. (1969). *In: Biological and Biochemical Applications of Electron Spin Resonance.* Adam Hilger Ltd., London.

Jiang, Y., Wilkins, P.C. and Dalton, H. (1993). Activation of the hydroxylase of sMMO from *Methylococcus capsulatus* (Bath) by hydrogen peroxide. *Biochim. Biophys. Acta.* **1163:**105-112.

Jollie, D.R. and Lipscomb, J.D. (1991). Formate dehydrogenase from *Methylosinus trichoporium* OB3b. Purification and spectroscopic characterisation of the cofactors. *Journal of Biological Chemistry.* **266(32):**21853-21863.

Kastrau, D.H.W., Heiss, B., Kroneck, P.M.H. and Zumft, W.G. (1994). Nitric oxide reductase from *Pseudomonas stutzeri,* a novel cytochrome *bc* complex.

Kazlauskaite, H., Hill, A.0., Wilkins, P.C., and Dalton, H. (1996). Direct electrochemistry of the hydroxylase of soluble methane monooxygenase from *Methylococcus capsulatus* (Bath). *European Journal of Biochemistry.* **241:**552-556.

Kleinekofort, W., Germeroth, L., van der Brock, J.A., Schubert, D. and Michel, H. (1992). The light-harvesting compex II (B800/850) from *Rhodospirillium molischianum* is an octamer. *Biochemica et Biophysica Acta.* **1140:**102-104.

Koh, S.-C., Bowman, J.P. and Sayler, G.S. (1993). Soluble methane monooxygenase production and trichloroethylene degradation by a type I methanotroph, *Methylomonas methanica 68-1. Appl. Environ. Microbiol.* **59:**960-967.

Laemmli, U.K. (1970). Cleavage of structural proteins during the assembly of the head of bacteriophage T4. *Nature,* London. **227:**680-689.

Large, P.J. and Bamforth, C.W. (1988). *Methylotrophy and Biotechnology.* Longman, Wiley, New York.

Leadbetter, E.R. and Foster, J.W. (1959). Incorporation of molecular oxygen in bacterial cells utilising hydrocarbons for growth. *Nature.* **184:**1428-1429.

Leak, D.J. and Dalton, H. (1983). *In vivo* studies of primary alcohols, aldehydes and carboxylic acids as electron donors for the methane monooxygenase in a variety of methanotrophs. *J. General Microbiology* **129:**3487-3497.

Leak, D.J. and Dalton, H. (1986a). Growth yields of methanotrophs, 1. Effect of copper on the energetics of methane oxidation. *Appl. Microbiol. Biotechnol.* **23:**470-476.

Leak, D.J. and Dalton, H. (1986b). Growth yields of methanotrophs, 2. A theoretical analysis. *Appl. Microbiol. Biotechnol.* **23:**477-481.

Leak, D.J. Stanley, S.H. and Dalton, H. (1985). Implications of the nature of methane monooxygenase on carbon assimilation in methanotrophs. *In: Microbial gas metabolism, mechanistic, metabolic and biotechnological aspects.* (Ed) R.K. Poole, and S.C. Dow. Academic press Ltd., London pp201-208.

Leak, D.J., (1992). Biotechnology and applied aspects of methane and methanol utilizers. *In*: *Methane and methanol utilizers.* Murrell, J.C and Dalton, H (ed). Plenum Press, New York. pp256-261.

Leak, D.J., Aikens, P.J. and Seyed-Mahmoudian, M. (1992). The microbial production of epoxides. *Trends in Biotechnol.* **10:**256-261.

Lelieveld, J., Crutzem, P.J. and Bruhl, C. (1993). Climate effects of atmospheric methane. *Chemosphere* **26:**739-768.

Lemos, S.S, Collins, M.L.P., Eaton, S.S., Eaton, G.R. and Antholine, W.E. (2000). Comparison of EPR-visible Cu^{2+} sites in pMMO from *Methylococcus capsulatus* (Bath) and *Methylomicrobium album* BG8. *Biophysical Journal.* **79:**1085-1094.

Lidstrom, M.E. and Semrau, J.D. (1995). Metals and Microbiology; The influence of copper on methane oxidation. *In: Aquatic Chemistry.* Eds: C.P. Huang, C.R. O'Melia and J.J. Morgan. American Chemical Society, Washington D.C. pp 195-201.

Lidstrom, M.E. and Stirling, D.I. (1990). Methylotrophs: Genetics and commercial applications. *Annu. Rev. Microbiol.* **44:**27-58.

Lipscomb, J.D., Lee, S.K., Froland, W.A., Andersson, K.K., Liu, Y., Neshein, J.C. (1993) Oxygen-activation by the oxygen-bridged di-iron cluster of the methane monooxygenase hydroxylase component. *FASEB Journal.* **7(7):**AlO54.

Liu, A.-M., Li, S.-B., Miao, D.-X., Yu, W.-L., Zhang, F. and Su, P. (1991). Isolation and purification of methane monooxygenase from *Methylomonas* sp. GYJ3. *Chinese Chem. Lett.* **2:**419-422.

Liu, K.E. and Lippard, S.J. (1991). Redox properties of the hydroxylase component of methane monooxygenase from *Methylococcus capsulatus* (Bath): effects of protein B, reductase and substrate. *Journal of Biological Chemistry* **266:**12836-12839.

Liu, Y., Nesheim, J.C., Lee, S.K. , and Lipscomb, J.D. (1995). Gating effects of components on oxygen activation by the methane monooxygenase hydroxylase component. *Journal of Biological Chemistry.* **270(42):**24662-24665.

Lloyd, J.S. (1997). Heterologous expression and site-directed mutagenesis of soluble methane monooxygenase. *PhD Thesis,* University of Warwick.

Lloyd, J.S., Bhambra, J., Murrel, J.C., and Dalton, H. (1997). Inactivation of the regulatory protein B of soluble methane monooxygenase from *Methylococcus capsulatus* (Bath) by proteolysis can be overcome by a Gly to Gln modification. *European Journal of Biochemistry.* **248:**72-79.

Lowry, O.H., Rosenbrough, N.J., Farr, A.L. and Randall, R.J. (1951). Protein measurement with the Folin phenol reagent. *J.Biol. Chem.* **193:**265-275.

Lund, J. and Dalton, H. (1985). Further characterisation of the FAD and Fe_2S_2 redox centers of component C, the NADH:acceptor reductase of the soluble methane monooxygenase of *Methylococcus capsulatus* (Bath). *Eur. J Biochem.* **147:**291-296.

Lund, J., Woodland, M.P. and Dalton, H. (1985). Electron transfer in the soluble methane monooxygenase of *Methylococcus capsulatus* (Bath). Eur. *J. Biochem.* **147:**297-305.

McTavish, H., Fuchs, J.A. and Hooper, A.B. (1993). Sequence of the gene coding for ammonia monooxygenase in *Nitrosomonas europaea. J.Bacteriol.* **175:**2436-2444.

Maniatis, T. (1989). Molecular cloning, a laboratory manual. Second Edition. Edited by J. Sambrook, E.F. Fritsch and T. Maniatis. Cold Spring Harbour Laboratory Press.

Marison, I.W. and Attwood, M.M. (1982). A possible alternative mechanism for the oxidation of formaldehyde to formate. *Journal of General Microbiology.* **128:**1441-1446.

Moir. J.W.B., Crossman, L.C., Spiro, S. and Richardson, D.J. (1996). The purification of ammonia monooxygenase from *Paracoccus denitrificans. FEBS Letters* **387:**71-74.

Moore, A.L, Umbach, A.L, and Siedow, J.N. (1995) Structure-Function relationships of the alternative oxidase of plant mitochondria: A model of the active site. *J. of Bioenergetics and Biomembranes.* **27(4):**367-377.

Murrell, J.C (1993). Molecular biology of methane oxidation. *In: Microbial Growth on C_1 compounds.* (Eds) J.C. Murrell. and D.P. Kelly. Intercept, Andover, pp 109-112.

Murrell, J.C (1994). Molecular genetics of methane oxidation. *Biodegradation.* **5:** 145-159.

Murrell J.C. and Holmes, A. (1996). Molecular biology of methane monooxygenase. *In: Microbial Growth on C_1 compounds.* (Eds) M.E. Lidstrom. and F.R. Tabita. Kluver Academic publishers, Netherlands, pp 133-140.

Murrell J.C., McDonald, I.R. and Gilbert, B. (2000). Regulation of expression of methane monooxygenase by copper ions. *Trends in Microbiology.* **8(5):**221-225.

Nakajima, T., Uchiyama, H., Yagi, O. and Nakahara, T. (1992). Purification and properties of a soluble methane monooxygenase from *Methylocystis* sp.M. Biosci. *Biotech. Biochem.* **56:**736-740.

Neese, F., Zumft, W.G., Antholine, W.E. and Kroneck, P.M.H. (1996). The purple mixed-valance Cu_A center in nitrous-oxide reductase: EPR of the copper-63-, copper-65- and [^{15}N] histidine enriched enzyme and a molecular orbital interpretation. *J Am. Chem. Soc.* **118:**8692-8699.

Nguyen, H.-H.T., Elliot, S.J., Yip, J.H.-K., and Chan, S.I. (1998). The particulate methane monooxygenase from *Methylococcus capsulatus* (Bath) is a novel copper containing three-subunit enzyme. *Journal of Biological Chemistry.* **273(14):**7957-7966.

Nguyen, H-H. T., Nakagawa, K.H., Hedman, B., Elliot, S.J., Lidstrom, M.E., Hodgson, K.O. and Chan, S.I. (1996b). X-ray absorption and EPR studies on the copper ions associated with the particulate methane monooxygenase from *Methylococcus capsulatus* (Bath). Cu(I) ions and their implications. *J. Am. Chem.* Soc. **118(50):**12766-12776.

Nguyen, H-H. T., Shiemke, A.K., Jacobs, S.J., Hales, B.J., Lidstrom, M.E. and Chan, S.I. (1994). The nature of the copper ions in the membranes containing the particulate methane monooxygenase from *Methylococcus capsulatus* (Bath). *J. Biol. Chem.* **269:**14995-15005.

Nguyen, H-H. T., Zhu, M., Elliot, S.J., Nakagawa, K.H., Hedman, B., Costello, A.M., Peeples, T.L., Wilkinson, B., Morimoto, H., Williams, P.G., Floss, H.G., Lidstrom, M.E., Hodgson, K.O. and Chan, S.I. (1996a). The biochemistry of the particulate methane monooxygenase. *In: Microbial Growth on C_1 Compounds* ppl50-158. Eds: M.E. Lidstrom and F.R, Tabita. Kluwer Academic Publishers, Dordrecht.

Nielsen, A.K., Gerdes, K., Degn, H. and Murrell, J.C. (1996a). Regulation of bacterial methane oxidation: transcription of the soluble methane monooxygenase operon of *Methylococcus capsulatus* (Bath) is repressed by copper ions. *Microbiology* **142:**1289-1296.

Nielsen, A.K., Gerdes, K., and Murrell, J.C. (1996b). Copper-dependent reciprocal transcriptional regulation of methane monooxygenase genes in *Methylococcus capsulatus* (Bath) and *Methylosinus trichosporium. Mol. Microbiol* **25:399-409.**

Nunn, D.N. and Lidstrom, M.E. (1986). Isolation and complementation analysis of 10 methanol oxidation mutant classes and identification of the methanol dehydrogenase structural gene of *Methylobacterium* sp. strain AMI. *Journal of Bacteriology.* **166:**581-590.

Nunn, D.N., and Anthony C. (1988). Cytochrome c_L. *Biochem. J.* **256:**673-676.

Nunn, D.N., Day, D., and Anthony C. (1989). The second subunit of methanol dehydrogenase of *Methylobacterium extorquens* AM1. *Biochemical Journal.* **260(3):**85762.

O'Neill, J.G. and Wilkinson, J.F., (1977). Oxidation of ammonia by methane-oxidising bacteria and effects of ammonia on methane oxidation. *J.Gen. Microbiol.* **100:**407-412.

Ortiz de Montellano, P.R. (1986) *In: Cytochrome P-450.- Structure, Mechanism, and Biochemistry.* (Ed) Ortiz de Montellano, P.R. Plenum Press, New York, pp.217-271.

Patel, R.N. and Felix, A. (1976). Microbial oxidation of methane and methanol: crystallization and properties of methanol dehydrogenase from *Methylosinus sporium. Journal of Bacteriology.* **128(l):**413-24.

Patel, R.N. and Savas, J.C. (1987) Purification and properties of the hydroxylase component of methane monooxygenase. *J. Bacteriol.* **169:**2313-2317.

Patel, R.N., Hou, C.T., Laskin and A.I., Felix (1982). Microbial oxidation of hydrocarbons: properties of a soluble methane monooxygenase from a facultative methane-utilising organism, *Methylobacterium* sp. strain CR-L-26. *Appl. Environ. Microbiol.* **44:**1130-1137.

Patel, R.N., Hou, C.T., Laskin, A.I., Felix, A. and Deiranko, P. (1979). Microbial oxidation of gaseous hydrocarbons. II. Hydroxylation of alkanes and epoxidation of alkenes by cell free particulate fractions of methane oxidising bacteria. *J. Bacteriology.* **139:**675-679.

Peisach, J. and Blumberg, W.E. (1974). Structural implications derived from the analysis of electron paramagnetic resonance spectra of natural and artificial copper proteins. *Archives of Biochemistry and Biophysics* **165:**691-708.

Peltola, P., Priha, P. and Laakso, S. (1993). Effect of copper on membrane lipids and on methane monooxygenase activity of *Methylococcus capsulatus (Bath). Archives of Microbiology* **159:**521- 525.

Peterson, G.L. (1977). A simplification of the protein assay method of Lowry which is more generally applicable. *Anal. Biochem.* **83:**346-356.

Pilkington, S.J. and Dalton, H. (1991). Purification and characterisation of the soluble methane monooxygenase from *Methylosinus sporium* 5 demonstrates the highly conserved nature of this enzyme in methanotrophs. *FEMS Microbiol. Lett.* **78:**103-108.

Pilkington, S.J., Salmond, G.P.C., Murrell, J.C. and Dalton, H. (1990). Identification of the gene encoding the regulatory protein B of the soluble methane monooxygenase. *FEMS Microbiol. Lett.* **72:**345-348.

Prior, S.D. and Dalton, H. (1985a). The effect of copper ions on membrane content and methane monooxygenase activity in methanol-grown cells *Methylococcus capsulatus* (Bath). *J. Gen. Microbiol.* **131:**155-163.

Prior, S.D. and Dalton, H. (1985b). Acetylene as a suicide substrate and active site probe for methane monooxygenase from *Methylococcus capsulatus* (Bath). *FEMS Microbiol. Letts.* **29:**105-109.

Quayle, J.R. (1987). An eightieth anniversary of the study of C_1 metabolism. *In*: *Microbial Growth on C_1-Compounds.* (Eds). Van Verseveld, H.W. and Duine, J.A.. Martinus Nijhoff, Dordrecht. pp 1 -5.

Ribbons, D.W. (1975). Oxidation of C_1 compounds by particulate fractions from *Methylococcus capsulatus*: distribution and properties of methane-dependent reduced nicotinamide adenine dinucleotide oxidase (methane hydroxylase). *J. Bacteriol.* **122:**1352-1363.

Ribbons, D.W. and Michalover, J.L. (1970). Methane oxidation by cell-free extracts of *Methylococcus capsulatus. FEBS Letters.* **11:**41-44.

Rich, P.R. (1981). Electron transfer reactions between quinols and quinones in aqueous and aprotic media. *Biochim. Biophys. Acta.* **637:**28-33.

Robinson, N.C., Wiginton, D. and Talbert, L. (1984). Phenyl-sepharose-mediated detergent-exchange chromatography: Its application to the exchange of detergents bound to membrane proteins. *Biochemistry.* **23:**6121-6126.

Rosenzweig, A.C., Frederick, C.A., Lippard, S.J. and Norlund, P. (1993). Crystal structure of a bacterial non-haem iron hydroxylase that catalyses the biological oxidation of methane. *Nature.* **366:**537-543.

Sayavedra-Soto, L.A., Hommes, N.G., Russell, S.A. and Arp, D.J. (1996). Induction of ammonia monooxygenase and hydroxylamine oxidoreductase mRNAs by ammonium in *Nitrosomonas europaea. Mol. Microbiol.* **20(3):**541-548.

Schägger, H. (1994). Chromatographic techniques and basic operations in membrane protein purification. *In: A practical guide to membrane protein purification.* Eds. G.V. Jagow and H. Schägger. Publishers: Academic Press.

Scott, D., Best, D.J. and Higgins, I.J. (1981a). Intracytoplasmic membranes in oxygen-limited chemostat cultures of *Methylosinus trichosporium* OB3b; biocatalytic implications of physiologically balanced growth. *Biotechnol. Lett.* **3**:641-644.

Scott, D., Brannan, J. and Higgins, I.J. (1981b). The effect of growth conditions on intracytoplasmic membranes and methane monooxygenase activities in *Methylosinus trichosporium* OB3b. *J Gen. Microbiol.* **125**:63-72.

Sealy, R.C., Hyde, J.S. and Antholine, W.E. (1985). Electron Spin Resonance. *In: Modem Physical Methods in Biochemistry, Part A.* Elsevier Science Publishers, BV.

Semrau, J.D., Christoserdov, A., Lebron, J., Costello, A., Davagnino, J., Kenna, E., Holmes, A.J., Finch, R., Murrell, J.C. and Lidstrom, M.E. (1995a). Particulate methane monooxygenase genes in methanotrophs. *J. Bacteriol.* **177**:3071-3079.

Semrau, J.D., Zolandez, D., Lidstrom, M.E. and Chan, S.I. (1995b). The role of copper in the pMMO of *Methylococcus capsulatus* (Bath): A structural vs. catalytic function. *J. Inorganic Biochem.* **58**:235 -244.

Shears, J.H. and Wood, P.M. (1986). Tri- and tetramethylhydroquinone as electron donors for ammonia monooxygenase in whole cells of *Nitrosomonas europaea. FEMS Microbiol. Lett.* **33**:281-284.

Shiemke, A.K., Cook, S.A., Miley, T. and Singleton, P. (1995). Detergent solubilisation of membrane-bound methane monooxygènase requires plastoquinol analogs as electron donors. *Archives of Biochemistry and Biophysics.* **321**:421-428.

Shigematsu, T. (1999). Soluble methane monooxygenase gene clusters from trichloroethylene-degrading *Methylomonas* sp. strains and detection of methanotrophs during *in situ* bioremediation. *Appl. Environ. Microbiol.* **65**:5198-5206.

Shinohara, Y., Uchiyama, H., Yagi,O. and Kusakabe, I. (1998). Purification and characterisation of component B of a soluble methane monooxygenase from *Methylocystis sp.M. Journal of Fermentation and Bioengineering.* **85**:37-42.

Shrope, M. (2000) Methane munchers go slow. *New Scientist* **166**:7.

Smith, D. and Dalton, H. (1989). Solubilisation of methane monooxygenase from *Methylococcus capsulatus* (Bath). *Eur. J Biochem.* **182**:667-671.

Stanley, S.H. (1985). *PhD Thesis, University of Warwick, Coventry.*

Stanley, S.H. and Dalton, H. (1982). Role of ribulose-1,5-bisphosphate carboxylase/oxygenase in *Methylococcus capsulatus* (Bath). *Journal of General Microbiology* **128**:2927-2935.

Stanley, S.H. and Dalton, H. (1992). The biotransformation of propylene to propylene oxide by *Methylococcus capsulatus* (Bath): 1. optimisation of rates. *Biocatalysis* **6:**163-175.

Stanley, S.H., Prior, S.D., Leak, D.J. and Dalton, H. (1983). Copper stress underlies the fundamental change in intracellular location of methane monooxygenase in methane-oxidising organisms: studies in batch and continuous cultures. *Biotechnol. Lett.* **5:**487-492.

Stirling, D. I., and Dalton, H. (1978). Purification and properties of an NAD(P)-linked formaldehyde dehydrogenase from *Methylococcus capsulatus* (Bath). *J.Gen. Microbiol.* **107:**19-29.

Stirling, D.I. and Dalton, H. (1979). Properties of the methane monooxygenase from extracts of *Methylosinus trichosporium* OB3b and evidence for its similarity to the enzyme from *Methylococcus capsulatus* (Bath). *Eur. J Biochem.* **96:**205-212.

Stolyar, S., Costello, A.M., Peeples, T.L., and Lidstrom, M.E. (1999). Role of multiple gene copies in particulate methane monooxygenase activity in the methane-oxidising bacterium *Methylococcus capsulatus* (Bath). *Microbiology.* **145:**1235-1244.

Suzina N.E, Chetina, E.V., Trotsenko Y.A and Fikhte, B.A. (1985). Peculiarities of the supramolecular organisation of intracytoplasmic membranes in methanotrophs. *FEMS Microbiology Letters.* **30:**111-114.

Suzuki, I., Kwok, S.-C., Dular, U. and Tsang, D.C.Y. (1981). Cell-free ammonia oxidizing system of *Nitrosomonas europaea:* general conditions and properties. *Can. J Biochem.* **59:**477-483.

Takeda, K., Tezuka, C., Fukuoka, S. and Takahara, Y. (1976). Role of copper ions in methane oxidation by *Methylomonas margaritae. J. Ferment. Technol.* **54:**557-562.

Takeguchi, M., Mijakawa, K., Kamachi, T. and Okura, 1. (1997). Purification and properties of particulate methane monooxygenase from *Methylosinus trichosporium* OB3b. *Journal of Inorganic Biochemistry* **65:**278-282.

Takeguchi, M., Fukui, K. Ohya, H. and Okura 1. (1999). Electron spin-echo envelope modulation studies on copper site of particulate methane monooxygenase from *Methylosinus trichosporium* OB3b. *Chem. Lett.* **(7):**617-618.

Takeguchi, M., Miyakawa, K. and Okura, I. (1998b). Purification and properties of particulate methane monooxygenase from *Methylosinus trichosporium* OB3b. *J. Mol. Catalysis A Chem.* **132:**145-153.

Takeguchi, M., Miyakawa, K. and Okura,. I. (1998a). Properties of the membranes containing the particulate methane monooxygenase from *Methylosinus trichosporium* OB3b. *Biometals.* **11:**229-234.

Tate, S. (1996). 'The modifier protein of formaldehyde dehydrogenase from *Methylococcus capsulatus* (Bath)'. *PhD. Thesis, University of Warwick.*

Tate, S. and Dalton, H. (1999). A low molecular-mass protein for *Methylococcus capsulatus* (Bath) is responsible for the regulation of formaldehyde dehydrogenase activity *in vitro*. *Microbiology UK.* **145:**159-167.

Tellez, C.M., Gaus, K.P., Aguilar-Aguil, A., Graham, D.W., Arnold, R.G. and Guzman, R.Z. (1997). Isolation of copper biochelates from *Methylosinus trichosporium* OB3b and sMMO^{c} mutants. *Appl. Environ. Microbiol.* **64:**1115-1122.

Tonge, G.M., Harrison, D.E.F and Higgins, I.J. (1977). Purification and properties of the methane monooxygenase system from *Methylosinus trichosporium* OB3b. *Biochem.* J **161:**333-344.

Tonge, G.M., Harrison, D.E.F., Knowles, C.J. and Higgins, I.J. (1975) Properties and partial purification of the methane-oxidising enzyme systems from *Methylosinus trichosporium. FEBS Lett.* **58:**293-299.

Tsien, H.C., Brusseau, G.A., Hanson, R.S. and Wackett, L.P. (1989). Biodegradation of trichloroethylene by *Methylosinus trichosporium* OB3b. *Appl. Enviro. Microbiol.* **55:**3155-3161.

Tukhvatullin, I.A., Korshunova, L.A., Gvozdev, R.I. and Dalton, H. (1996). Investigation of the copper center of membrane-bound methane monooxygenase from subcellular structures of *Methylococcus capsulatus* (strain M). *Biochemistry (Moscow)* **61:**886-891.

van Heel, M. and Frank, J. (1981). Use of multivariate statistics in analysing the images of biological macromolecules. *Ultramicroscopy.* **6(2):**187-194.

Von Jagow, G., Link, T.A. and Schägger, H. (1994) Purification strategies for membrane proteins. *In*: *A Practical Guide to Membrane Protein Purification.* (Eds) Gebhard Von Jagow and Hermann Schägger. Published by Academic Press.

Vorholt, J.A., Chistoserdova, L., Lidstrom, M.E., and Thauer, R.K. (1998). The NADP-dependent methylene tetrahydromethanopterin dehydrogenase in *Methylobacterium extorquens* AM1. *Journal of Bacteriology* **180(20):**5351-5356.

Vorholt, J.A., Chistoserdova, L., Stolyar, S.M., Thauer, R.K. and Lidstrom, M.E. (1999). Distribution of tetrahydromethanopterin-dependent enzymes in methylotrophic bacteria and phylogeny of methenyl tetrahydromethanopterin cyclohydrolases. *Journal of Bacteriology* **181:**5750-5757

Warne, A., Wang, D.N. and Saraste, M. (1995). Purification and two-dimensional crystallisation of bacterial cytochrome oxidases. *Eur. J. Biochem.* **234:**443-451.

Wertz, J.E. and Bolton, J.R. (1986). *In*: *Electron Spin Resonance, Elementary Theory and Practical Applications*. Chapman and Hall, New York, London.

Whittenbury, R. and Dalton, H. (1981). The methylotrophic bacteria. *In: The Prokaryotes.* (Eds) M.P. Starr, H.Stolph, H.G. Truper, A. B A. Balows, and H.G. Schlegel.. Springer-Verlag, Heidleburg. pp894-902

Whittenbury, R., Phillips, K.C. and Wilkinson, J.F. (1970). Enrichment, isolation and some properties of methane-utilising bacteria. *Journal of General Microbiology* **61:**205-218.

Wilkins, P.C., Dalton, H., Podmore, I.D., Deighton, N. and Symons, M.C.R. (1992). Biological methane activation involves the intermediacy of carbon centered radicals. *Eur. J Biochem.* **210:**67-72.

Wilkinson, B., Zhu, M., Priestly, N.D., Nguyen, H-H.,T., Morimoto, H., Williams, P.G., Chan, S.I. and Floss, H.G. (1996). A concerted mechanism for ethane hydroxylation by the particulate methane monooxygenase from *Methylococcus capsulatus* (Bath). *J. Am. Chem. Soc.* **118:**921-922.

Woodland, M.P. and Dalton, H. (1984). Purification and characterisation of component A of the methane monooxygenase from *Methylococcus capsulatus* (Bath). *J. Biol Chem.* **259:**53-59.

Woodland, M.P. and Dalton, R. (1989). Purification and characterisation of Component A of the methane monooxygenase from *Methylococcus capsulatus* (Bath). *Journal of Biological Chemistry.* **259:**53-59.

Woodland, M.P., Patil, D.S., Cammack, R. and Dalton, H. (1986). ESR studies of protein A of the soluble methane monooxygenase from *Methylococcus capsulatus* (Bath). *Biochim. Biophys. Acta.* **873:**237-242.

Wösten, M.M. (1998). Eubacterial sigma factors. *FEMS Microbiol. Rev.* **22:**127-150.

Yagi, T. (1991). Bacterial NADH-Quinone Oxidoreductases. *J. Bioenerg. Biomembr.* **23:**211-225.

Yagi, T. (1993). The bacterial energy-transducing NADH-Quinone oxidoreductases. *Biochim. Biophys. Acta.* **1141:** 1-17.

Yanagita, Y. and Kagawa, Y. (1986). *In*: *Techniques for the analysis of membrane proteins.* pp 61-76. (Eds) C.I.. Raglan and R.J. Cherry. Chapman and Hall, London.

Yoch, D.C., Chen, Y.-P., and Hardin, M.G. (1990). Formate dehydrogenase from the methane oxidizer *Methylosinus trichosporium* OB3b. *Journal of Bacteriology.* **172(8):**4456-4463.

Yuan, H., M. L. P. Collins, and Antholine, W. E. (1997). Low frequency EPR of the copper in particulate methane monooxygenase from *Methylomicrobium albus* BG8. *J. Am. Chem. Soc.* **119:**5073-5074.

Yuan, H., Collins, M. L. P. and Antholine W. E. (1998a). Concentration of Cu, EPR-detectable Cu, and formation of cupric-ferrocyanide in membranes with pMMO. *J. Inorg. Biochem.* **72:**179-185.

Yuan, H., Collins, M. L. P. and Antholine W. E. (1998b). Analysis of type 2 Cu(2+) in pMMO from *M. album* BG8. *Biophys. J.* **74:**A300.
217-271.

Yuan, H., Collins, M. L. P. and Antholine W. E. (1999). Type 2 Cu(2+) in pMMO from *Methylomicrobium album* BG8. *Biophys. J.* **76:**2223-2229.

Zahn, J.A. and DiSpirito, A.A. (1996). Membrane-associated methane monooxygenase from *Methylococcus capsulatus* (Bath). *Journal of Bacteriology* **178:**1018-1029.

Zatman, L. (1981). A search for patterns in methylotrophic pathways. *In: Microbial Growth On C_1 Compounds.* (Ed) Dalton, H. London:Heyden. pp. 42-54.